NASA CONTRACTOR REPORT

NASA CR-1663

DESIGN FOR A SPACE QUALIFIED LASER

Phase I

by W. B. Bridges

Prepared by
HUGHES AIRCRAFT COMPANY
Malibu, Calif.
for Electronics Research Center

NATIONAL AERONAUTICS AND SPACE ADMINISTRATION • WASHINGTON, D. C. • OCTOBER 1970

STANDARD TITLE PAGE

1. Report No.	2. Government Accession No.	3. Recipient's Catalog No.
NASA CR-1663		

4. Title and Subtitle	5. Report Date
DESIGN FOR A SPACE QUALIFIED LASER Phase I	October 1970 6. Performing Organization Code

7. Author(s)	8. Performing Organization Report No.
W. B. Bridges	

9. Performing Organization Name and Address	10. Work Unit No.
Hughes Research Laboratories Hughes Aircraft Co. Malibu, California	740-21-02-05-25 11. Contract or Grant No. NAS 12-579

12. Sponsoring Agency Name and Address	13. Type of Report and Period Covered
National Aeronautics and Space Administration Washington, D. C. 20546	Contractor Report 14. Sponsoring Agency Code

15. Supplementary Notes

None

16. Abstract

The research and development toward perfecting a space-qualified 5 mW He-Ne laser is reported. The laser and power supply, which are integrated into a single package, provide a rugged, lightweight, compact unit. The design details of the unit are presented. The results of special studies conducted in cold cathode geometry and lifetests; internal mirrors; mirror and window seals; and environmental testing are reported.

17. Key Words (Selected by Author(s))	18. Distribution Statement
Space Qualified Helium Neon Laser 1. Gas Lasers	Unclassified-Unlimited

19. Security Classif. (of this report)	20. Security Classif. (of this page)	21. No. of Pages	22. Price
Unclassified	Unclassified	121	$3.00

TABLE OF CONTENTS

LIST OF ILLUSTRATIONS

SECTION I

INTRODUCTION

This document summarizes work performed by the Hughes Aircraft Company, Research Laboratories and Electron Devices Divisions, for the National Aeronautics and Space Administration under Contract NAS 12-579, "Research Directed Toward Perfecting a Design for a Space-Qualified Laser." It is intended to cover, in outline form, the pertinent data presented verbally by Hughes personnel to NASA/ERC personnel at Cambridge, Massachusetts, on 1 February 1968.

The objectives of this program are best set forth in the Statement of Work:

"The Contractor shall supply the necessary personnel, facilities, services, and materials to accomplished the work as set forth below:

ITEM 1: Perfect a design for a space-qualified laser in accordance with the general specifications outlined in Exhibit A, attached hereto and made a part hereof. This shall include, but is not limited to, the following:

a. Calculations of the interaction of all critical parameters.

b. Laboratory experiments intended to support calculations of critical parameters.

c. Literature review.

d. Investigation of the state-of-the art in commercial lasers, including foreign ones.

e. Visits to NASA centers for elucidation of the spacecraft configurations and environmental conditions.

f. Visits to universities or non-NASA government laboratories for information exchange purposes.

ITEM 2: Upon completion of Item 1 an oral presentation and review will be held at NASA/ERC, Cambridge, Massachusetts. Four (4) copies of all pertinent data shall be made available to the contract monitor one week before said review. This shall include a set of design specification requirements which meet all the performance environment needs, and a list of materials.

Monthly Technical Reports are required and shall be prepared in accordance with Contractor Report Exhibit, dated January 13, 1967, attached hereto and made a part of this contract. Quarterly Technical, Interim Scientific and Final Technical Reports are not required."

The general specifications as set forth in Exhibit A are quoted from the contract:

"GENERAL SPECIFICATIONS FOR SPACE-QUALIFIED LASER

1. To operate at 6328Å with He-Ne.

2. To operate in a single transverse mode, ($TEM_{ooq} \rightarrow TEM_{ooq+j}$).

3. To operate at an initial output power level not less than five (5) milliwatts, CW.

4. To demonstrate the capability of an operating/shelf life of three (3) years, the operating portion of which shall be not less than 10,000 hours. The output power shall not drop below 3 mW at 7000 hours operating time and 2 mW at 10,000 hours operating time.

5. To operate with a polarized output, linear to one part in 1000.

6. To operate with a beam diameter not greater than two (2) millimeters.

7. To operate with a beam divergence consistent with the diffraction limit for the selected beam diameter. The beam is to be round.

8. To operate with no detectable lasing at the 3.39μ or 1.15μ wavelengths.

9. To operate without liquid cooling.

10. To operate within a light-tight enclosure.

11 To operate without any significant magnetic field leakage.

12. To operate normally in space vacuum environments after rocket launch.

13. To operate with a minimum angular deviation of the beam axis as a function of temperature, time, vehicle spin, laser age, magnetic field, etc. Quantitative definition of this parameter will be made later before Phase II work begins.

14 To operate with a minimum of discharge and mode noise in the output radiation. The final specification of this parameter will be made consistent with the state-of-the-art at design freeze.

15. To operate with a power supply and control package developed on this contract along with the laser head and meeting identical environmental specifications. Minimum control functions would be: (a) turn on supplies, (b) start discharge, and (c) power check telemetry.

16. The mounting design shall be as nearly universal as possible, consistent with meeting all other objectives. The design shall permit beam axis alignment with associated apparatus in the satellite assembly phase.

17. The weight, size, and power demand shall be as low as possible consistent with meeting all other objectives.

18. The topics of resonator configuration, type of discharge, type of cathodes (if used), method for maintaining mirror alignment, need for magnetic shielding, dust protection, heat removal, etc. are to be determined in Phase I of this contract.

19. Particular lasers of this design may be converted to emit at 1.15 μ or 3.39 μ wavelengths. Minor consideration should be given to this desired capability.

20. The materials used must be compatible with generally accepted space practice."

The Statement of Work, as given above, has been fulfilled. The design of a Space Qualified Laser (SQL) required under Item I is presented in detail in Section II of this document. The results of our work on subtasks a through f under Item I are detailed in Section III, along with the results of additional subtasks undertaken at the contractor's option.

SECTION II

SPACE-QUALIFIED LASER DESIGN

In this section we present the details of the laser design developed under the present contract. The final design version, now designated Hughes type 3072H, is substantially the same as that described in our proposal dated May 1967. During the present contract we have confirmed by experiment those design features which represented new departures in laser construction: all metal-ceramic tube envelope; high-temperature window seals; high efficiency, all solid-state, regulated power supply. During the program we also confirmed our values for the basic parameters of the laser design: length, bore diameter, and cold-cathode operation. We have the highest confidence that lasers fabricated according to the design presented will meet or surpass all of the requirements given in "Exhibit A" (quoted in Section I), as well as those additional specifications which will be imposed by the particular mission requirements.

The outstanding features of our design are summarized below.

- Rugged all metal-ceramic construction, allowing high temperature bakeout and precision manufacture
- Long-life cold-cathode discharge, permitting highest operating efficiency and minimum heat generation within the optical cavity support structure
- Internal mirrors, reducing optical cavity losses and simplifying the dust-sealing requirements while retaining a polarized output
- Optimized optical cavity support structure, using materials and geometry to minimize the effects of thermal gradients, vibration, and external mechanical stresses
- Integrated tube and power supply package with a helium atmosphere, minimizing altitude-induced stresses on the optical cavity support structure, promoting component cooling, and minimizing corona problems
- All solid-state dual power supply with precision current regulation and space-proven circuitry.

The over-all weight of the proposed unit is approximately 11.6 lb, and the total power consumption is approximately 30 W from the 28 V dc line.

A. METAL-CERAMIC TUBE

The reasons for our choice of a metal-ceramic laser tube envelope were discussed in detail in our proposal. The choice was based on years of experience in developing both glass and metal-ceramic microwave tubes and, more recently, glass, fused silica, and metal-ceramic lasers. All our experience indicates the ultimate superiority of metal-ceramic construction, particularly for applications requiring operation in unfavorable environments. A prototype metal-ceramic laser was fabricated during the present program with no unexpected difficulties, thus confirming the correctness of our choice. A photograph of this tube is shown in Fig. II-1.

Figure II-2 shows the construction details of the metal-ceramic prototype fabricated under the present program. The proposed design is identical to that shown in the figure, except that the over-all dimension is shortened to 14.75 in. (the metal and ceramic parts and subassemblies were ordered for the prototype before the final dimensions were fixed). Figure II-2 shows both the metal-ceramic discharge tube and the optical cavity support and adjustment structure. The items called out in the figure are named in Table II-1 and are described in further detail below.

High purity Al_2O_3 is used for the ceramic bore (1). The active bore dimensions for the prototype tube are 14 in. by 2.5 mm i.d.; for the proposed tube these will become 10 in. by 1.5 mm. The bore is metallized and sealed to the internal bore support (2) and the end bore supports (3) and (10). The cantilever bore section shown in the figure will be reduced by 30% in the proposed design, materially increasing the resonant frequency of this section. Vibration tests (see Section III-F) performed on glass tubes with even larger cantilever sections have indicated that this is not a problem area.

The cathode support cylinders (8) with end (3) and (10) form a gas reservoir with approximately 600 cm^3 volume in the present design, and 400 cm^3 in the proposed design. The results of our life tests to date indicate this will be more than sufficient for 10,000 hours operating life. The cathode consists of a processed tantalum cylinder (23) with end caps (6) slipped inside the vacuum envelope (8). Life test data (discussed in Section III-F) indicate that this cathode type will also be suitable for 10,000 hours operation.

The anodes of this dual discharge design are formed by the metal bellows (12) on each end of the discharge tube. Each bellows is brazed to an adapter ring (11) which is, in turn, heliarced to the flange (4) brazed to the metallized ceramic bore. The vacuum envelope is completed by the prism holder (14) and mirror holder (15) (see View A

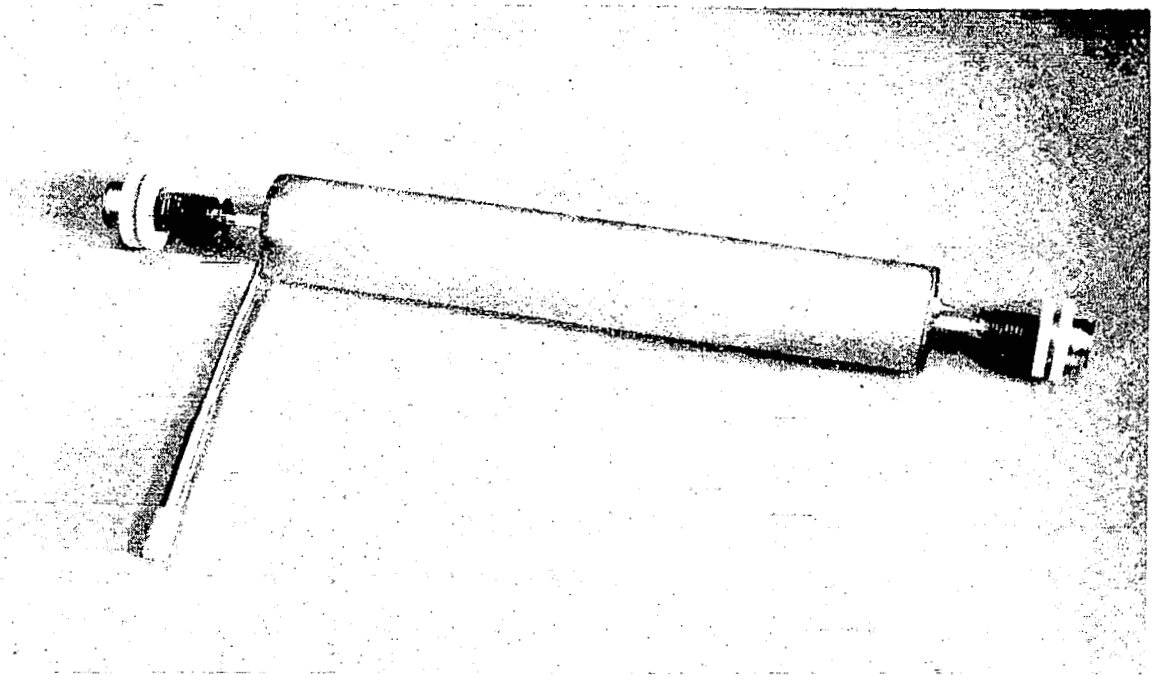

Fig. II-1. Photograph of completed metal-ceramic tube.

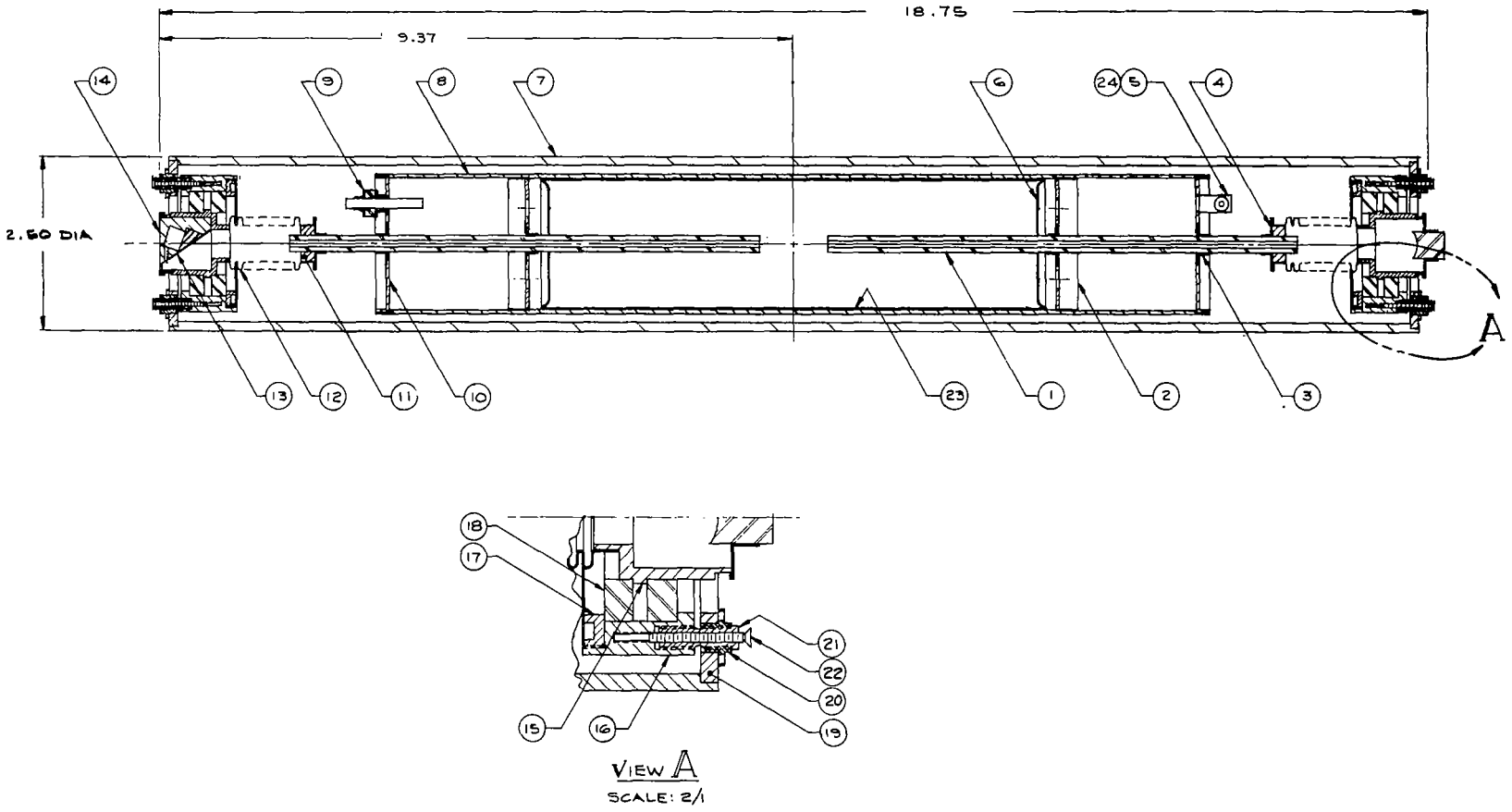

Fig. II-2. Metal-ceramic tube cross sectional view.

TABLE II-1

Legend for Figure II-2

1	Ceramic Bore
2	Internal Bore Support
3	Pumpout Bore Support
4	Heliarc Flange Adapter
5	Pumpout
6	Cathode End Cap
7	Cavity Support Cylinder
8	Cathode Vacuum Jacket
9	Getter Feedthrough
10	Getter Bore Support
11	Bellows Adapter
12	Bellows
13	Prism Clamp
14	Prism Holder
15	Mirror Holder
16	Adjusting Mirror Support
17	Retainer Ring
18	Insulator
19	Mirror Support
20	Coarse Adjustment
21	Differential Screw
22	Locking Screw
23	Processed Tantalum Cathode
24	Tipoff

for (15)). The coated Brewster's angle half prism used for the high reflectance mirror provides the polarization reference for the beam. This prism is held mechanically in part (14) and does not form a portion of the vacuum envelope. The output mirror attached to part (15) forms part of the vacuum envelope. The technique for making these metal-to-metal heliarc sealed mirrors was worked out during the present program and is described in detail in Section III-G.

Electrical connection to the getter is made through a ceramic feedthrough insulator (9). This connection is used only during initial tube processing. An alternate stacked ceramic disc seal was indicated in our proposal, but the feedthrough shown in (9) is simpler and has proven quite reliable on other metal-ceramic microwave tubes and in the Hughes EDD appendage ion vacuum pumps. The vacuum tipoff (24) is made by pinching the copper vacuum pumpout (5) in the usual vacuum tube fashion.

The vacuum envelope (8) is held rigidly to the optical cavity support cylinder (7) with a layer of potting compound suitable for use in spacecraft. The mirrors are held rigidly with respect to the outer cylinder by adjustable mounts (see View A, Fig. II-2). The mirror holder (14) or (15) is held in a retainer ring (17) via insulators (18), necessary to allow the optical support structure to remain at ground (cathode) potential while the mirror holder floats at anode potential. The retainer (17) is positioned with respect to the support structure end plate (19) by locking differential screw mechanisms (21), (22), and (23). These screw mechanisms are adaptations of the design now being used successfully in our airborne argon ion laser, and other Hughes military optical equipment.

Many considerations enter into the realization of a successful laser design. The tube design shown in Fig. II-2 is a consequence of several choices among alternative approaches. Detailed discussions of the engineering considerations involved in the choice of envelope materials, mirror geometry, cathode type, etc., were given in our original proposal. The conclusions reached in those discussions have been further borne out by our work during the present Phase I program. The arguments for the critical design choices made in arriving at the present proposed design are reviewed only briefly here.

1. Choice of a Cold Cathode

The cold cathode design proposed originally and also incorporated in the present design has evolved from many experiments performed at Hughes. Although early cold-cathode tubes proved to have short life compared with simple hot-cathode versions, the pioneering work of Hochuli and Haldemann (Ref. II-1) with aluminum oxide films

suggested that practical cold-cathodes could be made. We made some early experiments with oxidized aluminum, following Hochuli, but abandoned this approach because of the relatively poor qualities of aluminum as a clean, bakable vacuum tube material. A better cathode material was then developed in the form of an oxidized tantalum surface, built as a hollow structure. The layer of Ta_2O_5 formed by proper processing should, in theory, have even higher sputtering resistance than Al_2O_3, because of the higher heat sublimation of Ta_2O_5 (although neither rate has been actually measured because of the extremely low yield for both materials).

The theory of cold-cathode emission through insulating layers and the appropriate cathode configuration was covered briefly in our proposal. Thin oxide films, although insulators, can be made to supply low emission densities by tunneling, in which the electron penetrates the insulating surface quantum mechanically. The emission density must be kept low so that the electric field causing the tunneling is not sufficiently high to punch through the film. The exact hollow cathode configuration used is also of great importance. A design with an objective life of >10,000 hours must have very uniform, low emission density; a localized high-emission region could produce orders of magnitude more sputtering than neighboring low emission regions. The uniformity of emission is controlled by the electrode and plasma configuration. The design proposed for the 3072H space-qualified laser is essentially a doubled version of that used in the 3082H alignment laser tube made by Hughes for Keuffel and Esser Co. Life tests on the 3082H tubes have gone over 7000 hours to date with unchanged discharge or laser characteristics. The details of these life test cathode studies on the 3072H type cathodes are given in Section III-F. We are confident that the cathode design proposed herein is suitable for a 10,000 hour tube life.

2. Choice of a Dual Bore Design

The proposed design utilizes a split discharge column employing two anodes and a common cathode. This choice was made not only to reduce the discharge voltage by a factor of two but also to provide operating redundancy. Either half of the tube may be operated independently provided separate power supplies are used. This allows the laser to be operated with approximately 35% of full power if desired. It also offers operation at 35% output if one power supply section should fail. In this design the mirror surfaces are far removed from the cathode region where sputtering (if any) occurs, thus affording maximum protection to the optical surfaces.

3. Choice of Internal Mirrors

The various factors entering into the choice of mirror coatings and cavity configuration were discussed in our original proposal. The decision to use "hard" coated mirrors in an internal mirror configuration, with a coated Brewster's angle half-prism to provide polarization, was borne out by our subsequent experiments, discussed in Section III-G. We found that "hard," ultraviolet-resistant coatings are available with losses equal to or smaller than the best commercial soft coatings (Spectra-Physics). We also found that a significant increase in power could be obtained by eliminating the Brewster's angle windows. A sealing technique was developed which will allow the fabrication of a bakable internal mirror tube (although with further development this same sealing technique could also be applied to Brewster's angle windows). The simplicity and compactness of the internal mirror design is also superior to an external mirror arrangement with separate hermetically sealed compartments between the windows and mirrors. We feel confident that this mirror configuration will result in the most practical tube for space use.

B. OPTICAL CAVITY SUPPORT STRUCTURE DESIGN

The optical cavity support structure was shown in cross section in Fig. II-2 as a simple tubular member connecting the mirror adjustment mechanisms on either end. In our proposed design we intend to make this tubular member as a composite structure consisting of an inner and outer tube spaced apart by ribs or posts, as shown in Fig. II-3. The reduction of externally generated azimuthal temperature gradients around the inner tubular member (to which the end mirror retaining assemblies are attached) should greatly reduce the misalignment due to bending. We may think of the outer tube as "shorting out" the externally driven thermal gradients induced, for example, by asymmetry in the mounting bracket, as shown in Fig. II-3.

We have chosen beryllium as the material for the cavity support structure. While one might think that a lower-expansion material such as fused silica would be superior, a careful analysis of the problem shows this is not correct. The support structure must resist deformation caused by changes in mechanical stresses and by stress originating from thermal gradients. The resonant frequency of the mirror support assembly also must be maintained as high as possible in order to minimize the effects of spacecraft low frequency vibrations.

In Table II-2 the physical properties of materials pertinent to this discussion are listed for several possible candidates for the cavity support tube. The rigidity of a simply supported overhanging beam of

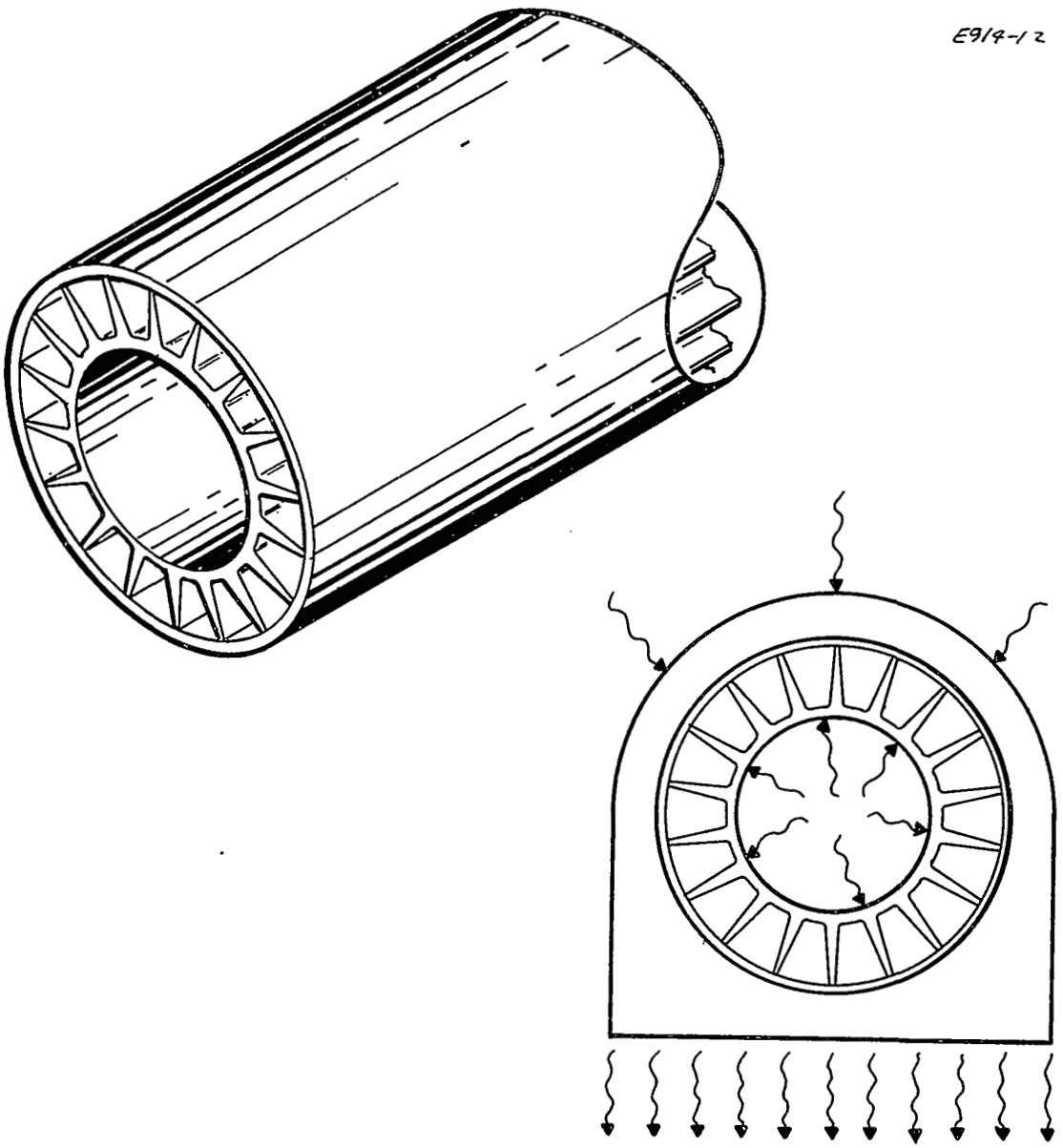

Fig. II-3. Proposed composite mirror support structure.

TABLE II-2

Pertinent Physical Properties of Possible Cavity Support Tube Materials

Material	E, psi	ρ, lb/in.^{3}	K, in./in./$^\circ$C	σ, cal/cm-sec/$^\circ$C	E/ρ, in.	K/σ, (cm-sec)/cal
Aluminum	9.0×10^6	9.75×10^{-2}	23.6×10^{-6}	5.3×10^{-1}	9.23×10^7	4.45×10^{-5}
Beryllium	42×10^6	6.7×10^{-2}	11.6×10^{-6}	3.5×10^{-1}	62.7×10^7	3.32×10^{-5}
Invar	21.4×10^6	31.4×10^{-2}	9.0×10^{-6}	0.26×10^{-1}	6.82×10^7	3.44×10^{-5}
Lockalloy	28×10^6	7.56×10^{-2}	16.6×10^{-6}	4.9×10^{-1}	37.0×10^7	3.38×10^{-5}
Magnesium	5.77×10^6	6.28×10^{-2}	27.1×10^{-6}	3.67×10^{-1}	9.2×10^7	7.19×10^{-5}
Pyroceram	12.5×10^6	7.94×10^{-2}	0.20×10^{-6}	0.048×10^{-1}	15.8×10^7	4.17×10^{-5}
Quartz	10.4×10^6	7.94×10^{-2}	0.55×10^{-6}	0.033×10^{-1}	13.1×10^7	16.7×10^{-5}
Tantalum	27×10^6	60×10^{-2}	6.5×10^{-6}	1.3×10^{-1}	4.5×10^7	5.0×10^{-5}
Titanium	16.8×10^6	16.3×10^{-2}	8.41×10^{-6}	0.27×10^{-1}	10.3×10^7	30.8×10^{-5}

uniform cross section is directly proportional to the ratio E/ρ; the deformation of the beam due to the stress exerted by the weight of the end plate is inversely proportional to E. Therefore, from the standpoint of mechanical rigidity, a material of a large modulus of elasticity E and a low density ρ is required. The desirability of a high resonant frequency also demands a material with a large E/ρ ratio since the resonant frequency of the tube is directly proportional to $(E/\rho)^{1/2}$. If the weight of the assembly is to be minimized, a low density material is desirable. This is true for a simple tube or a composite structure as shown in Fig. II-3.

In order to minimize beam distortion resulting from stresses caused by thermal gradients, it is imperative that the material have a low ratio of thermal coefficient of expansion to thermal conductivity (K/σ). Referring to Table II-2, it is quite apparent that beryllium surpasses all the other candidates in every requirement. Beryllium has the largest modulus of elasticity, the smallest density, the largest ratio of E/ρ, and the smallest ratio of K/σ. It is also quite clear from Table II-2 that aluminum, magnesium, and quartz are all considerably poorer in the mechanical ratio E/ρ, and quartz is also poorer by a factor of 5 in the thermal ratio K/σ.

We have chosen a single-point mounting foot for the cavity support tube, as shown in Fig. II-4. This mounting foot provides both mechanical support and a thermal path to the heat sink (spacecraft frame). The single foot support serves to isolate the cavity support cylinder from torques or stresses which the laser package or spacecraft heat sink might undergo.

The resonant frequency for a cantilever arrangement as shown in Fig. II-4 (but with 18.75 in. over-all length) was calculated to be 4090 Hz, assuming a simple center support and a solid beryllium tube with a 0.25 in. wall thickness. This frequency is sufficiently high to be out of the high amplitude range of low frequencies typical of spacecraft vibrations. For the 14.75 in. structure actually proposed, the resonant frequency is even higher — approximately 7000 Hz. For the ribbed or post separated composite tube, the resonant frequency will be still higher. We are confident that this method of support is superior to two-point or two-ring mounts, even though these have slightly higher resonant frequencies, because of the isolation from external torques and stresses provided by the single-foot mount.

C. PACKAGE DESIGN

The key feature of our proposed package design is that the laser and power supply are integrated into one hermetically sealed

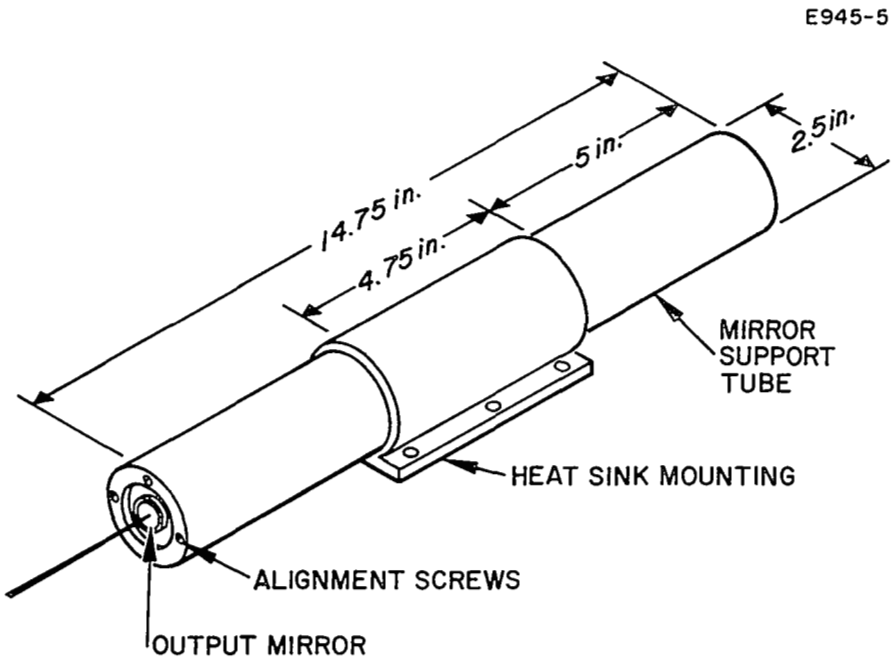

Fig. II-4. Over-all view of cavity support structure and mounting bracket for 3072H laser.

helium-filled package, as shown in Fig. II-5. This arrangement has the following advantages:

- The laser cavity is exposed to a relatively constant-pressure helium atmosphere, so that changes in the forces on cavity structure in traveling from the earth's surface to space are minimized.

- No high voltage connectors or cables are needed to connect the laser to the power supply. All high voltage leads are contained within a sealed helium atmosphere, thus allowing operation through critical altitude without special design of the power supply or cables to suppress corona.

- The minimum lead length between the laser discharge tube and power supply minimizes the shunt capacitance and provides the maximum stability with the minimum values of series stabilizing resistors.

- The helium atmosphere helps prevent hot spots from forming in the electronic circuitry by providing a high thermal conductivity path to the package walls.

The proposed package material is magnesium alloy (AZ-61 or AZ-91) heliarced or dip brazed. Interior ribs and edge flanges are used to stiffen the structure and allow the use of light stock material for the walls. The input connectors for the 28 V prime power and telemetry are helium-leak-tight assemblies. The output window is antireflection coated and sealed to the package with a metal compression seal capable of remaining leak tight under pressure and temperature cycling. A tubulation for evacuation and helium filling is also provided. The final seal after helium filling is made at this tubulation.

Two physical arrangements are proposed, with the choice between them being made on a mission requirements basis. The first version, shown in Fig. II-5, is similar to the demonstration laser prototype built under the present program (see Section III-H), except that the length has been reduced from 20-7/8 in. to 16 in. over-all. The volume is approximately 380 $in.^3$. The alternative arrangement is shown in Fig. II-6; the volume is approximately the same, and the two arrangements differ only in the power supply circuit board layout. Since both arrangements use the same laser tube, cavity support structure, and power supply components, the qualification of both versions would take little more effort than either alone.

Both package versions use the same method of boresight alignment. Once the laser is adjusted and sealed inside, a precision edge is machined on a corner of the package parallel to the experimentally

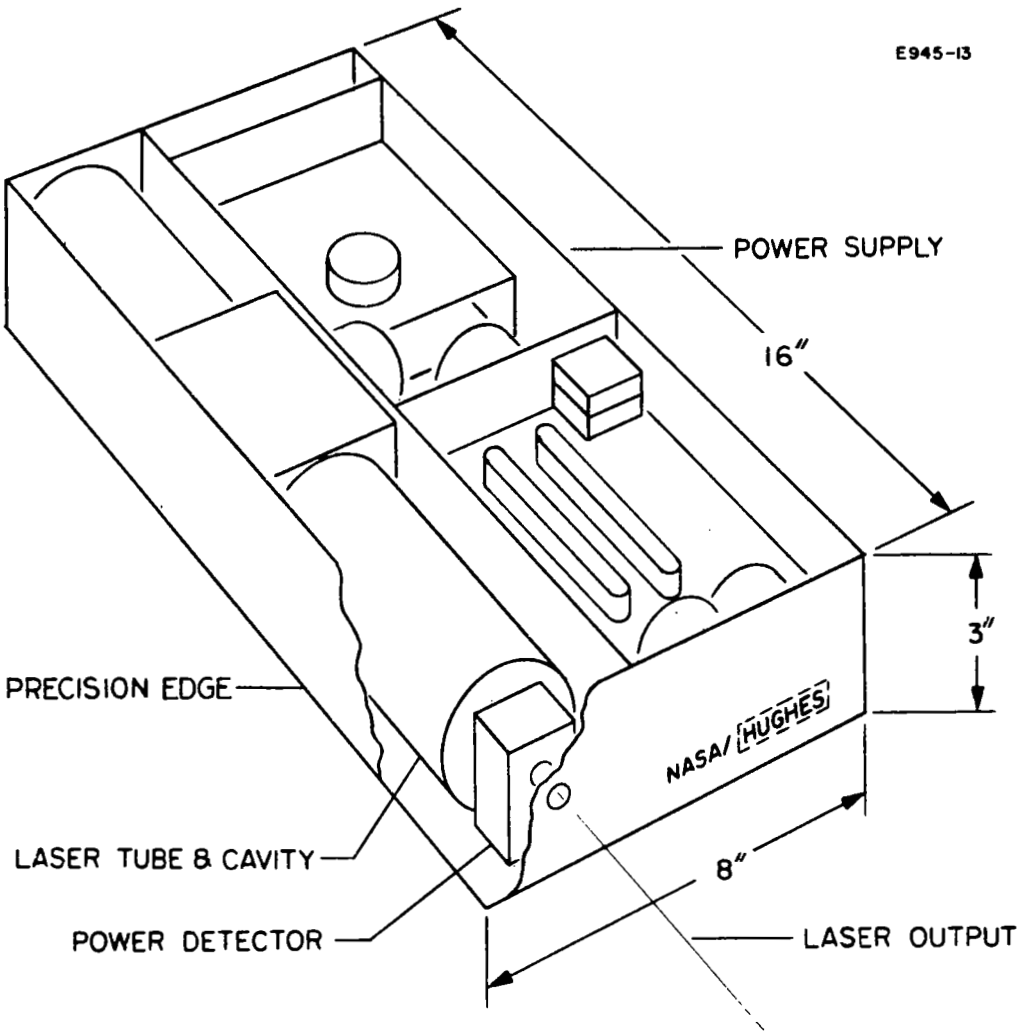

Fig. II-5. Package arrangement alternative 1.

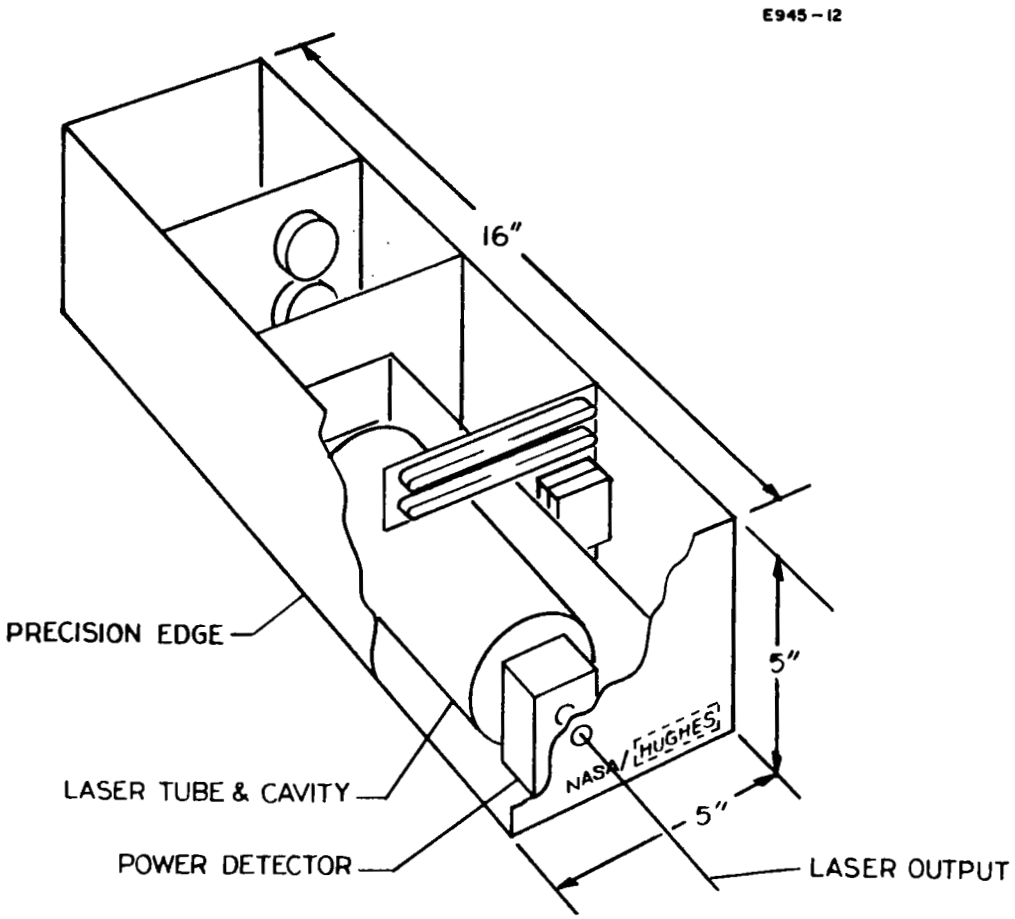

Fig. II-6. Package arrangement alternative 2.

determined optical output axis. In this way units mounted and aligned with this edge as a guide can be interchanged at will without readjustment. The precision edge runs nearest the mounting foot of the laser, as indicated in Figs. II-5 and II-6, so that errors in alignment between the edge and the laser otpical axis due to external torques or stresses applied to the mounting base plate are minimized. Mounting of the laser to the base plate is accomplished by bolting through the external flange of the package as shown in Fig. II-7. Heat transfer from the package to the base plate occurs over the large area of the package bottom.

The over-all package sizes given in Figs. II-5 and II-6 are the maximum proposed. Measurements described in Section III-B assure that these will be adequate. Some additional effort should be expended on further decreasing the package size and weight by the use of the side "bulges" out to the flange dimensions and the use of exterior stiffener ribs to allow reduction in the wall thickness used. The exact package strength (and hence size and weight) will be determined by the qualification program itself.

Although not required by the present contract, some consideration was given to the problem of using an electro-optical modulator in conjunction with the proposed laser. Intracavity modulation devices would of course require a complete mechanical redesign of the laser tube, since internal mirrors are used. External modulation is easily added, however, and we believe that the integrated sealed package approach could be used to advantage. The same laser tube and cavity structure could be used with the electro-optic modulator mounted directly on the end of the mirror support structure, with the laser package lengthened to accommodate this extension. The modulator driver (also requiring high voltage, low capacity leads) could be placed in the lengthened portion of the power supply compartment. All the advantages mentioned with regard to the laser then accrue to the modulator. Additional qualification testing of the modulator components and driver and the over-all unit would be necessary, of course, but the procedures would amount to no more than separately qualifying the modulator alone, since the laser tube and power supply would be already in proven form.

D. POWER SUPPLY DESIGN

The detailed design for an all solid-state dual power supply was evolved during the Phase I contract. The supply was fabricated and tested, and the test results are given in Section III-H. Briefly, the proposed supply provides current to the laser discharge with approximately 0.3% variation over the input voltage range from 24 to 32 V dc, a 0.6% variation over the temperature range from -20°C to +50°C and

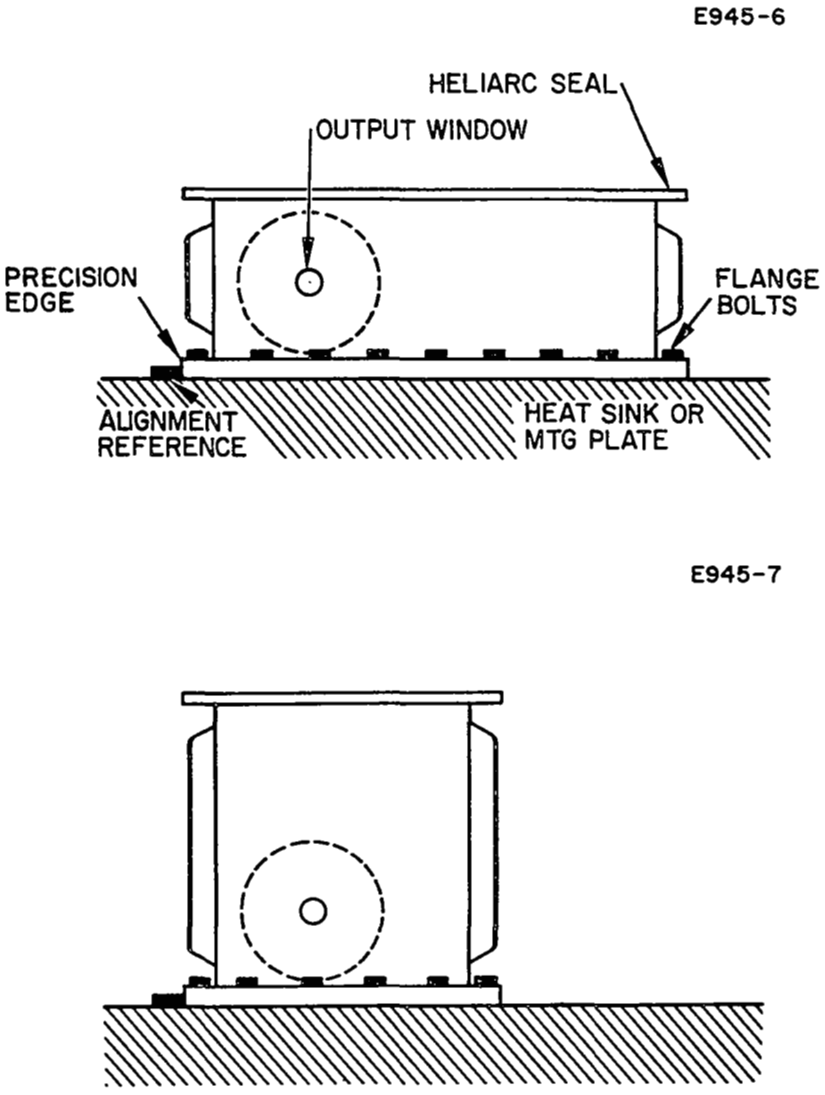

Fig. II-7. View showing package mounting flange and alignment edge.

a 1% variation over the load resistance range from 130 kΩ to 160 kΩ (corresponding to a laser discharge voltage range of 1100 to 1360 V).

Figure II-8 shows a block diagram of the dual supply. The power supply is made up of the following seven subcircuits:

- control logic
- current regulator
- dc to dc converter
- high voltage filter
- current sensing
- starting circuitry
- telemetry monitoring circuitry

The first six subcircuits are duplicated, with one set to operate each anode of the laser. The function of these seven circuits is detailed as follows. For component identification, reference should be made to the complete schematic B190074 attached to this document.

1. Control Logic

Two special power turn-on circuits are provided so that the entire power supply can float on the dc bus and be activated or turned off by means of low level signals.

Transistors Q5 and Q6 comprise the remote power turn-on circuit. A low level input signal will turn on Q5, which provides additional bias to turn on transistor Q3 in the regulator circuit. To turn off the power supply, the low level signals are removed. Either anode may be turned on or off independently of the other.

2. Current Regulator

The function of the pulse width type regulator is to provide a regulated laser current from 24 to 32 V dc input source. It is capable of regulating this current to better than ±5% for changes in input voltage and temperature. The over-all efficiency of the regulator circuit alone is 89 to 94%, depending on the temperature and input voltage.

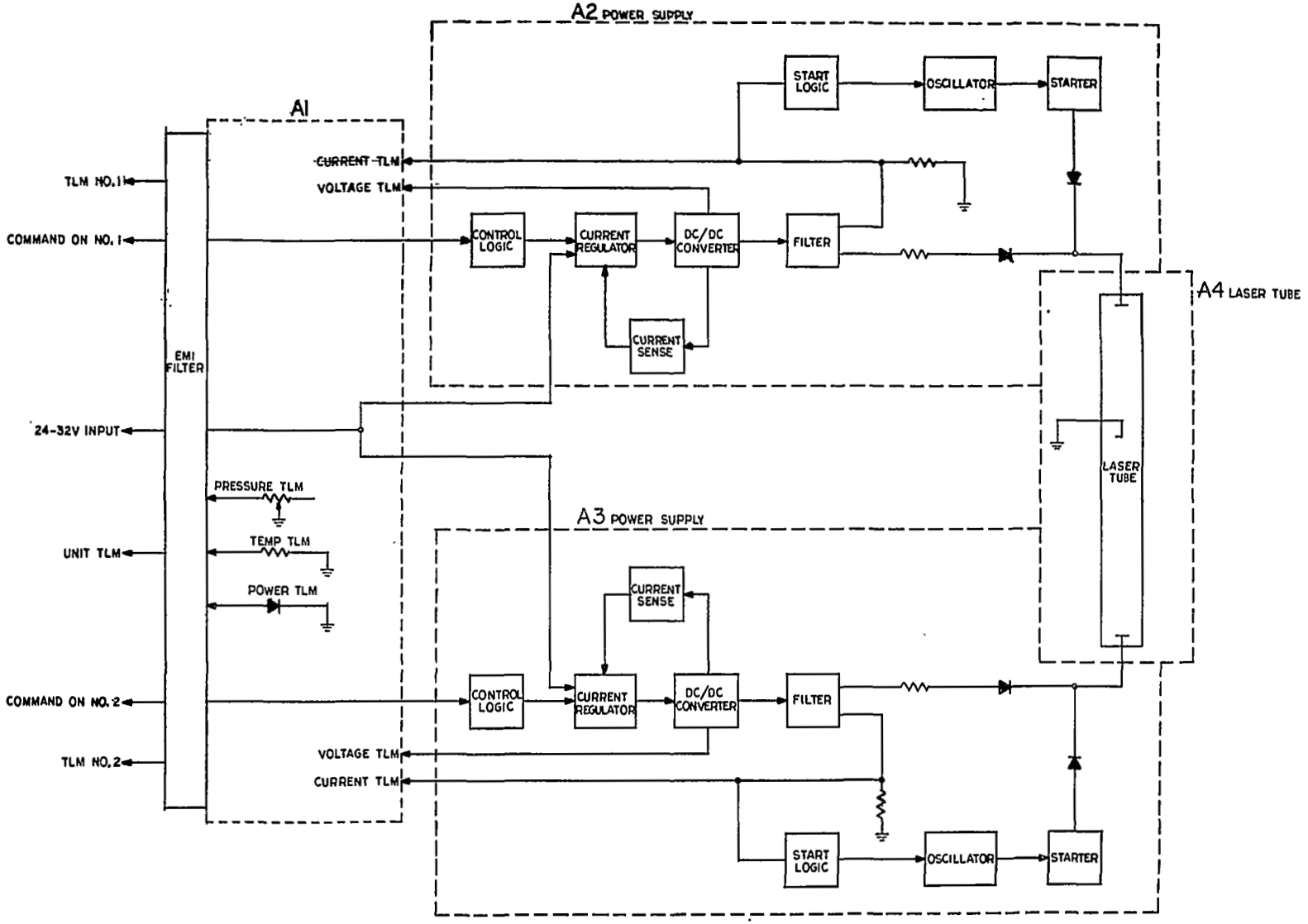

Fig. II-8. Block diagram of SQL power supply.

Transistors Q1 and Q14 are the switched pass transistors which produce rectangular pulses to L3 and C9 for smoothing. Q2, 3, 4, 7 and 8 provide the amplification which maintains a low bus voltage ripple. The signal produced at the junction of CR29 and R18 is the sensing voltage which is proportional to output current.

3. DC to DC Converter

The dc/dc converter is used to convert the input bus voltage to about 1300 V dc to operate the laser anodes. It also supplies low voltages to operate the starting circuitry and the saturable reactor in the current feedback loop.

Transistors Q11 and Q12 and transformers T1 and T2 form a switching circuit which generates squarewave ac voltages in the windings of T2. The frequency of these square waves is determined by the volt-second capacity of the transformer T1, and is approximately 4000 Hz in the present design. Q9 provides forward bias to the switching circuit to initiate oscillation but is then shut off through CR12 and CR13, thus ensuring a higher efficiency with R20 removed electrically.

4. High Voltage Filter

The high voltage filter provides filtering for the anode voltages through use of L2, C14, and C13. The output ripple from this filter is below 1% peak to peak (0.3% rms).

5. Current Sensing

Current sensing is accomplished by means of saturable reactor SR1. The output from SR1 is rectified by CR31 through 34, filtered by C15, and then used as the sensing signal to control the switching regulator.

6. Starting Circuitry

The starting circuitry causes high voltage pulses from T3 to appear across the laser electrodes through steering diodes CR27 and CR28 until the laser starts. SCR Q15 discharges C12 into T3 from a winding on T2, through diodes CR16-CR19 and R27. Transformer T3 continues to receive input voltage pulses so long as Q13, a unijunction transistor, is allowed to oscillate and provide pulses to Q15. As soon as anode current flows, diode CR 20 becomes forward biased and disables Q13.

7. Telemetry

Standard telemetry outputs (0 to 5 V dc) are provided to monitor each laser anode voltage through an auxiliary winding on the dc to dc converter. The anode currents are monitored directly by R34. Pressure telemetry is provided by a transducer MT1, similar to that used on the HS 308 and ATS programs. Temperature telemetry will be provided by thermistors at as many points as required. A single temperature telemetering circuit is shown using R39, R36 and R38.

The optical power monitoring circuit is not shown on Schematic B190074, since some further evaluation is needed. Approximately 1% of the output power (50 μW at full output) will be diverted by a beam splitter to drive the power monitor sensor. Two optical detectors are being considered for this sensing task: a standard silicon solar cell and a photo-FET. The solar cell has the advantage of being a fully space-qualified component. The photo-FET has the advantage of a higher output signal requiring less amplification to the 0 to 5 V telemetry level, but it has not yet been exposed to space environmental testing. In either case, a balanced bridge circuit using two detectors will be used to compensate as much as possible for temperature variations, and several stages of solid-state amplification will be necessary to convert the 50 μW signal into the 5 V telemetry output. The over-all size and power consumption of this power monitor circuitry should be negligible, however.

8. Efficiency

One of the major emphases during the development of this power supply was to obtain the highest energy conversion efficiency. A measured worst-case efficiency of 77% occurs at high line voltage and high temperature, when the power loss in R28 is neglected. (R28 is a laser biasing resistor necessary for obtaining an over-all positive resistance from the plasma tube and is individually chosen for the particular discharge tube used.) Under other combinations of line voltage and temperature, the over-all efficiency is greater than 77%.

E. RELIABILITY AND QUALITY ASSURANCE PROVISIONS, PHASE II

In this section and in Appendices A, B, and C we shall describe the Reliability and Quality Assurance provisions to be implemented during Phase II of the Space Qualified Laser Program:

Appendix A: Reliability Program, Phase II

Appendix B: Qualification-Reliability Test Plan

Appendix C: Quality Assurance System.

Hughes reliability and quality assurance provisions are intended to conform to the objectives outlined for Phase II. The program described herein is designed to provide

1. effective planning and management of the reliability and quality assurance effort

2. assurance of a closed loop monitoring and evaluation system

3. definition of the major qualification and reliability tests

4. the necessary documentation for qualifying the integrated laser and power supplies.

The Reliability Program Plan is presented as Appendix A. It describes the Hughes Electron Dynamics Division organizational structure and interfaces. This plan also describes the Reliability Engineering tasks to be undertaken during Phase II. It should be noted that this plan suggests the use of Mil-Spec parts for Phase II and High-Reliability parts for later flight units. The major reliability effort will be directed toward (1) improving the lifetime characteristics, (2) elimination of failure modes and mechanisms, and (3) over-all reliability assessment. These reliability tasks will be conducted in a manner time-phased with the engineering effort.

The Qualification-Reliability Test Plan is presented as Appendix B. It describes the Qualification and the Reliability tests to be performed as an integral part of the Phase II program. These tests are designed to insure that the integrated laser and power supplies can meet the requirements of the severe space environments. The data collected from these tests will be used for reliability evaluation and analysis.

The Quality Assurance System described in Appendix C is designed to provide effective management of the quality control plans and procedures. The provisions in this section describe the methods for control drawings, specifications, procuring material and parts, packaging and shipping provisions, etc. The Quality Assurance System will be utilized as a criterion for determining conformance to Phase II requirements.

SECTION III

PHASE I SUBTASKS

Work performed in satisfaction of Item 1, subtasks a through f and additional subtasks, is documented in this section.

A. CALCULATION OF CRITICAL LASER PARAMETERS

A review of basic helium-neon laser mechanisms was given in our proposal and the resulting scaling laws were discussed. We repeat the scaling law summary here as an introduction to the parameter calculation.

Certain relationships have been found empirically for optimum He-Ne laser operation. Some of these have been put on a reasonably firm theoretical basis by Gordon and White (Ref. III-1), while others remain essentially empirical. The measurements are accurate enough for the proper design of an optimum laser, however, so that no further research is necessary to determine the scaling relationships. We simply state the results below and show how they may be used to design the required laser.

- The optimum ratio of helium pressure to neon pressure has been determined to be approximately 5:1. The exact proportion is not too critical and a broad optimum exists.

- Isotopically pure He^3 has proven to be superior to He^4 as shown by White (Ref. III-2). The reason is that the He^3 atoms have higher velocities and hence more rapid collision rates with neon atoms.

- The optimum total gas pressure for a tube of diameter D is

$$pD = 2.9 \text{ to } 3.6 \text{ Torr-mm} \quad . \qquad \text{(III-1)}$$

  with the lower value appropriate for smaller diameter tubes (1 to 2 mm).

- The electron temperature is a function only of pD and is therefore the same for all optimum lasers. It is approximately independent of current. These relations have been confirmed by Labuda and Gordon (Ref. III-3) and Wada and Heil (Ref. III-4). Constant T_e and constant pD imply a

constant E/p for the discharge; that is, E/p is a measure of the energy gained by electrons in the electric field E between collisions with gas atoms. These relations also imply constant (E/p) (pD) = ED for the discharge; since $E \approx V_{tube}/L$, then V_{tube} D/L is a constant. Consistent with the above relationships is the observed relation I/D = a constant. Thus, (V_{tube} D/L) (I/D) = V_{tube} I/L is also a constant, an expression that the input power per unit length for an optimum laser is approximately the same no matter which diameter is chosen.

- The optimum small signal gain coefficient at 0.6328 μ is given approximately by

$$g \approx \frac{0.3}{D} , \qquad \text{(III-2)}$$

where D is in millimeters and g is in (m^{-1}). This relationship has been measured independently at several laboratories and is reasonably accurate over the range of D from 1 to 10 mm.

The variation of power output with the various atomic and physical parameters (or measurable combinations of these parameters) has been discussed by Rigrod (Ref. III-5); White, Gordon, and Rigden (Ref. III-6); and Smith (Refs. III-7 to III-9). The latest work by Smith compares all three approaches and yields the most accurate comparisons with experiment. The development of the theory is given in Ref. III-7, the measurement of the critical medium parameters in Ref. III-9, and the comparison between theory and experiment in Ref. III-8. For a multimode laser (i.e., TEM_{00} operation, but several longitudinal modes oscillating simultaneously), Smith finds the relation (Ref. III-7)

$$P_{out} = \frac{\pi D^2}{10} (Aw_o) G(1 - \sqrt{a/G})^2 \qquad \text{(III-3)}$$

where D is in millimeters, (Aw_o) is a constant with the empirically determined values of 300 mW/(mm)^2, G is the small-signal gain per pass (= gL), and a is the loss per pass. The output coupling is assumed to be at its optimum value given by

$$t_{opt} = G(\sqrt{a/G} - a/G) . \qquad \text{(III-4)}$$

From these relations, the power output and optimum coupling coefficient can be determined once the diameter, length, and cavity losses are specified. One assumption necessary to arrive at eqs. (III-3) and (III-4) that was not stated previously is that the optical mode cross-sectional area is assumed to be about 1/5 the physical tube area. This is a reasonable approximation for TEM_{00} operation in the usual cavity configuration. Equations(III-3) and (III-4) are derived for the case of symmetrical mirrors, with equal outputs from each end. If the output is taken from one end only, a factor of two should be added to the right hand sides of both (III-3) and (III-4).

Similar relationships are expected to hold for the 1.15 μ and 3.39 μ transitions, but the values of Aw_o and gD have not been determined accurately for these lines.

Smith has obtained very good agreement (Ref. III-8) between eq. (III-3) and the actual output of several BTL lasers. He uses the value 0.3% for the loss per pass which is made up of 0.1% loss in the window and 0.2% in the mirror. Mirror losses this small are quite difficult to realize (although the group at BTL under Gordon has in fact produced mirrors with losses this small; these were the same mirrors used in the experiments Smith compares). A more realistic figure for mirror loss in the soft coating material is $\approx 0.5\%$, and for the hard materials 0.5 to 0.8%. Using these values we may compute an approximate design for the 5 mW laser required for this program. For a single ended output, eq. (III-3) becomes

$$P = 190\, D^2 G(1 - \sqrt{a/G})^2 \text{ mW}, \qquad \text{(III-5)}$$

and eq. (III-4) becomes

$$t_{opt} = 2G\,(\sqrt{a/G} - a/G)\,. \qquad \text{(III-6)}$$

Figure III-1 shows the output power to be expected from a 30.5 cm (12 in.) active length as a function of the single-pass loss for different bore diameters, as given by (III-5). The curves of course assume that the optimum output mirror transmission given by eq. (III-6) and shown in Fig. III-2 is used at each point. The same data are in given in Figs. III-3 and III-4 for a 23 cm (9 in.) active length. These two lengths were used in tubes fabricated during the SQL program. We see that the total single-pass loss must be less than 2% to achieve 5 mW output from the 30.5 cm bore with diameters in the practical range 0.8 to 3 mm and less than 1.1% for the 23 cm bore. We also note that the behavior with diameter is not monotonic for optical

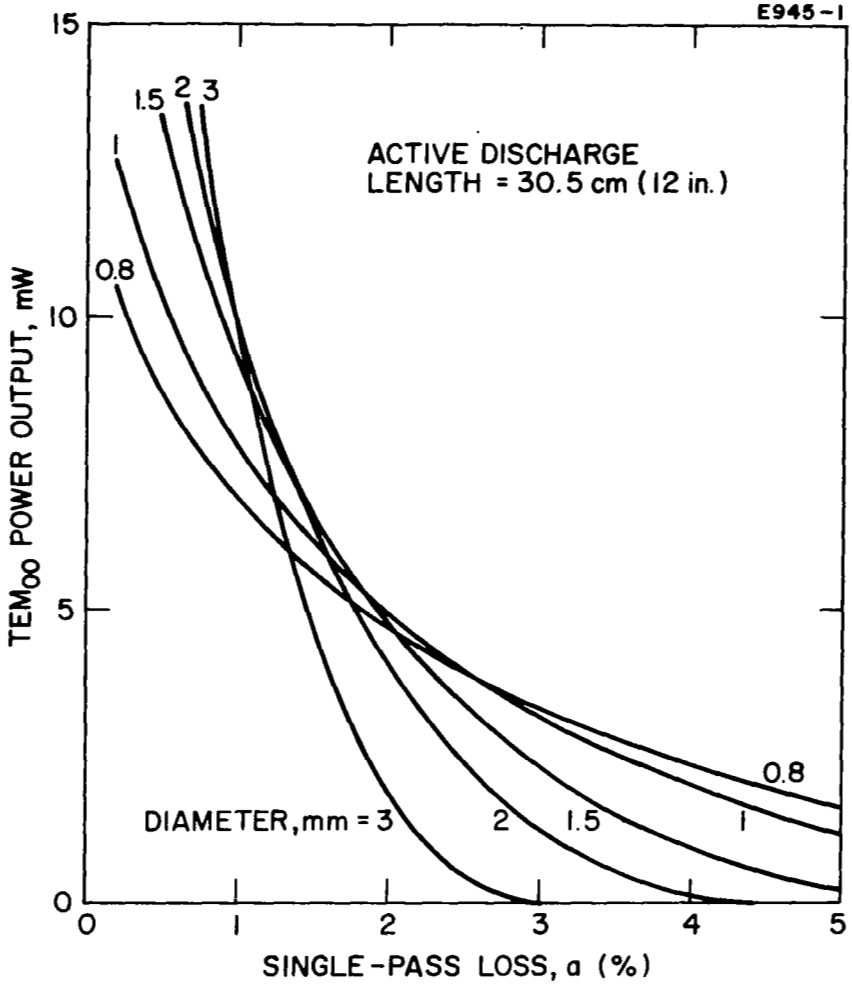

Fig. III-1. Power output as a function of loss parameter a, for a 12 in. tube length.

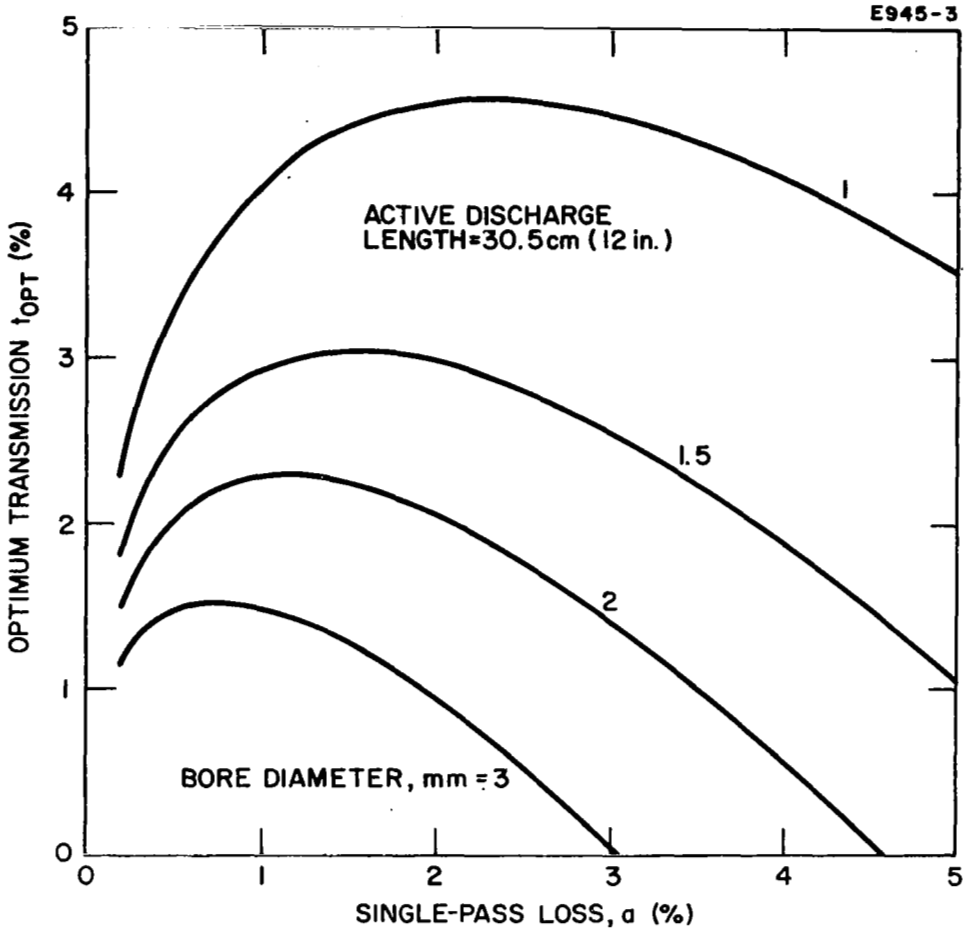

Fig. III-2. Optimum mirror transmission as a function of loss parameter a for a 12 in. tube length.

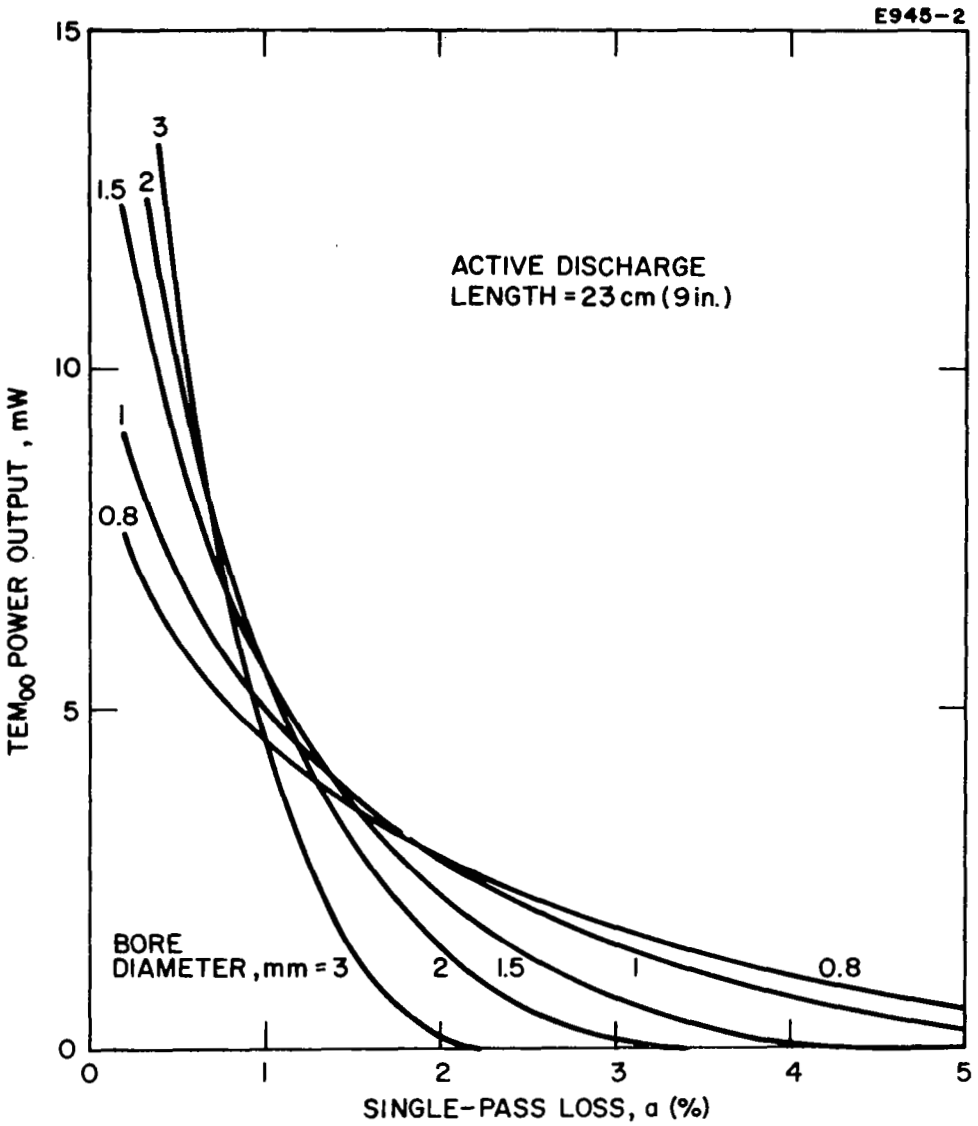

Fig. III-3. Power output as a function of loss parameter a, for a 9 in. tube length.

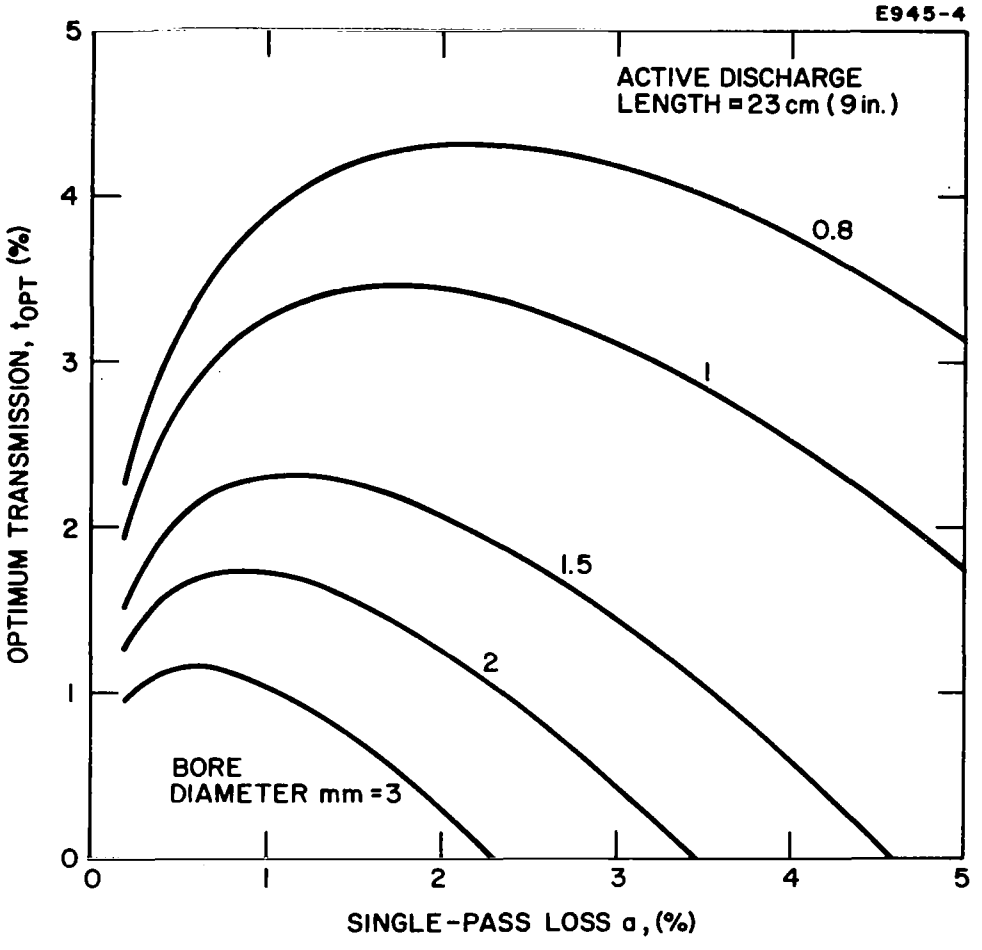

Fig. III-4. Optimum mirror transmission as a function of loss parameter a, for a 9 in. tube length.

losses in the range which yields 5 mW output. Comparison with experiment is also complicated by the fact that the mirror transmission is not actually optimized at each point during the measurements. The results of measurements on tubes fabricated during the program are given in Section III-B.

B. MEASUREMENT OF CRITICAL LASER DESIGN PARAMETERS

Several tube variations were fabricated under this program to check the designs made on the basis of the calculations given in the previous section. Tube diameters of 3, 2.5, 2, and 1.5 mm, and active bore lengths of 12 in. and 9 in. were used (although not all combinations of these diameters and lengths were tried). The most serious unknown parameter in attempting a comparison of the experiments with theory was the mirror loss a. While mirrors with losses as low as 0.2% have been made, a more typical value for practical dielectric mirrors lies in the range from 0.5 to 1%. In addition, the limited selection of mirror transmissions readily available prevented the exact optimization for each set of diameter, length, and loss. Nevertheless, a reasonably good agreement with theory was obtained.

Reference to Fig. III-1 indicates that for total signal-pass losses (mirror plus Brewster's angle window) of about 1%, optimized output powers of 9 to 10 mW should be possible from 1.5 to 3 mm bore tubes with 30.5 cm active lengths. The corresponding optimum mirror transmission ranges from $\approx$ 1.5% to 3%. Figures III-5 and III-6 give the typical performance characteristics of 2 mm x 30.5 cm bore tubes. Power outputs in the range from 6 to 8 mW were obtained at various fill pressures. The output was obtained in the TEM_{10} mode, which does not exactly fit the theoretical assumptions, but should not be too far off. The mirror transmission used (0.8%) is also not in the optimum range $\approx$2%; therefore, we may conclude that the optical losses are somewhat less than 1% and that more power would be realized by a 2% mirror with the same losses.

The optimum pressure of $\approx$2 Torr agrees reasonably well with the 1.5 to 1.8 Torr predicted by (III-1). Higher gas fills would be used in practice to slow down any sputtering cleanup of gas.

The degree of loss in power due to mode selection is indicated in Fig. III-7. For the mirror radii shown, approximately 20% reduction in output occurred from TEM_{10} to TEM_{00}. This effect is even smaller in the smaller bore (1.5 mm) tubes measured later in the program and proposed for the metal-ceramic design.

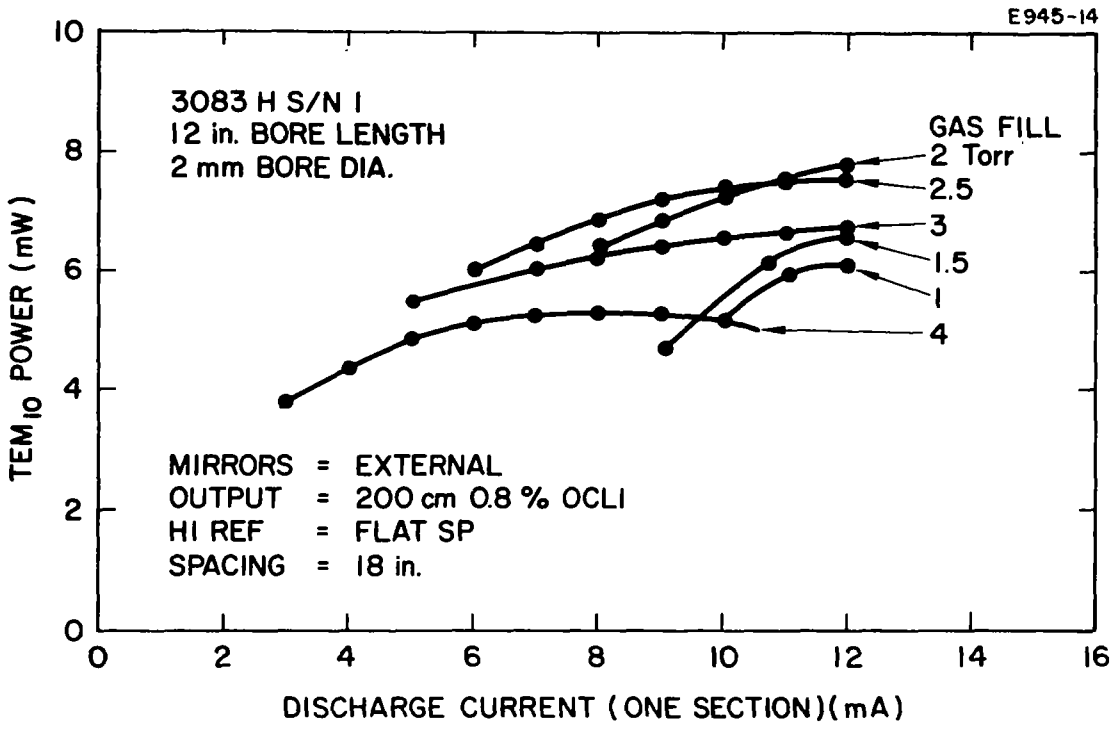

Fig. III-5. Measured power output as a function of discharge current for a 3083H glass tube (No. 1).

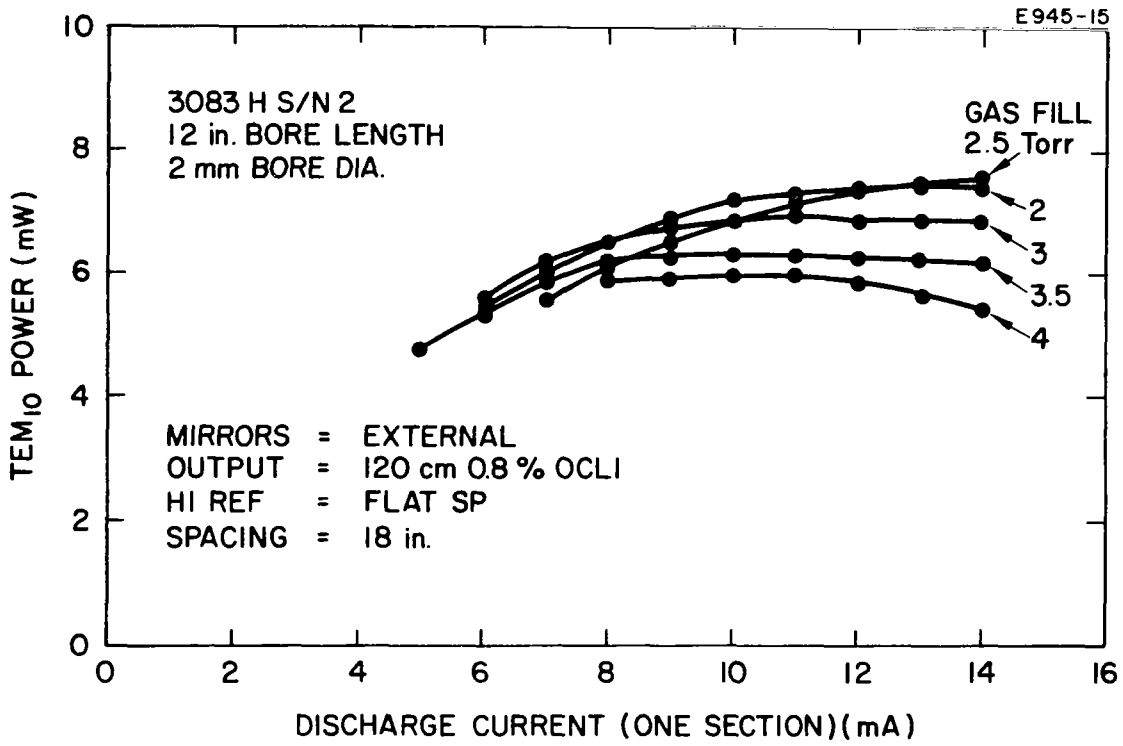

Fig. III-6. Measured power output as a function of discharge current for a 3083H glass tube (No. 2).

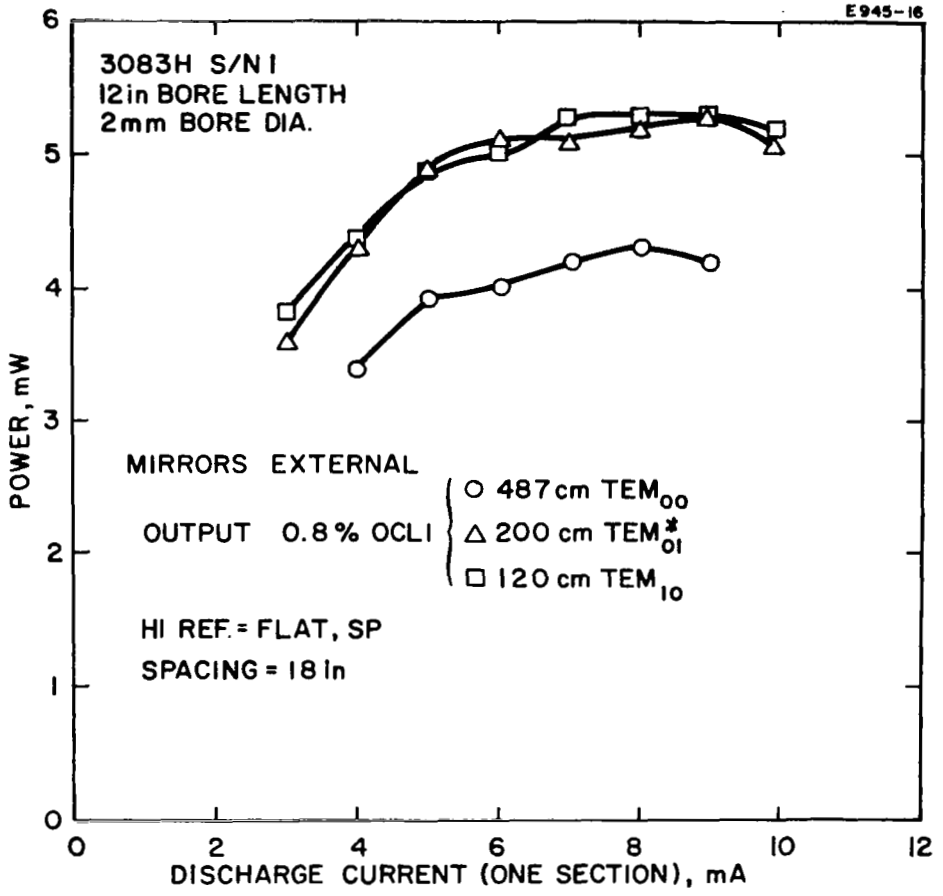

Fig. III-7. Measured output power for TEM_{00}, TEM^{*}_{01}, TEM_{10} modes for tube 3083H (No. 1).

Because we had realized 6 to 8 mW output in our early external mirror tubes, we felt that it would be proper to reduce the over-all tube length by 25%. The additional power needed to realize 5 mW output in the smaller bore length (9 in.) would be made up by using a smaller bore diameter and internal mirrors. Figures III-8 and III-9 confirm these conclusions. Figure III-8 shows the results obtained with a 3083H shortened from 12 in. to 9 in. active bore length and diameter decreased from 2 mm to 1.5 mm, but used with Brewster's angle windows. A maximum output of ≈ 4 mW was obtained, with the optimum pressure increasing and the optimum current decreasing in the proper ratio. Figure III-9 shows the effect of using the same mirrors and tube, but with the Brewster's angle windows removed and the mirrors epoxied directly onto the tube ends. Approximately 5.5 mW output is obtained with the best mirror combination. It is interesting to note that the theory predicts an optimum mirror transmission $\geq 2\%$ for the loss range from 0.4% to 2%, while the experiment indicates that the power actually decreased when the transmission increased from 1% to 1.8%. Both mirrors were manufactured by Spectra-Physics, but it is possible that they have substantially different losses.

A comparison of output powers obtainable from the short 3083H type tubes at 0.6328, 1.15, and 3.39 μ is given in Fig. III-10. Slightly over 50% of the 0.6328 μ power is available at 1.15 μ and slightly under 50% is available at 3.39 μ. We do not know how closely these mirror transmissions approached the optimum values.

C. LITERATURE REVIEW AND STATE-OF-THE-ART SUMMARY

No special literature search was made for this program since all personnel were actively engaged in development on helium-neon lasers at the program inception and were thoroughly familiar with publications in the field. A summary of the theory and scaling laws associated with He-Ne lasers was given in our proposal. The key publications on laser theory and scaling laws are Refs. III-1, III-2, and III-5 through III-10. Useful survey papers have also been written by Haisma (Ref. III-1) and Allen and Jones (Ref. III-12). Few good papers on technological problems have appeared; of those published, the most interesting are the papers on cold cathodes by Hochuli and Haldemann (Ref. III-13) and life limitations in rf excited He-Ne lasers by Turner, et al. (Ref. III-14). (The conclusions reached in Ref. III-14 are not all in agreement with unpublished observations on rf excited He-Ne made at Hughes Research Laboratories, particularly regarding cleanup rates with different wall materials.)

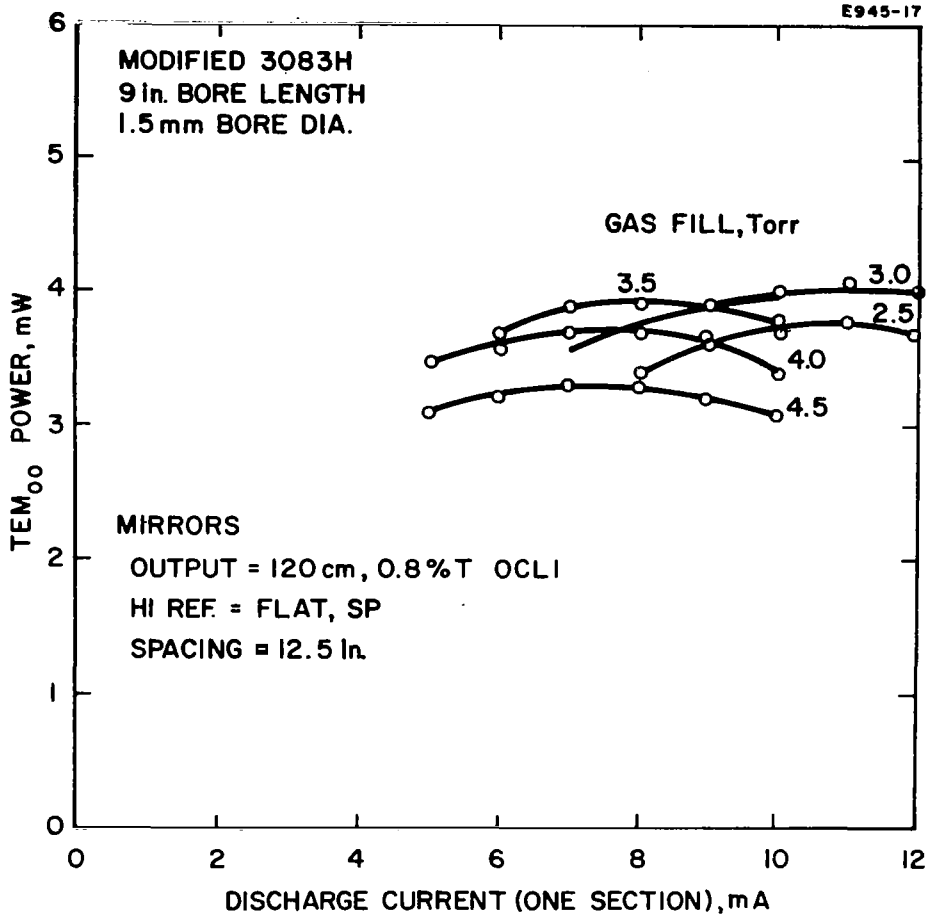

Fig. III-8. Measured TEM_{00} power output for a short (9 in.) bore 3083H.

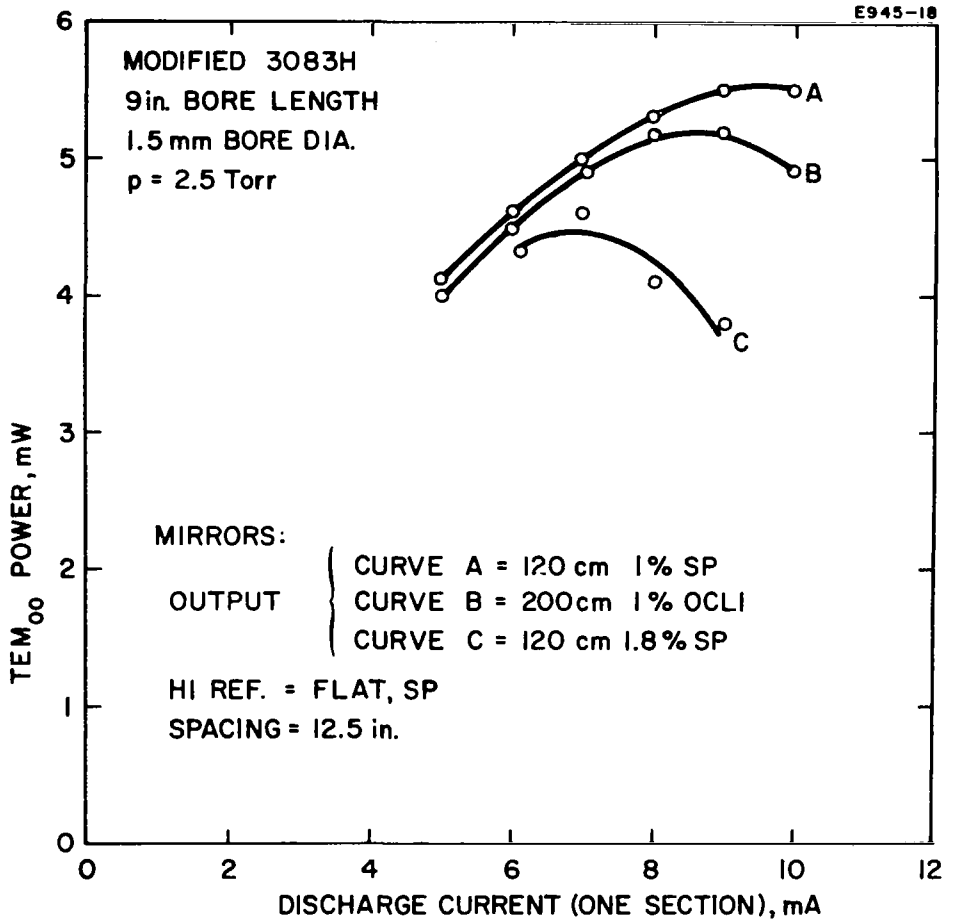

Fig. III-9. Measured TEM_{00} power output for a short (9 in.) bore 3083H with different radius mirrors.

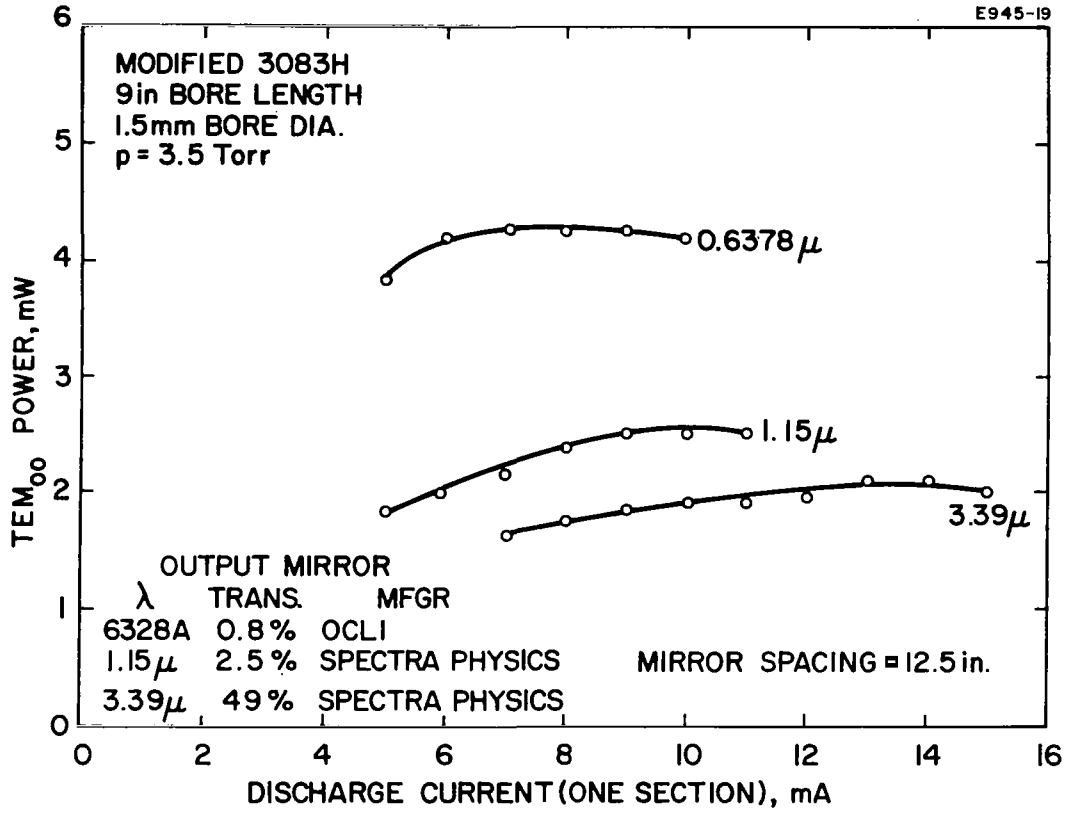

Fig. III-10. Measured TEM_{00} output from a short (9 in.) bore 3083H at 0.63μ, 1.15μ, and 3.39μ.

The state of the art in helium-neon lasers was assessed both from journal articles and also from commercial advertising brochures. Table III-1 summarizes the salient characteristics of commercially available He-Ne lasers, both foreign and domestic, with TEM_{00} outputs in the range 1 to 10 mW. Direct comparison with the proposed SQL design is difficult because none of the lasers listed were designed for 5 mW output, space environment, or spacecraft power supply characteristics. The most notable is the Soviet ЛГ-56, with 2 mW TEM_{00} output and a laser head weight of 2.65 lb. The descriptive brochure states that the laser "... is characterized by high resistivity to mechanical effects and to ambient temperature changes and can be used under conditions of considerable dust and moisture content." Furthermore, a temperature range of -30^{o} to $+40^{o}$C is quoted and dynamic mechanical limits of 4.5 g vibration (20-80 Hz), 15 g repeated shock, and 75 g single shock are quoted. "Precision light ranging" is mentioned as a possible application in the brochure. It is only recently that U.S. manufacturers have been concerned with the development of lasers for surveying and equipment guidance.

It is evident from the specifications given for the proposed Hughes 3072H SQL that it exceeds the commercial state of the art in specific power output per unit length, power output per unit weight, efficiency, and life. While somewhat greater powers have been observed in laboratory versions of this length, we believe the proposed 3072H design specifications represent a realistic and reproducible set of operating characteristics obtainable in severe environments.

D. SUMMARY OF VISITS TO NASA FACILITIES

Conferences were held with (1) NASA Headquarters, Washington, D.C.; (2) Electronic Research Center, Cambridge, Massachusetts; (3) Marshall Space Flight Center, Huntsville, Alabama; and (4) Manned Spacecraft Center, Houston, Texas, during the fifth month of Phase I. The purpose of these meetings was to solicit suggestions concerning the laser performance specifications, environmental conditions, and physical configuration as these factors pertain to definitive requirements. The proposed laser specifications and design approach were reviewed, and an operable prototype for the tentative design was demonstrated. The following NASA personnel were in attendance at the above listed centers.

1. NASA Headquarters, Washington, D.C.

H. L. Anderton
J. Meson
H. Fosque
H. H. Plotkin

TABLE III-1

Commercial Laser Characteristics

Manufacturer	Model Number	Power		Head		Power Supply		Life	Input Power, W	Brochure Date	$\frac{TEM_{00}\ Power,\ mW}{Length,\ in.}$
		TEM_{00}, mW	TEM_{mn}, mW	Weight, lb	Size L x D or L x W x H (in inches)	Weight, lb	Size, in.				
CSF	F9094	1	2	2.65	13.4 x 2.4	14	?	?	?	1967	0.075
EIMAC	300	1	-	?	14.5 x 1.9	?	12.8 x 13.8 x 9	2000 hours	165	1966	0.069
EIMAC	303	3	-	?	25 x 1.9	?	12.8 x 13.8 x 9	2000 hours	165	1966	0.12
EOA	LAS102	1	2	3	13.5 x 2	?	?	2000 hours	?	1966	0.074
Ferranti	GP-2	1	-	11	20.3 x 5.4 x 6.2	included in head		500 hours	?	1967	0.049
Ferranti	SL-5	2.5	-	6.6	18 x 3.5 x 2.9	20	?	500 hours	?	1967	0.139
Jodan	GL-60	3	-	?	>22	?	?	?	?	1967	<0.136
OTI											
Perkin-Elmer	5600	1.3	-	5.5	17.5 x 2.25	20	12 x 6 x 14	1 year	80	1967	0.074
Perkin-Elmer	5300	8	15	34	36 x 4	20	12 x 6 x 14	1 year	?	1965	0.222
Quantum Physics	LS-30	1.5	4	10 total	13 x 3 x 4.5	included in head		1 year	?	1967	0.116
Quantum Physics	LS-31	2	6	14 total	>14 x 1.75	-	4.5 x 8 x 7	1 year	?	1967	<0.143
Quantum Physics	LS-35	7	15	18 total	>24 x 2.5	-	4.5 x 8 x 10	1 year	?	1967	<0.292
Radiation Physics	RPI-75	7	-	15 total	24 x 2	-	3 x 6 x 8	1 year	?	1967	0.292
Siemans	LG-64	1	10	11	26.2 x 5.1 x 4.8	28	14.4 x 7.5 x 7.4	1000 hours	?	1966	0.038
Spectra Physics	122	3	-	10	16 x 3.3 x 3.3	4.5	4.2 x 3 x 12	1 year	125	1967	0.188
Spectra Physics	123	7	-	15	22 x 3.3 x 3.3	4.5	4.2 x 3 x 12	1 year	180	1967	0.318
U.S.S.R	ЛГ-56	2	-	2.65	13.7 x 2.3	11	11.7 x 5.9 x 5.9	500 hours	66	1966	0.146
	ЛГ-126	10	-	31	37 x 5.7	44	20.5 x 13.8 x 11.4	500 hours	500	1967	0.27
Hughes	3072H	5	-	11	16 x 3 x 8	included in head		10,000	30	1968	0.313

2. Electronic Research Center, Cambridge, Massachusetts

P. Hanst
R. Paananen
P. Fletcher
J. Morneal
J. Early
P. Ryan
T. Lawrence
W. Laurie
S. Korp

3. Marshall Space Flight Center, Huntsville, Alabama

P. Marrero
E. Reinbolt
D. Lee

4. Manned Spacecraft Center, Houston, Texas

D. Lilly
R. Hotz
R. Kelly
E. Walters
H. Erwin
S. Derry

Hughes personnel making the presentation were

W. B. Bridges (Project Manager)
R. A. Brenan
W. P. Kolb
A. G. Peifer
T. Hummel (at ERC, MSFC, MSC)
C. J. Eliades (at ERC)
J. Juncker (at MSFC)
C. McKinney (at HQ)

A copy of the Hughes proposal and a questionnaire were submitted to the above centers for review prior to the meetings. It was hoped that future requirements for a space He-Ne laser could be tentatively defined as to the performance and environmental conditions.

Only a little information on future specifications was available, however, since the specific space projects discussed were not far enough along to generate firm specifications. As pointed out in Appendix A, each mission will generally define a special set of requirements if the mission goals are specified in advance of the component development. Table II of Appendix A lists the environmental specifications for many of the space traveling-wave tubes built by the Electron Dynamics Division of Hughes Aircraft Company. However, it is believed that the goals set forth for this program are realistic and once the laser is qualified, many space experiments can be designed around the laser specification.

In reviewing the proposed design, the following comments were discussed. All centers were in agreement that the two-anode design approach which makes possible power supply redundancy was a good feature. This feature allows operating the laser at reduced power upon command and can be used to perform certain experiments. In addition, for communication experiments, consideration should be given in the future to a means of modulating the optical output. This is discussed in Section II-C.

The operational temperature range specified in Exhibit D of the RFP from -107°C to +150°C could be relaxed for any projected applications. The recommended temperature range based upon prior experience is a deviation of 50°C, as indicated in Table II of Appendix A. However, the center temperature of this 50°C will vary from mission to mission.

The operational model demonstrated at the centers was representative of the design approach. Refinement of this design has resulted in reduction of the over-all package length to 16 in. and a square cross sectional outline. A rectangular cross section is proposed as an alternative. It was the general feeling that a square cross-sectional package would probably be more suitable for integrating with the spacecraft.

E. CONTACTS WITH NON-NASA PERSONNEL

In private conversations with W. B. Bridges, E. I. Gordon of Bell Telephone Laboratories reported that life tests are continuing there on both hot and cold cathode He-Ne lasers. Elapsed time on these lasers is in excess of 5000 hours.

A conference was held at EDD with T. Musset and D. Morelli, Optical Coating Laboratories, to discuss hard coated ultraviolet-resistant mirrors for use in internal mirror lasers. Such mirrors have been subjected to experiments at OCLI to verify initial operation and have been found satisfactory. Subsequently, we obtained samples of these coatings from OCLI and have also found them satisfactory.

Dr. U. Hochuli, University of Maryland, was visited by A. G. Peifer to discuss results of the extensive cold cathode experiments being performed there. The experiments are essentially an extension of those reported at the conference on Laser Engineering and Applications, Washington, D.C., June 1967. The results, although pertaining to aluminum cathodes, certainly add validity to the proposition that cold cathode He-Ne lasers can have extremely long life. This is also verified by Hughes life tests using cold cathode devices.

F. LIFE TESTS AND CATHODE STUDIES

At the beginning of the program, life tests were already under way on the Hughes Model 3082H tubes, shown in Fig. III-11. This tube is manufactured by Hughes for the K &E alignment laser. The cold cathode used in this tube is oxidized tantalum hollow cathode structure which had proven reliable in several previous tube designs. The proposed SQL design required approximately twice the active bore length, so that a structure consisting of two 3082H tubes joined at the open end of the cathode (left end on Fig. III-11)was proposed. The resulting glass tube, now designated type 3083H, is shown in Fig. III-12. Eight such tubes were fabricated on the program: SQL s/n-1 through s/n-6, and 3083H s/n 1 and 2. In addition, two modified 3083H tubes (identical to that in Fig. III-12 but 3 in. shorter) were built. Of these tubes, SQL s/n 2, s/n 3, s/n 4, and s/n 6 were placed on life test during the contract term. The over-all results are summarized in Table III-2.

The 3082H tubes are all still operating with no change in V-I or laser output characteristics (except for s/n 13, which apparently developed a leak). The SQL (3083H type) tubes all failed on life test in 400 to 1300 hours because of gas cleanup. Spectroscopic examination of the discharge after laser action had ceased proved that no contaminants were present – only helium and neon emission lines were seen. These four tubes were subsequently taken apart and the cathodes were examined. It was quite evident from a visual examination of the inside of the cathode can that insufficient oxidation of the surface had occurred during the processing cycle. Consequently, the cathodes had sputtered at the rate determined by pure tantalum, and gas cleanup occurred in a short time. (The 160 hour life of s/n 3 probably can be attributed to an experimental cathode configuration which has subsequently proven unsatisfactory.) To confirm that the lack of proper oxidation occurred during the process cycle and not by removal during tube operation, 3083H type cathodes were run through the normal process cycle and then cut open without being run in a discharge tube. The insides of the cathodes were usually shiny metal, with no trace of the dull grey surface charactistic of the properly oxidized surface. We conclude that the change in geometry introduced by closing both ends of the cathode can prevented adequate oxidation of the inner surface when processed with the 3082H process cycle. A special fixture was made to assure oxygen entry into this region, but no cathodes have yet been processed with the new schedule and equipment. It is quite clear from the successful operation of the 3082H tubes that proper cathode processing will result in a life greater than 7000 hours.

M 5920

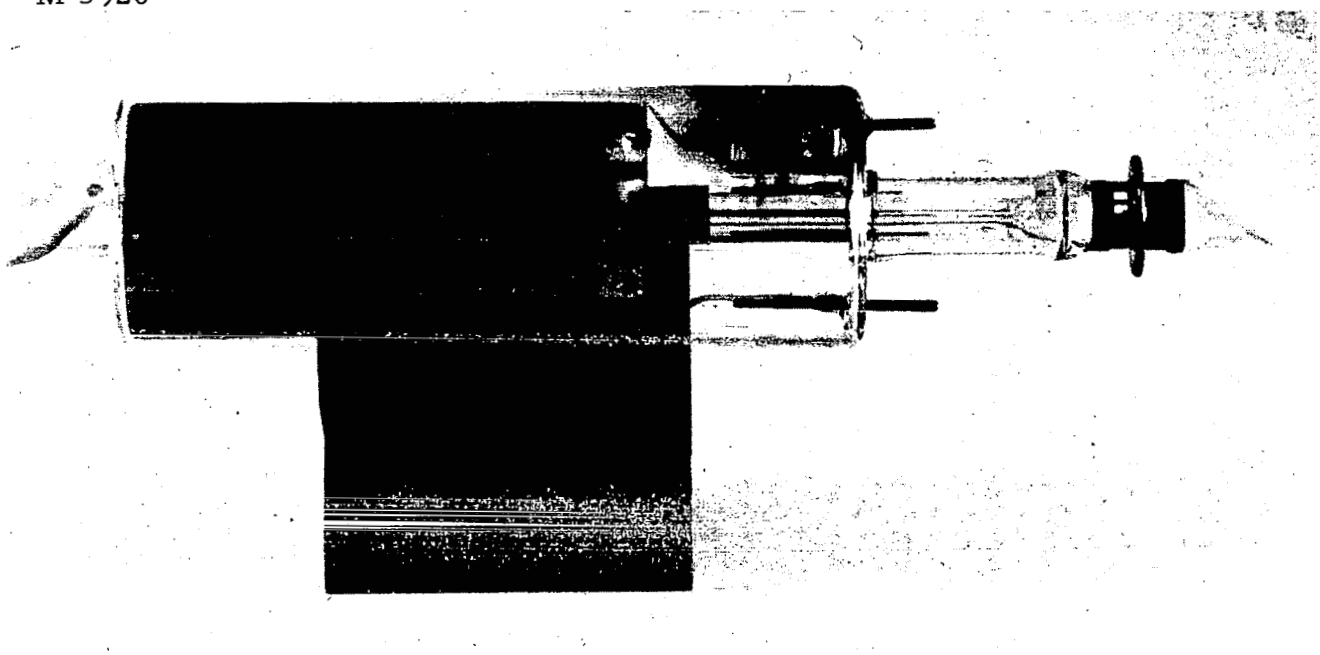

Fig. III-11. Hughes Model 3082H discharge tube.

M 5919

Fig. III-12. Hughes Model 3083H discharge tube

TABLE III-2

Life Test Results (to 18 January 1968)

Type	S/N	Feature	Status	Hours	Comment
3082H	5	-	Running	7062	No change
3082H	13	-	Failed	1450	Contamination, Dev. Leak.
3082H	25	-	Running	2872	No change
3082H	27	Current Mod. at 10 kHZ	Running	2801	No change
3082H	43	-	Running	521	No change
SQL	2	-	Failed	1347	Gas cleaned up
SQL	3	Reentrant Cathode	Failed	161	Gas cleaned up
SQL	4	Ceramic Bore	Failed	404	Gas cleaned up
SQL	6	-	Failed	435	Gas cleaned up

A vibration shake test was also run on two additional type 3082H tubes to insure that the cantilever bore was not a weak point. Both tubes survived sinusoidal vibration in three mutually perpendicular axes at 0.2 in double amplitude in the range 5 to 30 Hz, and 8.6 g in the range 30 to 2000 Hz. The vibration frequency was swept up and back at a rate of 1 octave/min. In addition, vibration was continued for 2 min at each main resonance. One tube suffered a spotweld failure at a cathode lead. We may conclude that the cantilever bore (which will be even shorter and better supported in the 3072H) will cause no problems.

G. MIRROR MEASUREMENTS AND FABRICATION TECHNIQUES

It is quite evident from Figs. III-1 and III-3 that obtaining dielectric coated mirrors with the lowest possible losses is crucial to the realization of a high performance laser. For this reason, we

attempted to compare the best mirror coatings for their performance, both in external mirror lasers and internal mirror lasers. The latter test was necessary to determine if the discharge ultraviolet or other possible discharge agents would degrade the mirror performance with operation. The problems of ultraviolet mirror degradation were discussed at length with Dr. T. Musset of Optical Coating Laboratories, Inc., Santa Rosa, California, who recently has been concerned with mirror development for internal mirror He-Ne lasers. OCLI has developed special ultraviolet-resistant coatings for such lasers which, at the same time, retain the "hardness" and durability of the standard TiO_x-SiO_x coatings. Normal and ultraviolet-resistant hard coatings were obtained from OCLI and soft coatings from Spectra-Physics, Mountain View, California, for evaluation. Table III-3 lists the characteristics of the mirrors compared. The last five mirrors in the list are dielectric-coated Brewster's angle half-prisms of the type proposed for the final design. The remaining mirrors were coated on standard 15 mm diameter by 11 mm thick fused-silica substrates.

It would have been most desirable to have a full range of transmissions and radii of curvature from each manufacturer so that mirror loss alone could be compared. Considerations of economy and delivery time limited our selection somewhat to mirrors and substrates on hand or readily available. Because of the variability of transmission in the Spectra-Physics commercial coatings, we were able to cover a somewhat larger range of transmissions than we originally thought. Figure III-13 compares output powers for a few of the mirrors measured. It would appear that about 1% transmission was the optimum value for this laser; however, such a conclusion would require that the losses in the mirrors compared all were equal and that the same cavity mode oscillated each time. For 200 and 300 cm mirrors the modes were similar and of the order of TEM_{20} in a 3 mm tube. The higher power output of the 120 cm mirrors shown on Fig. III-13 results from the larger filling factor of the TEM_{40}-TEM_{50} modes typical in a 3 mm tube. These experiments were performed with the test rig shown in Fig. III-14 (tube SQL s/n-1 in place) which could be run as an internal mirror laser or Brewster's angle window laser. The latter arrangement was used for most of the comparisons; the internal-mirror comparisons reported in Section III-B were all made with sealed-off tubes.

From several intercomparisons of both output and high reflectance mirrors, we determine that the best hard coatings, both normal and ultraviolet-resistant, performed as well as the best soft coatings. Both produced satisfactory output power (better power per unit length than the best lasers listed in the state-of-the-art survey, Section III-C).

The coated prisms were also compared among themselves and with dielectric-coated flat mirrors. A typical comparison is shown in Fig. III-15. From these and other runs we conclude that the best coated prisms are almost as good as the best flat mirrors and would

TABLE III-3

Mirror Characteristics

S/N	MFGR	Radius, cm	Trans. Nom., %	Trans. Meas., %	Comment
314	OCLI	200	0.7	0.6	Normal, hard coating
315	OCLI	200	0.7	0.6	Normal, hard coating
318	OCLI	∞	< 0.01	< 0.01	Normal, hard coating
SP-A	SP	300	1.6	2.0	Commercial, soft coating
SP-B	SP	300	1.6	2.3	Commercial, soft coating
SP-C	SP	∞	0.05	< 0.1	Commercial, soft coating
SP-D	SP	∞	0.05	< 0.1	Commercial, soft coating
SP-E	SP	120	0.5	1.0	Commercial, soft coating
SP-F	SP	120	0.5	0.7	Commercial, soft coating
SP-G	SP	300	1.6	1.5	Commercial, soft coating
SP-H	SP	300	1.6	2.4	Commercial, soft coating
0-1	OCLI	200	1.0	-	UV-Resistant, hard coating
0-2	OCLI	∞	1.0	-	UV-Resistant, hard coating
0-3	OCLI	200	1.0	-	UV-Resistant, hard coating
0-4	OCLI	487	1.0	-	UV-Resistant, hard coating
0-5	OCLI	∞	0.001	-	UV-Resistant, hard coating
0-6	OCLI	∞	0.001	-	UV-Resistant, hard coating
0-7	OCLI	∞	0.001	-	UV-Resistant, hard coating
0-8	OCLI	200	0.001	-	UV-Resistant, hard coating
SP-X	SP	∞	0.05	(prism)	Normal, soft coating
SP-Y	SP	∞	0.05	(prism)	Normal, soft coating
SP-Z	SP	∞	0.05	(prism)	New type, hard coating
0-X	OCLI	∞	< .01	(prism)	UV-Resistant, hard coating
0-Y	OCLI	∞	< .01	(prism)	UV-Resistant, hard coating

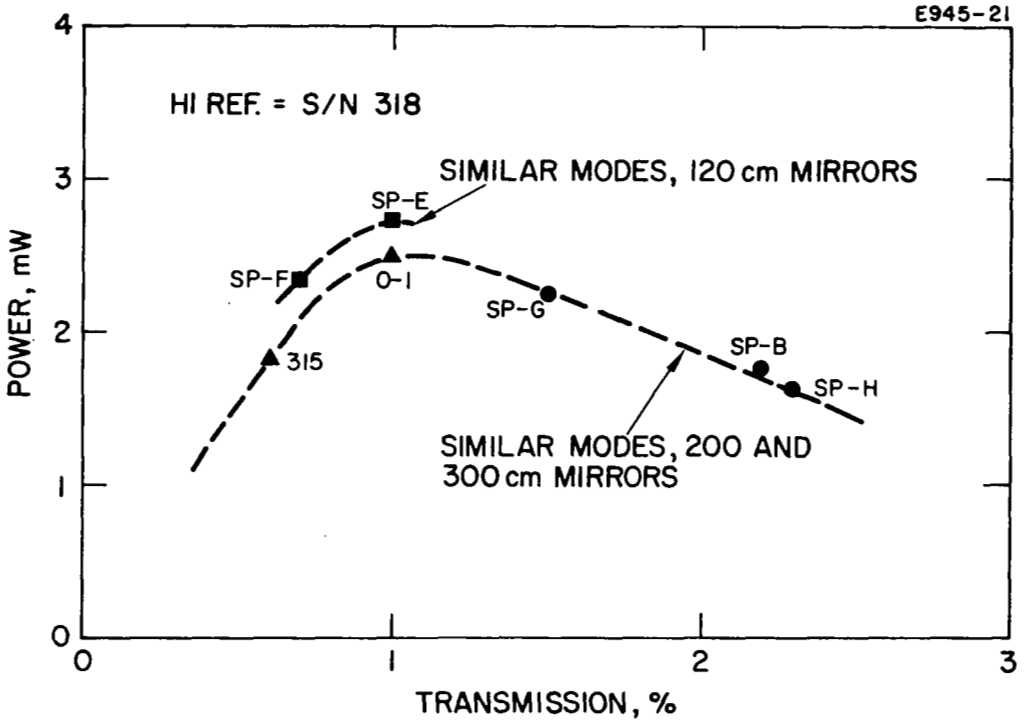

Fig. III-13. Output power as a function of mirror transmission (tube SOL S/N 1).

M 5713

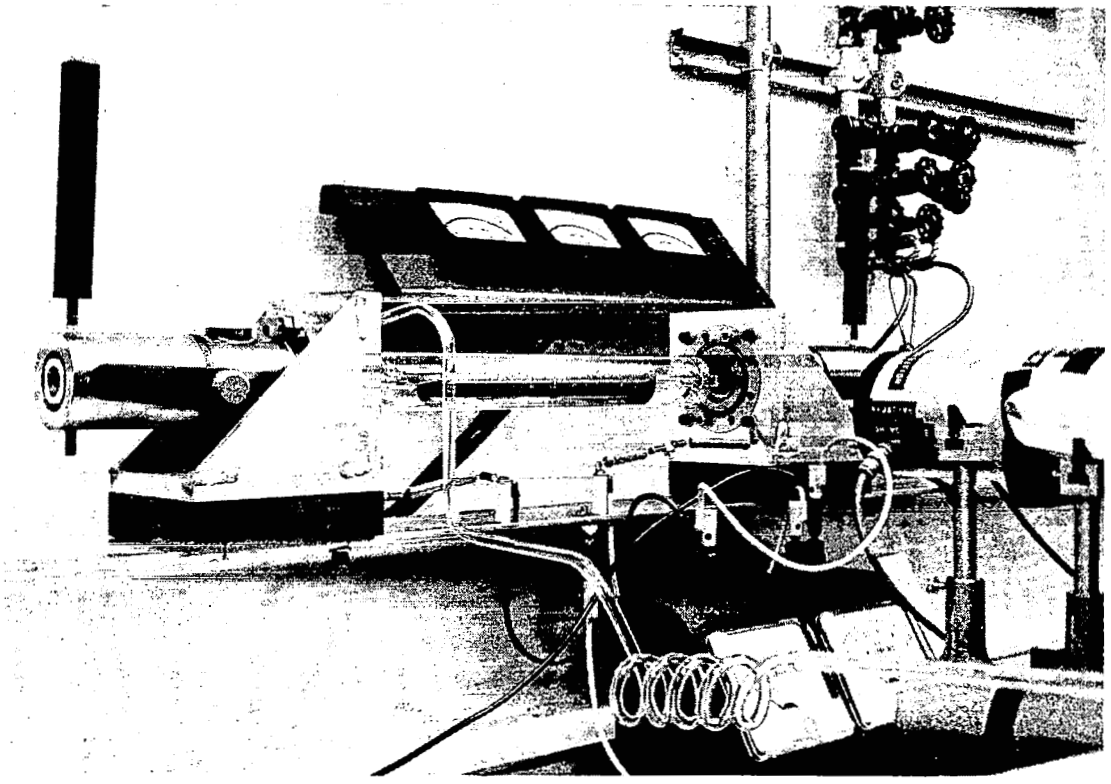

Fig. III-14. Mirror test laser used at beginning of program. Tube shown is SQL S/N 1.

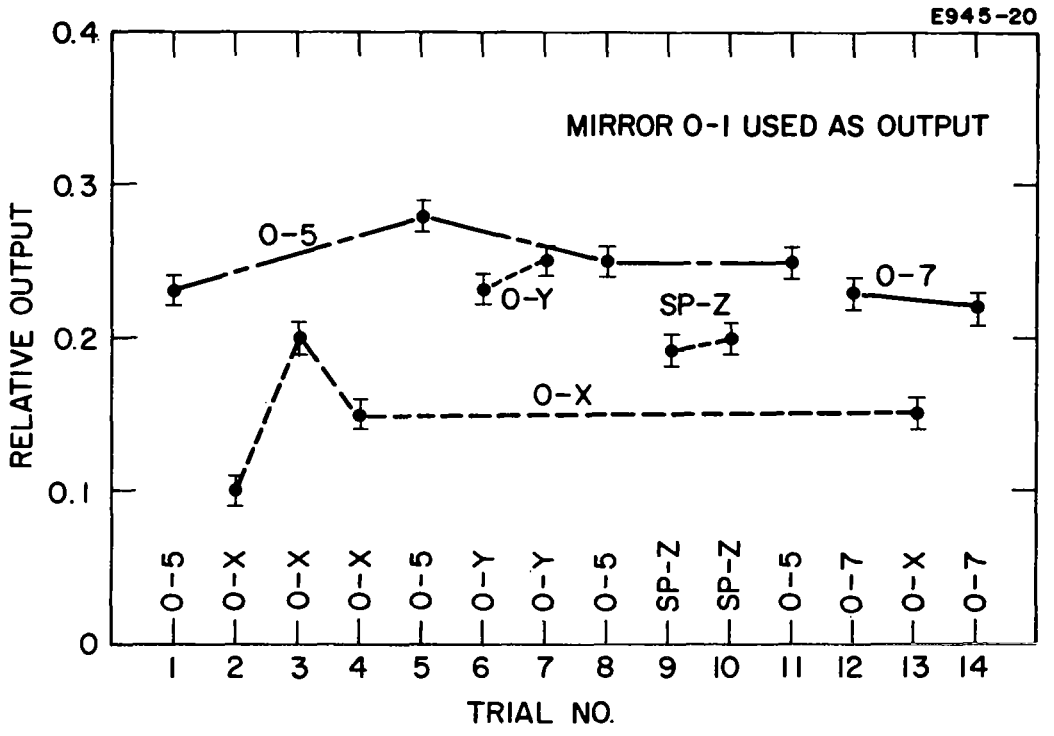

Fig. III-15. Relative output for several mirrors and coated Brewster angle half-prisms. Measurements were all taken in the sequence shown to assure no changes in output from sources other than mirror loss.

undoubtedly be better than a flat mirror-plus-Brewster's angle window. We had hoped to make this last comparison directly, but did not have sufficient time.

In addition to verifying satisfactory operation of existing coatings, a technique was worked out for sealing the output mirror (or window) onto the laser without the need for epoxy or other cement. The technique developed allows heliarc welding of the mirror onto the completed metal-ceramic tube as the final assembly step, thus assuring the cleanest possible tube and mirror surfaces. Figure III-16 shows a cross section drawing and a picture of the mirror blank. In this technique, a plug of Corning 7052 Kovar sealing glass is wetted onto a Kovar eyelet, and then both front and back surfaces are ground and polished. After coating, the Kovar flange is heliarced to a similar flange on the completed metal-ceramic envelope. Sixteen mirror blanks were fabricated in this manner; several were examined for strains or distortion in a Twyman-Green interferometer after polishing and also after welding to the vacuum test fixture shown in Fig. III-17. No distortion was observed in any case. Ten blanks were sent to OCLI for grinding (to 200 cm spherical surface) and coating. Unfortunately, these mirrors were not received in time to be compared for output power with the other mirrors used in the test rig. However, these metal-to-metal mirrors are being used on the metal-ceramic envelope now being assembled.

An alternative technique was also investigated and found satisfactory (although somewhat more bulky). Figure III-18 shows a cross section view of a mirror assembly fixture using a metal V-seal* used in checking this concept with a quartz flat. A calculated compression in the V-ring is achieved by close control of the fixture dimensions. The spring metal base of the V-ring maintains this pressure even under wide temperature variations, while the ductile metal plating on the ring supplies the seal. We feel this method is a satisfactory alternative to the heliarced mirror, although it requires a somewhat more massive structure to handle the compressive forces. The V-seal also would be attractive in lasers requiring mirror substrates other than 7052 glass (for example, the CO_2 laser).

H. POWER SUPPLY TEST RESULTS

The proposed power supply design was discussed in detail in Section II-D. In this section we present test results on a breadboard version of one complete section. (In addition to this breadboard

*Trade name of Parker Metal V-Seal Rings, Parker Seal Company, Culver City, California.

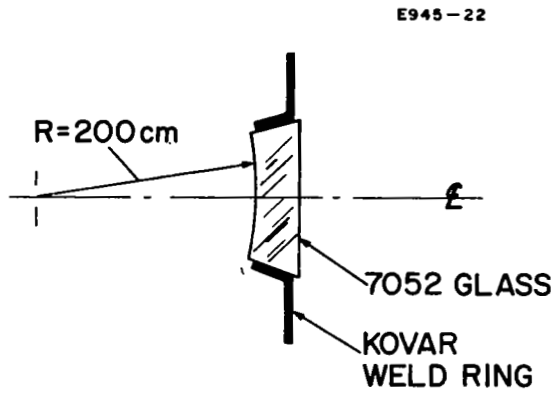

M 5921

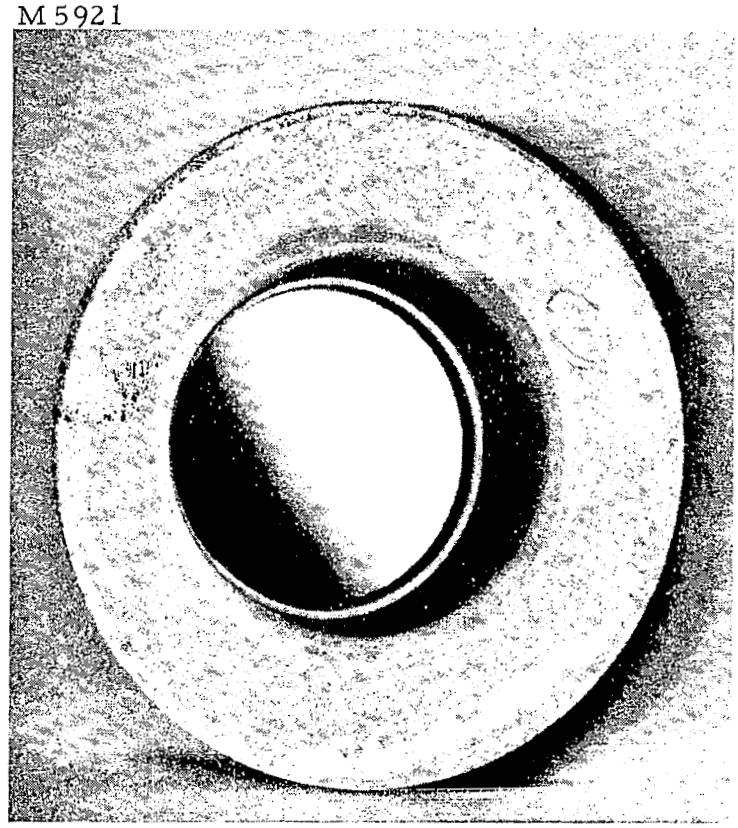

Fig. III-16. Cross section sketch and photograph of metal-to-metal mirror developed under present program.

M 5922

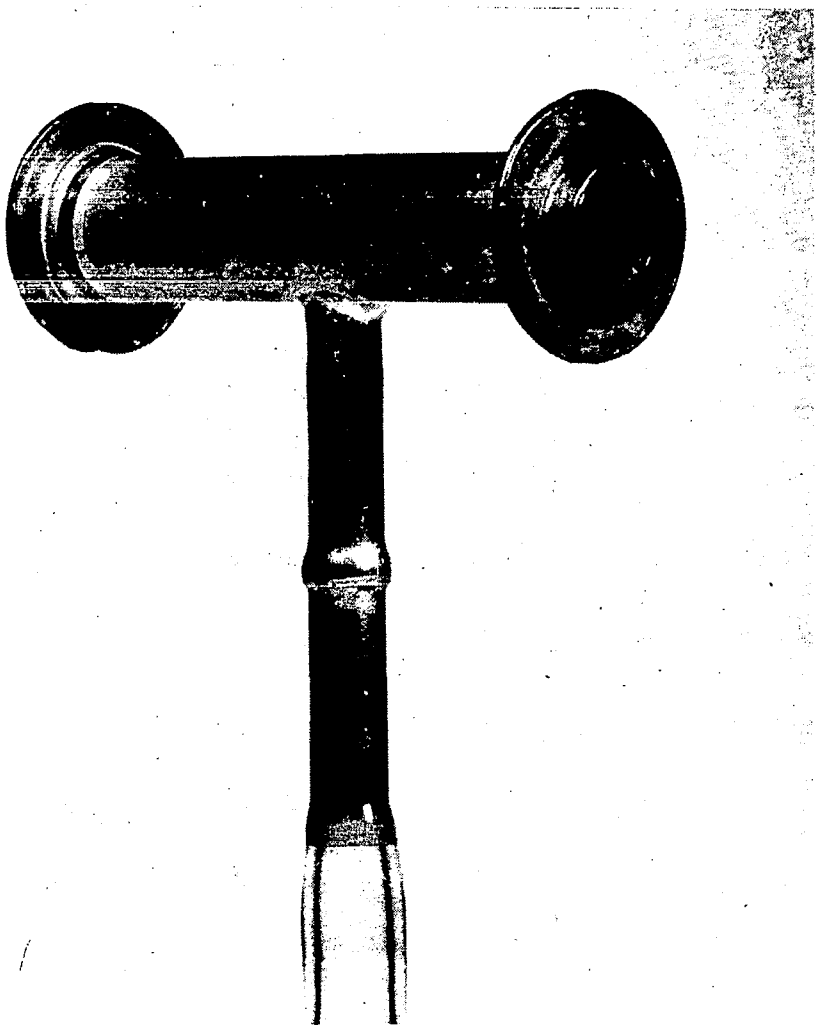

Fig. III-17. Fixture to test welding procedures and vacuum properties of metal-to-metal mirrors.

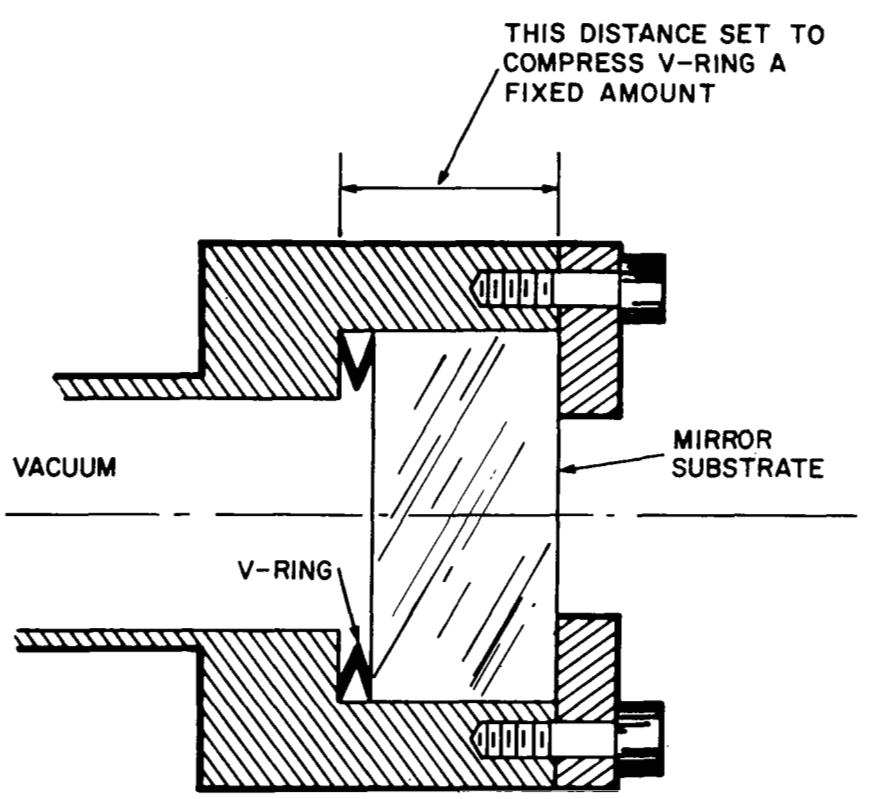

Fig. III-18. Cross sectional view of alternative mirror sealing technique using a compressed metal V-ring.

version, one complete dual power supply was built without the magamp regulators and telemetry circuits and incorporated into the demonstration unit described in the next section.)

Figure III-19 gives the current variation in a resistive load (not the laser) when the input line voltage is changed from 24 to 32 V. Figure III-20 gives the current variation experienced when the value of the resistive load is changed. The probable excursion of the laser impedance during changes in gas pressure during the useful life of the tube is indicated on the figure. Figure III-21 shows the variation of the current in a resistive load with temperature over the range -20°C to +50°C for both high and low line voltages. Figure III-22 shows the same data but with a 3083H laser tube as a load. Evidently the laser discharge characteristics change with temperature and yield better over-all regulation for the combination than for a simple resistive load.

I. PROTOTYPE LASER UNIT

Although not required to build an operating laser by the contract work statement, we felt that the best method of uncovering new critical laser design areas was to build a prototype unit, including laser, cavity support, power supply, and exterior package in the configuration originally proposed. Such a unit was fabricated and demonstrated to NASA personnel in October 1967 (see Section III-E). The demonstration prompted several comments and suggestions. There was general agreement that it would be highly desirable to decrease the over-all length, if possible, from 21 in. to 16 in. We have determined that this is feasible, and our proposed design is now for a 16 in. over-all package length. The prototype did serve to confirm the practicality of our power supply and package design. The laser tube and cavity support were not intended to be exact prototypes because of time and economic limitations: a glass tube with external mirrors was used rather than a metal-ceramic version, and a simple tubular aluminum cavity support system was employed rather than the composite beryllium type proposed. Nevertheless, the prototype worked extremely well while being transported to the various NASA facilities, without mirror or other adjustments being required. Figure III-23 shows the exterior of the laser and Figure III-24 the interior. The over-all dimensions are given in Fig. III-25.

Building the prototype also allowed us to make an accurate weight projection. The measured weight budget for the prototype is given in Table III-4. Using magnesium and beryllium instead of aluminum would have reduced the prototype from 16.1 to 13.4 lb.

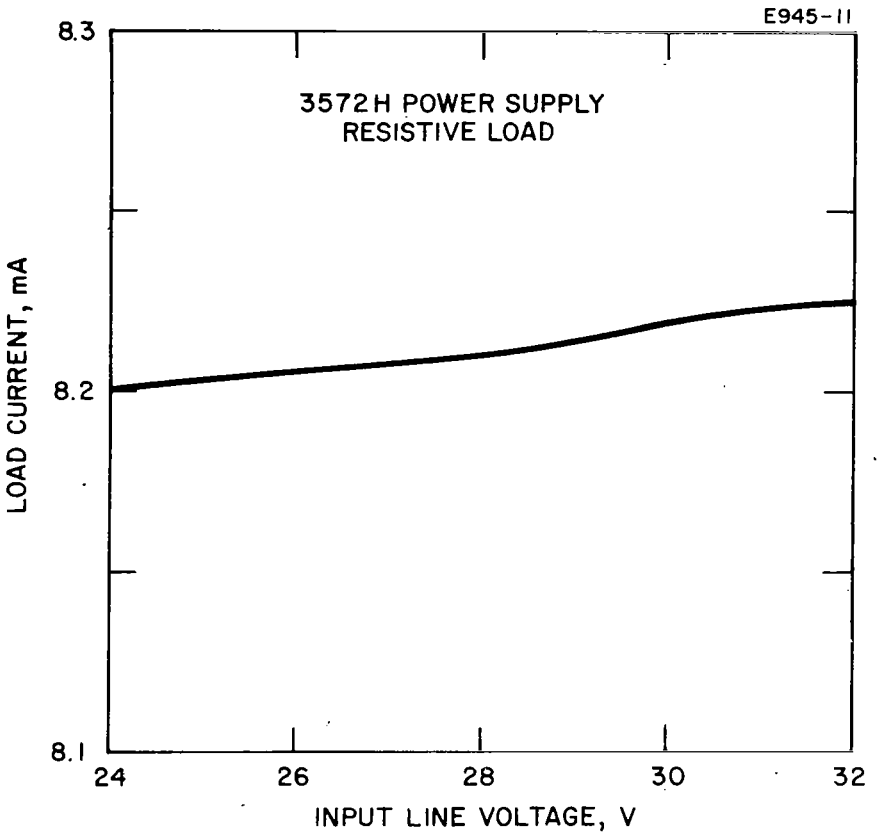

Fig. III-19. Load current variation for input line voltages in the range 24 to 32 V dc.

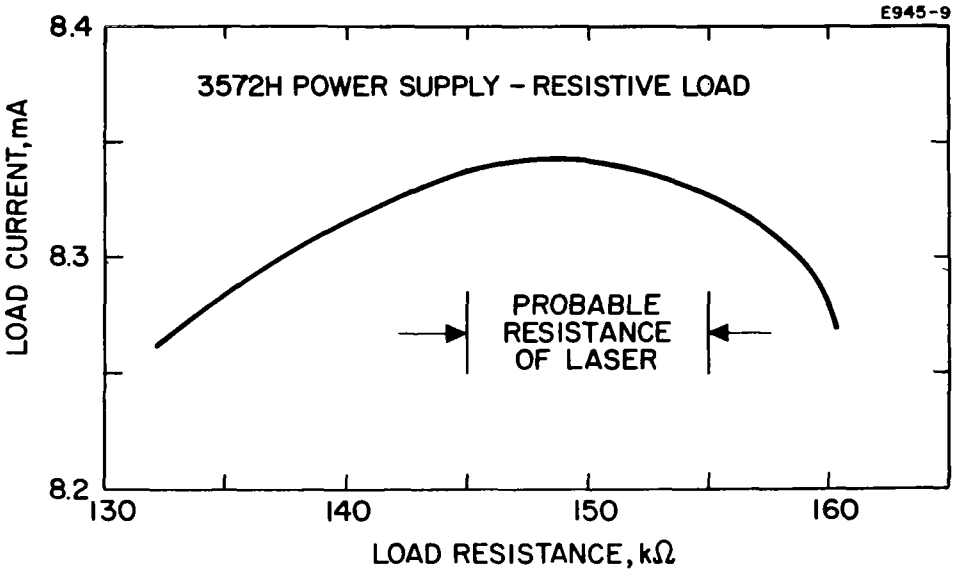

Fig. III-20. Load current variations for load resistances in the range 130 kΩ to 160 kΩ.

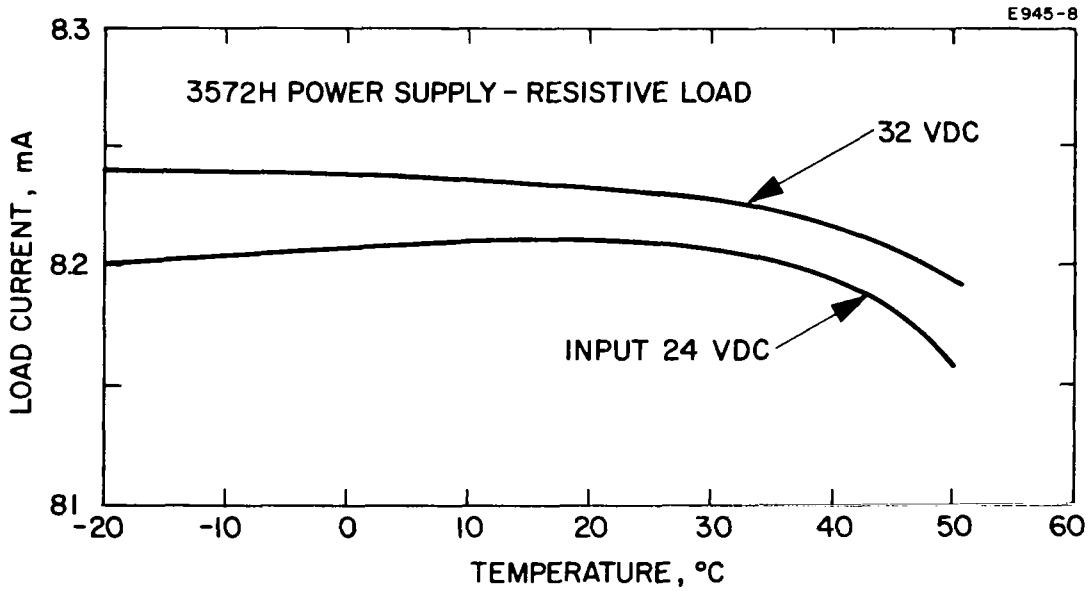

Fig. III-21. Load current variations for temperatures in the range - 20 to +50°C with a resistive load.

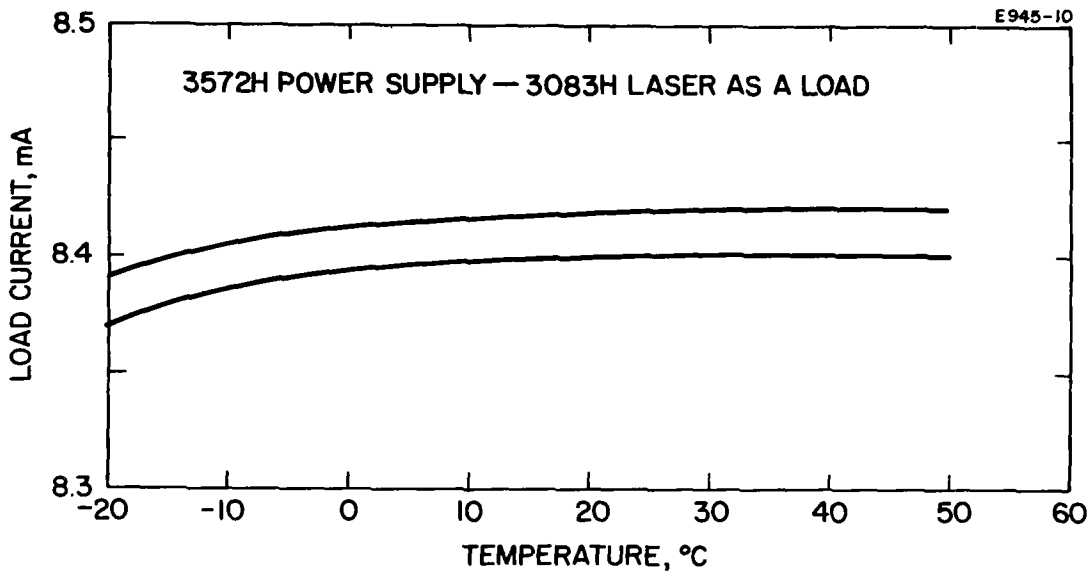

Fig. III-22. Load current variations for temperatures in the range -20 to +50°C with a 3083H laser as load.

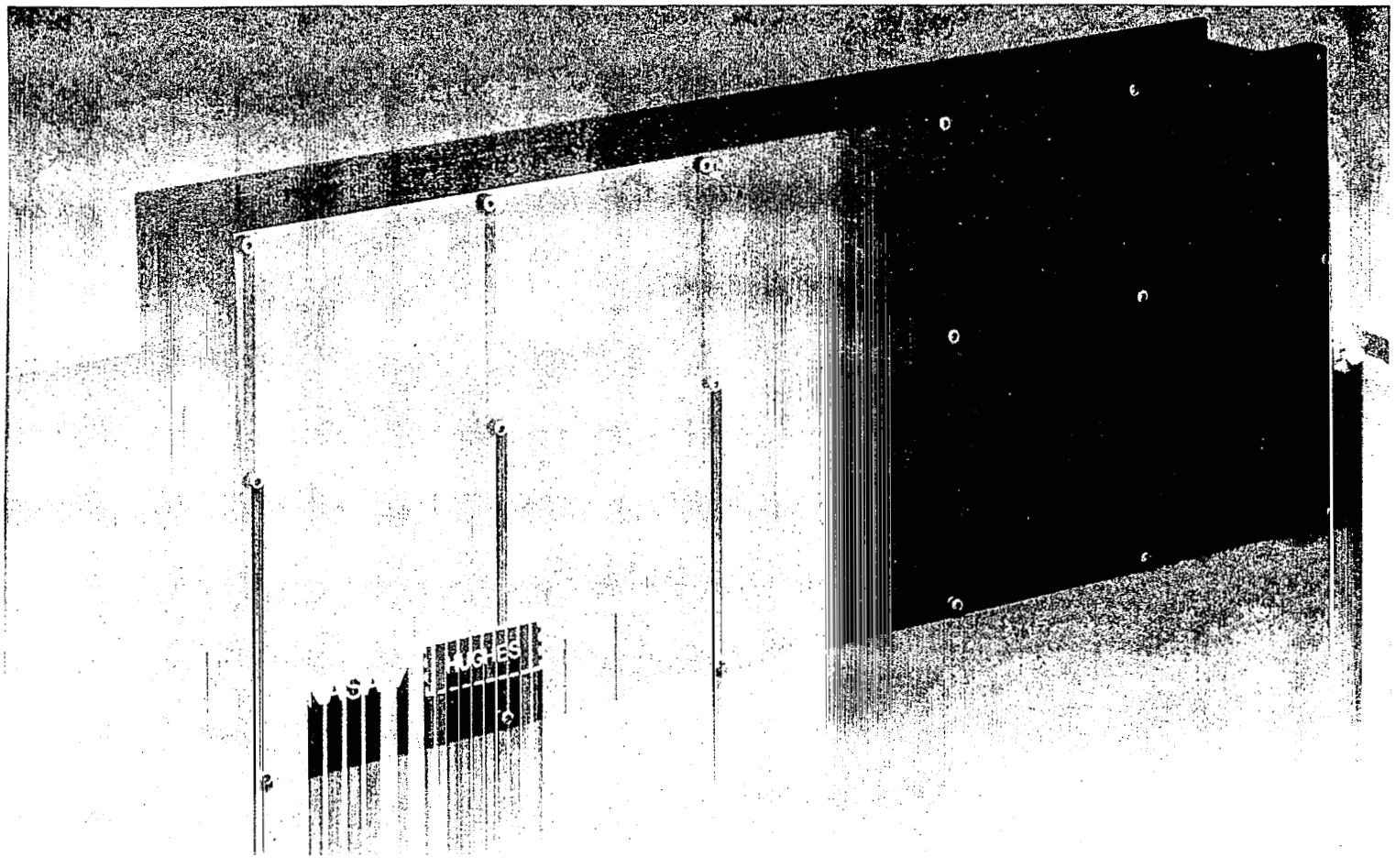

Fig. III-23. Photograph of prototype SQL demonstration unit.

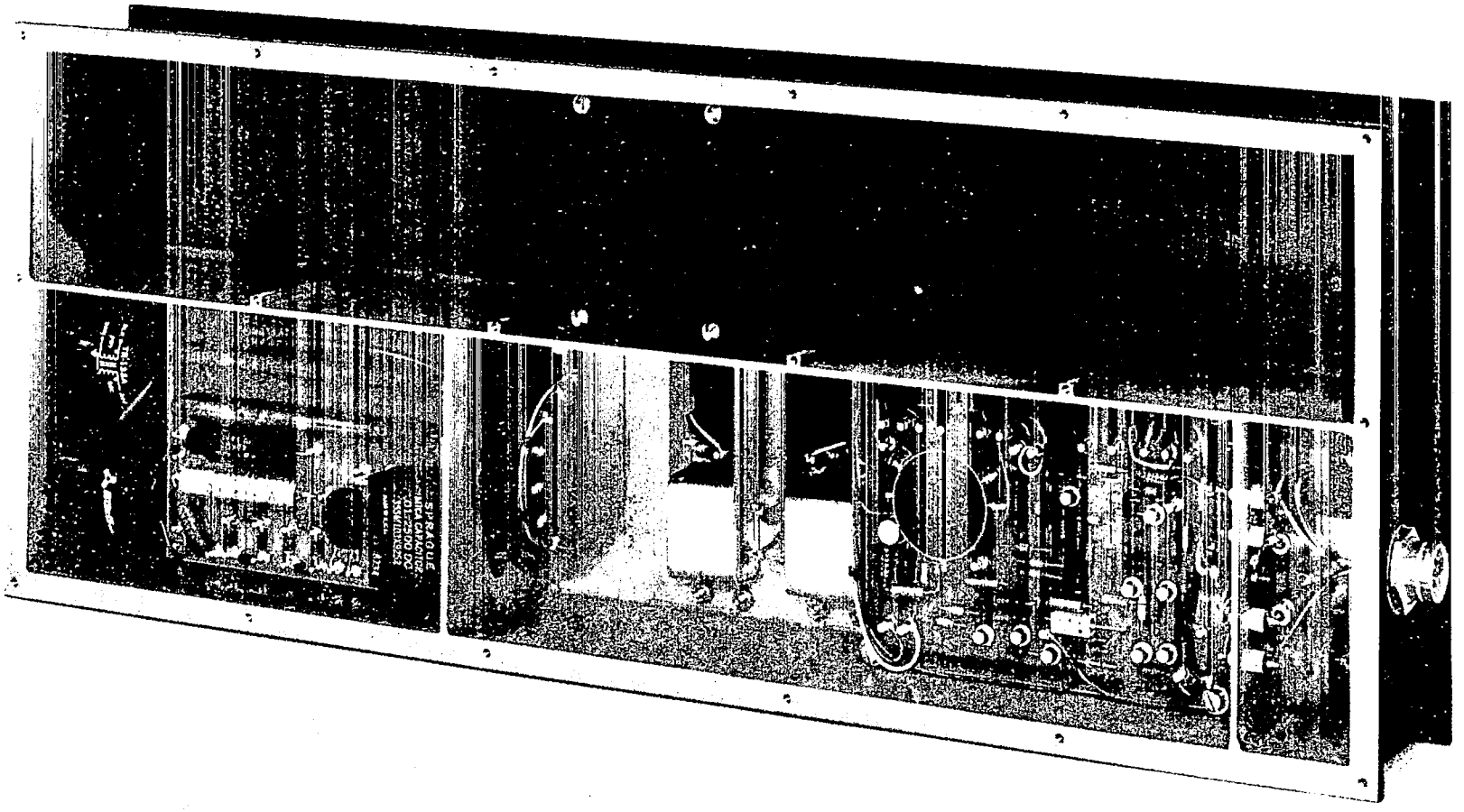

Fig. III-24. Photograph of prototype SQL interior showing laser mirror support structure and power supply circuit boards.

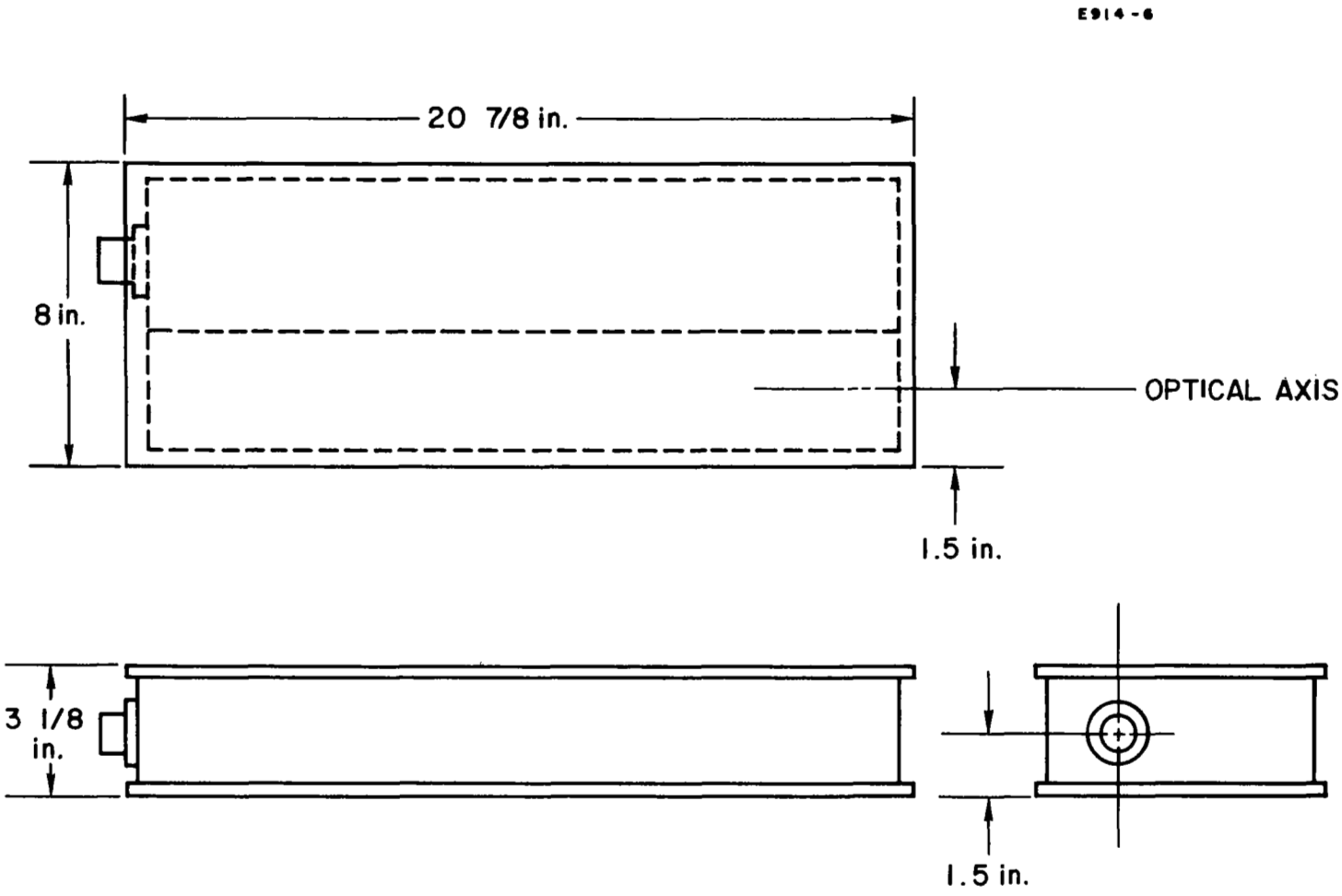

Fig. III-25. Dimensions of prototype unit. Proposed design has been reduced to 16 in. over-all length.

TABLE III-4

Weight Budget

E945-24

ITEM	PROTOTYPE (21 in.) (ACTUAL)	PROTOTYPE (21 in.) (PROPOSED MATERIALS)	PROPOSED DESIGN (16 in.)
PACKAGE	5.9 lb (Al)	3.8 lb (Mg)	2.9 lb (Mg)
POWER SUPPLY	4.7	4.7	4.7
OPTICAL CAVITY	4.0 (Al)	2.8 (Be)	2.2 (Be)
TUBE	0.5 (GLASS)	1.5 (M/C)	1.2 (M/C)
POTTING	1.0	0.3	0.3
TELEMETRY	—	0.3	0.3
TOTAL	*16.1 lb*	*13.4 lb*	*11.6 lb*

Shortening the laser to the new proposed length should further reduce the weight to 11.6 lb. A slightly greater weight saving may be realized by further power supply optimization, especially in magnetics, since the magnetics for the present supply were very conservatively designed.

J. RELIABILITY PREDICTION AND STRESS ANALYSIS FOR 3072H LASER

The over-all reliability of the integrated laser and power supplies may be expressed as the product of the probability of mission success for each of its major subassemblies. In the Phase I design, the over-all laser unit has two discharge sections within a common metal-ceramic vacuum envelope. Each section has separate power supplies which provide the anode and starting voltages. Note that the cathode is at ground potential and operates in the "cold" mode. Thus, the probability that the integrated laser provides full power output of 5 mW (i.e., no failures) may be expressed as the probability that all subassemblies operate:

$$R_{laser} = R_{PS}^2 \times R_{LDS}^2 \times R_{VEP}$$

where

R_{laser} ≡ reliability of the integrated laser and its power supplies (probability everything works)

R_{PS} ≡ reliability of one power supply

R_{LDS} ≡ reliability of one discharge section

R_{VEP} ≡ reliability of the common laser tube vacuum-envelope and package.

The Phase I design effectively provides a redundant mode of operation which, upon failure of one power supply or discharge element, allows performance at approximately 35% of the power output. Thus, effective redundancy allows a mode of degraded performance (Mode 2). The probability of successful operation in this mode is expressed by the series-parallel mission success diagram of Fig. III-26. The mission success diagram demonstrates that the laser output will fail only when both power supply-laser tube combinations or the vacuum envelope fails. The fall-off of output power due to cathode wearout or contamination is a phenomenon which could be predicted if statistical data were available. Therefore, this is not considered a MTBF, but a lifetime

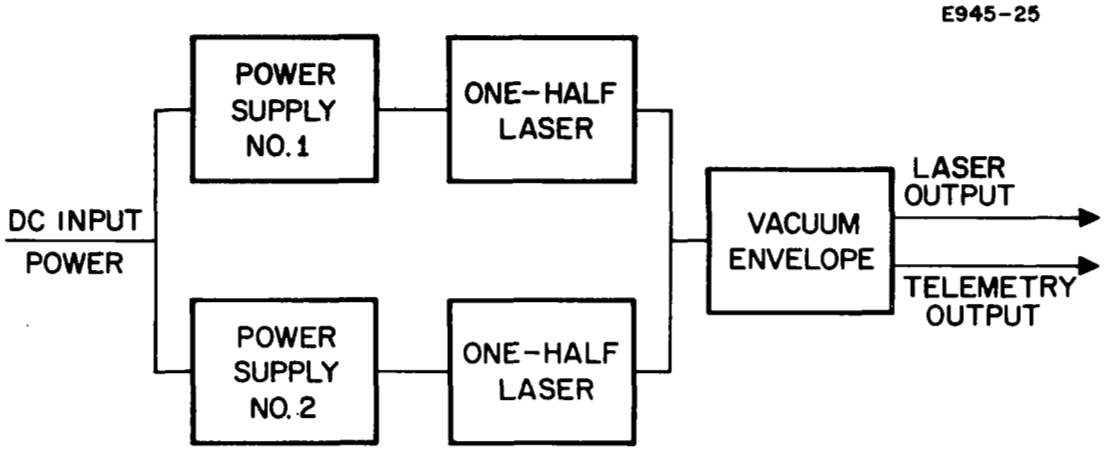

Fig. III-26. Reliability diagram, degraded mode 2 operation.

limiting factor. The probability that the integrated laser will operate in the degraded mode is R_{DL} expressed from the reliability block diagram as follows:

$$R_{DL} = \left[1-(1-R_{PS}R_{LDS})^2 \right] R_{VEP}$$

The predicted reliability of the 3072H laser unit is shown in Fig. III-27. This figure shows the reliability and mean-time-between-failures for no failure (full performance) and for the degraded mode of operation which provides 35% of the power output at the time of failure. In addition, curves are provided for the effect on reliability and MTBF of using Mil-Spec parts (proposed for Phase II) and the use of high reliability parts which may be directly substituted in any follow-on flight unit program. This analysis of reliability is based upon actual Hughes laser life test experience and failure rate data collected from electronic components.

Hughes/EDD has accrued over 15,000 hours of life test operation on the cold cathode 5 mW 3082H, He-Ne (cw) family of lasers. These data are summarized in Table III-5. These data are further supported by 18,000 hour lifetimes achieved by U. Hochuli, et al. (Ref. III-15). With these data and the rapidly changing state of the art, a conservative 25,000 hour mean-time-between-failures or greater is predicted for the 5 mW He-Ne laser. This prediction is only limited by the amount of data accrued to date. As a comparison, the initial predicted levels for the Hughes medium power TWT's were 20,000 hours mean-time-to-failure based upon limited life test data. Subsequent life tests have shown that these metal ceramic tubes exhibit an inherent mean-time-to-failure of greater than 1.5 million hours.

Many of the techniques used in these high reliability tubes are being used in perfecting the metal-ceramic Phase II He-Ne laser. For example, the Hughes metal-ceramic seal techniques used in these tubes are being used for the laser vacuum envelope. This type of vacuum seal has accrued over 1.5 million hours of failure free performance on such space programs as Surveyor, Syncom, ATS, Early Bird, Intelsat, Pioneer, and Lunar Orbiter.

The reliability prediction for each power supply is based upon an analysis using actual electrical stress levels for all components. Circuit design and derating levels have been selected to optimize efficiency, reliability, weight, etc. This analysis presents failure rates for a power supply which employs either Mil-Spec level or high reliability parts. It is proposed that the Mil-Spec electronic parts be incorporated into the lasers fabricated for Phase II achieving the

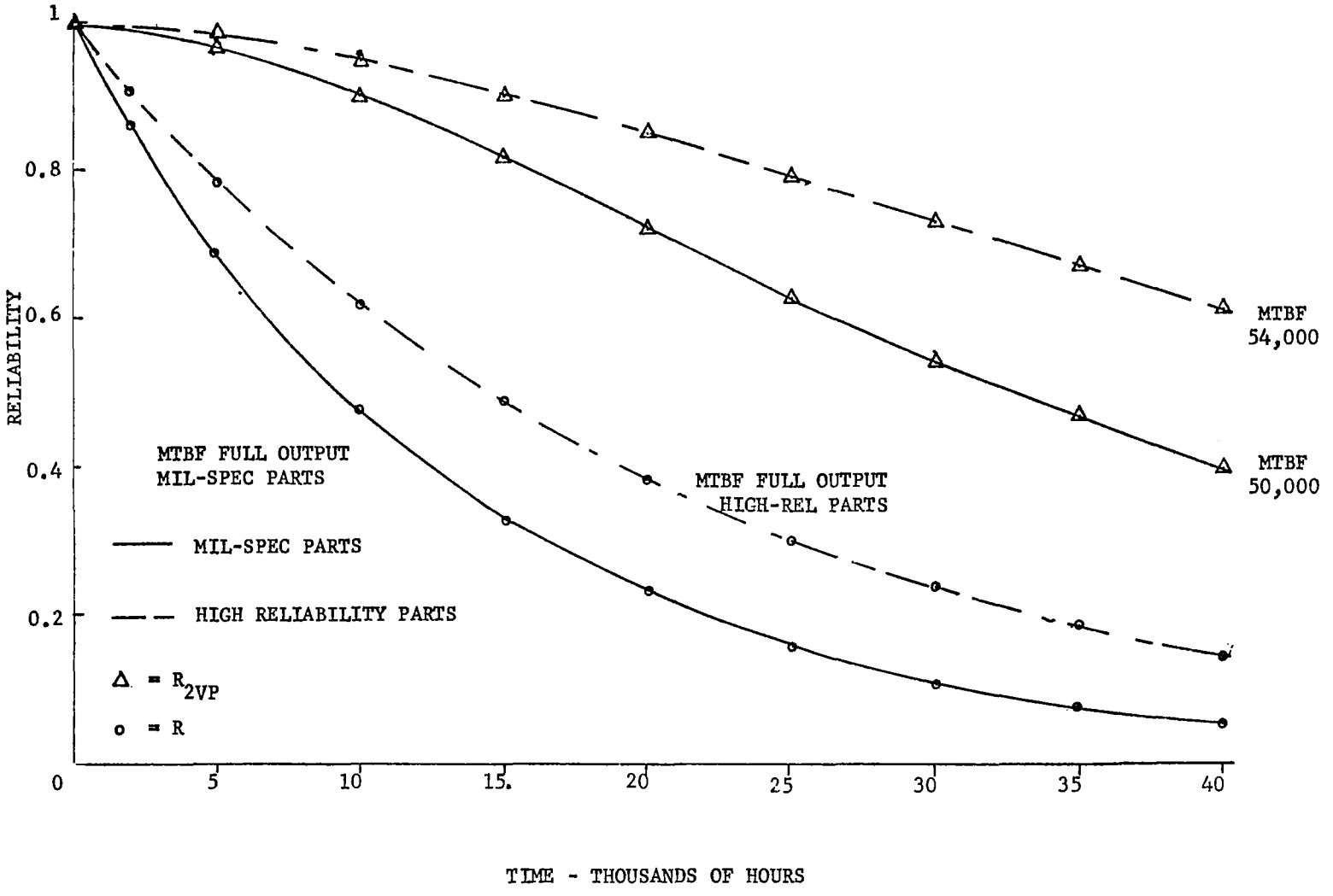

Fig. III-27. Reliability as a function of time for Mil Spec parts and High Reliability parts.

TABLE III-5

Power Supply Parts Count and Failure Rate Data
(For One Power Supply)

Part Type	Number of Components	MIL-Spec. $\lambda \times 10^{-6}$	HI-Reliability $\lambda \times 10^{-6}$
Transistors	15	3.510	0.778
Diodes	34	8.550	1.596
Capacitors	15	2.404	0.890
Resistors	41	0.291	0.156
Magnetics and Feed-Through Caps	9	1.800	0.180
Total Failure Rate ($\lambda \times 10^{-6}$)		16.555	3.600

reliability level indicated by Fig. III-27. Additional part preconditioning and parameter screening may be employed for space flight hardware in order to achieve the high reliability part level.

The failure rates using Mil-Spec parts are selected from those given in MIL-HDBK-217A, "Reliability Stress and Failure Rate Data for Electronic Equipment." These high reliability part failure rates are conservatively based upon Hughes space programs part data and the document entitled, "Dormant Operating and Storage Effects on Electronic Equipment and Part Reliability," written under Rome Air Development Center's Technical Report Number TR-66348. It should be noted that there is a significant improvement in reliability by using high reliability components (see Fig. III-27). Hughes failure rate data have proven valid for Hughes space qualified parts. These failures on Hughes spacecraft have been predicted based upon these failure rates, with only two occurring to date.

The reliability of the telemetry circuits has not been included in this preliminary analysis. The telemetry portion of the laser and power supply is designed to be failsafe; i.e., failure of any telemetry point will not cause a catastrophic failure of the power supply or laser. Since the telemetry circuits are designed failsafe, they will not alter the over-all reliability of the integrated power supply and laser.

The detailed component part stress and derating analysis is presented in the following pages for one power supply. The second power supply operates under identical conditions and exhibits the same failure rate. This stress analysis is based upon calculated electrical and thermal stress levels experienced during equipment operation encompassing critical parameters for each part. The parts count is based upon the power supply design as defined by the schematic Diagram B190074 dated 15 January 1968. The analysis shows that the applied parts derating levels are consistent with space program requirements of a reliable design with maximum performance at a minimum dc input power level.

The component part stress and derating analysis is presented in tabulated form by generic part type. In general, the worst condition was used to calculate the electrical stress. The maximum saturation voltage, maximum leakage current, maximum applied voltage, and other such component part parameters were used to obtain the maximum stress levels. These values are compared with the rating of the component part at an estimated baseplate temperature of 50°C. The rated value for each component includes derating due to the temperature rise above this base plate temperature. The stress analysis sheets for one power supply follow.

STRESS ANALYSIS SHEET

PRELIMINARY

CIRCUIT SYMBOL	PART NUMBER	PARA. ohms	MAX. VOLTAGE (VOLTS)		MAX. CURRENT (ma)		MAX. POWER (WATTS)			TEMPERATURE IN °C					STRESS RATIO	*HR. *MIL FAILURE RATE 10^{-6}	
			ACTUAL	RATED	ACTUAL	RATED	ACTUAL	RATED	DUTY	RATED MAX.	RATED MIN.	RATED T_s	RATED Δ/°C T.C.	AMB.			
R1	RS1-A	350					NIL	1		275	-55	25	.36	75	0.00	.003	.003
R2	RS1-A	15.0					0.006	1		275	-55	25	.36	75	0.00	.003	.003
R3	RN60C..	7.15K					0.005	0.125		175	-55	125	2.0	75	0.04	.004	.004
R4	RS1-A	3.5K					0.023	0.125		275	-55	25	.36	75	0.22	.007	.008
R5	RN60C..	1.0K					0.037	0.125		175	-55	125	2.0	75	0.29	.007	.010
R6	RN60C..	5.11K					0.006	0.125		175	-55	125	2.0	75	0.05	.004	.004
R7	RN60C..	71.5K					0.012	0.125		175	-55	125	2.0	75	0.12	.005	.005
R8	RN60C..	10.0K					0.080	0.125		175	-55	125	2.0	75	0.64	.010	.030
R9	RN60C..	2.15K					0.008	0.125		175	-55	125	2.0	75	0.06	.004	.004
R10	RN60C..	5.11K					0.014	0.125		175	-55	125	2.0	75	0.11	.005	.005
R11	RN60C..	21.5K					0.045	0.125		175	-55	125	2.0	75	0.36	.009	.020
R12	RN60C..	51.1					0.020	0.125		175	-55	125	2.0	75	0.02	.004	.004
R13	RN60C..	10.0K					0.036	0.125		175	-55	125	2.0	75	0.29	.007	.010
R14	RN60C..	10.0K					0.040	0.125		175	-55	125	2.0	75	0.32	.008	.020
R15	RN60C..	10.0K					0.040	0.125		175	-55	125	2.0	75	0.32	.008	.020
R16	RN60C..	10.0K					0.020	0.125		175	-55	125	2.0	75	0.02	.004	.004
R17	RN60C..	12.4K					0.004	0.125		175	-55	125	2.0	75	0.04	.004	.004
R18	RN60C..	12.4K					0.005	0.125		175	-55	125	2.0	75	0.04	.004	.004
R19	RN60C..	6.81K					0.020	0.125		175	-55	125	2.0	75	0.02	.004	.004
R20	RS-2C	400.0					0.44	1		275	-55	25	.36	75	0.20	.004	.008

T_s = Temperature at which derating begins

T.C. = Derating slope

STRESS ANALYSIS SHEET

PRELIMINARY

CIRCUIT SYMBOL	PART NUMBER	PARA.	MAX. VOLTAGE (VOLTS)		MAX. CURRENT (ma)		MAX. POWER (WATTS)			TEMPERATURE IN °C					STRESS RATIO	FAILURE RATE 10^{-6} HRS. H.R	FAILURE RATE 10^{-6} HRS. MIL
										RATED							
			ACTUAL	RATED	ACTUAL	RATED	ACTUAL	RATED	DUTY	MAX.	MIN.	T_s	T.C.	AMB.			
R21	RN60C--	21.5K					0.02	0.125		175	-55	25	2.0	75	0.02	.004	.004
R23	RN60C--	221K					0.00	0.125		175	-55	25	2.0	75	0.00	.003	.004
R24	RS1-A	270					0.01	1		275	-55	25	.36	75	0.01	.003	.004
R25	RS1-A	25.0					0.04	1		275	-55	25	.36	75	0.05	.003	.005
R26	RN60C--	1.0K					0.00	0.125		175	-55	25	2.0	75	0.00	.003	.004
R27	RS-5	33.0K					0.10	5		275	-55	25	.36	75	0.02	.003	.004
R28	RS-10	50.0K					5.0	10.0		275	-55	25	.36	75	0.61	.006	.030
R29	RN60C--	5.11K					0.006	.125		175	-55	25	2.6	75	0.05	.004	.004
R30	RS1-A	30.0					0.04	1.0		275	-55	25	.36	75	0.04	.004	.004
R31	RS1-A	30.0					0.04	1.0		275	-55	25	.36	75	0.04	.004	.004
R32	RN60C--	619					0.07	.125		175	-55	25	2.0	75	0.60	.010	.030
R33	RN60C--	S.F.T. ≈ 6K					0.00	.250		175	-55	25	2.0	75	0.00	.003	.003
R34	RN60C---	310					.03	.125		175	-55	25	2.0	75	0.20	.007	.008
R40	RN60C---	41.1K					.010	.125		175	-55	25	2.0	75	0.11	.005	.005
R41	RN60C---	8.25K					.003	.125		175	-55	25	2.0	75	0.04	.004	.004

T_s = Temperature at which derating begins

T.C. = Derating slope

STRESS ANALYSIS SHEET

PRELIMINARY

CIRCUIT SYMBOL	PART NUMBER	PARA.	MAX. VOLTAGE (VOLTS)		MAX. CURRENT (ma)		MAX. POWER (WATTS)			TEMPERATURE IN °C					STRESS RATIO	H.R. FAILURE RATE 10^{-6} HRS	MIL
										RATED							
		uf	ACTUAL	RATED	ACTUAL	RATED	ACTUAL	RATED	DUTY	MAX.	MIN.	T_s	T.C.	AMB.			
C1	137D__	78	32.0	60						125	-55	85		75	.19	.028	.150
C2	350D__	.022	4.0	60						125	-55	85		75	.08	.024	.140
C3	350D__	022	32.0	50						125	-55	85		75	.65	.076	.250
C4	350D__	1.0	6.0	50						125	-55	85		75	.13	.026	.160
C5	96P___	.0022	14.0	100						125	-55	85		75	.14	.010	.05
C6	96P___	.0022	40.0	100						125	-55	85		75	.40	.015	.062
C7	96P___	.0022	40.0	100						125	-55	85		75	.40	.015	.062
C8	350D___	2.2	14.0	50						125	-55	85		75	.07	.024	.130
C9	135D___	94	20.3	50						125	-55	85		75	.10	.026	.060
C10	350D___	2.2	6	50						125	-55	85		75	.13	.026	.160
C11	350D___	0.22	25	50						125	-55	85		75	.50	.050	.250
C12	96P___	.33	275	400						125	-55	85		75	.69	.400	.590
C13	355M__	.01	1400	2500						125	-40	85		75	.56	.050	.070
C14	355M__	.01	1400	2500						125	-40	85		75	.56	.050	.070
C15	350D__	10	22	50						125	-40	85		75	.45	.070	.200

T_s = Temperature at which derating begins

T.C. = Derating slope

STRESS ANALYSIS SHEET

PRELIMINARY

CIRCUIT SYMBOL	PART NUMBER	PARA.	MAX. VOLTAGE (VOLTS)		MAX. CURRENT (ma)		MAX. POWER (WATTS)			TEMPERATURE IN °C					STRESS RATIO	H.R. FAILURE RATE 10^{-6}	MIL FAILURE RATE 10^{-6}
										RATED				AMB.			
			ACTUAL	RATED	ACTUAL	RATED	ACTUAL	RATED	DUTY	MAX.	MIN.	T_s	mw/°C T.C.				
CR1	PS760B	I_f			1.3	100	0.007	5.0		175	-65	25	2.0	75	0.00	.007	.200
		V_R	32	50													
		V_f		0.50													
CR2	PS760B	I_f			>.01	100	0.000	5.0		175	-65	25	2.0	75	0.00	.007	.200
		V_R	0.50	50													
		V_f		.50													
CR3	PS760B	I_f			>.01	100	0.000	5.0		175	-65	25	2.0	75	0.00	.007	.200
		V_R	0.50	.50													
		V_f		0.50													
CR4	PS510B	I_f			23.0	400	0.018	0.600		175	-65	25	2.0	75	0.06	.007	.200
		V_R	0.50	225													
		V_f		.80													
CR5	IN4942	I_R			>.001	1.00	0.000	5.00		175	-65	25	1	75	0.00	.007	.200
		V_R															
CR6	IN4371A	I_{zm}			7.0	140	0.018	0.400		175	-65	25	3.2	75	0.08	.032	.350
		V_z		2.7													
CR7	PS6313	I_{zm}			3.0	68.3	0.026	0.600		175	-65	25	—	75	0.09	.032	.350
		V_z															

T_s = Temperature at which derating begins

T.C. = Derating slope

STRESS ANALYSIS SHEET

PRELIMINARY

CIRCUIT SYMBOL	PART NUMBER	PARA.	MAX. VOLTAGE (VOLTS)		MAX. CURRENT (ma)		MAX. POWER (WATTS)			TEMPERATURE IN °C					STRESS RATIO	H.R FAILURE RATE 10^{-6}	MIL FAILURE RATE 10^{-6} HRS
										RATED							
			ACTUAL	RATED	ACTUAL	RATED	ACTUAL	RATED	DUTY	MAX.	MIN.	T_s	mw/°C T.C.	AMB.			
CR8	1N825	I_{zm}			1.38	1.75	0.009	0.400		175	-55	50	3.2	75	0.00	.026	.350
		V_z			6.18	6.2											
CR9	PS510B	I_f			>0.01	400	0.000	0.600		175	-65	25	2.0	75	0.00	.007	.200
		V_R	20	225													
		V_f		.80													
CR10	PS760B	I_f			6.0	100	0.024	0.250		175	-65	25	2.0	75	0.19	.010	.250
		V_R	30	50													
		V_f		0.50													
CR11	PS760B	I_f			6.0	100	0.024	0.250		175	-65	25	2.0	75	0.19	.010	.250
		V_R	30	50													
		V_f		0.50													
CR12	PS510B	I_f			>0.01	400	0.000	0.600		175	-65	25	2.0	75	0.00	.007	.200
		V_R	65	225													
		V_f		0.80													
CR13	PS510B	I_f			>0.01	400	0.000	0.600		175	-65	25	2.0	75	0.00	.007	.200
		V_R		225													
		V_f		.80													

T_s = Temperature at which derating begins

T.C. = Derating slope

STRESS ANALYSIS SHEET

PRELIMINARY

CIRCUIT SYMBOL	PART NUMBER	PARA.	MAX. VOLTAGE (VOLTS)		MAX. CURRENT (ma)		MAX. POWER (WATTS)			TEMPERATURE IN °C					STRESS RATIO	H.R. FAILURE RATE 10^{-6} HRS	MIL
										RATED							
			ACTUAL	RATED	ACTUAL	RATED	ACTUAL	RATED	DUTY	MAX.	MIN.	T_s	T.C.	AMB.			
CR14	PS510B	I_f			20.0	400	0.024	0.600		175	-65	25		75	.08	.008	.250
		V_R	5.0	225													
		V_f	1.2														
CR15	PS510B	I_f			20.0	400	0.024	0.600		175	-65	25		75	.08	.008	.250
		V_R	5.0	225													
		V_f	1.2														
CR16	IN4249	I_f			1.0	1000	.001	1.2		175	-65	25		75	.00	.001	.200
		V_R	275	1000													
		V_f		1.2													
CR17	IN4249	I_f			1.0	1000	.001	1.2		175	-65	25		75	.00	.001	.200
		V_R	275	1000													
		V_f		1.2													
CR18	IN4249	I_f			1.0	1000	.001	1.2		175	-65	25		75	.00	.001	.200
		V_R	275	1000													
		V_f		1.2													
CR19	IN4249	I_f			1.0	1000	.001	1.2		175	-65	25		75	.00	.001	.200
		V_R	275	1.000													
		V_f		1.2													
CR20	PS510B	I_f			.001	400	.001	0.600		175	-65	25		75	.00	.001	.200
		V_R	5	2.25													

T_s = Temperature at which derating begins

T.C. = Derating slope

STRESS ANALYSIS SHEET

PRELIMINARY

CIRCUIT SYMBOL	PART NUMBER	PARA.	MAX. VOLTAGE (VOLTS)		MAX. CURRENT (ma)		MAX. POWER (WATTS)			TEMPERATURE IN °C					STRESS RATIO	H.R. FAILURE RATE 10^{-6}	MIL FAILURE RATE 10^{-6} HRS
										RATED							
			ACTUAL	RATED	ACTUAL	RATED	ACTUAL	RATED	DUTY	MAX.	MIN.	T_s	T.C.	AMB.			
CR21	PS510B	I_f			5	400	.006	.600		175	-65	25		75	.01	.007	.200
		V_R	25	225													
		V_f		0.80													
CR22	PS510B	I_f			5	400				175	-65	25		75	.01	.007	.200
		V_R	25	225													
		V_f		0.80													
CR23	IN3667	I_f			2.5	250	.125	1.0		175	-65	25		75	.125	.009	.250
		V_R	1400	2500													
		V_f		5.0													
CR24	IN3667	I_f			2.5	250	.125	1.0		175	-65	25		75	.125	.009	.250
		V_R	1400	2500													
		V_f		5.0													
CR25	IN3667	I_f			2.5	250	.125	1.0		175	-65	25		75	.125	.009	.250
		V_R	1400	2500													
		V_f		5.0													
CR26	IN3667	I_f			2.5	250	.125	1.0		175	-65	25		75	.125	.009	.250
		V_R	1400	2500													
		V_f		5.0													

T_s = Temperature at which derating begins

T.C. = Derating slope

STRESS ANALYSIS SHEET

PRELIMINARY

CIRCUIT SYMBOL	PART NUMBER	PARA.	MAX. VOLTAGE (VOLTS)		MAX. CURRENT (ma)		MAX. POWER (WATTS)			TEMPERATURE IN °C					STRESS RATIO	H.R FAILURE RATE 10^{-6} HRS	MIL FAILURE RATE 10^{-6} HRS
										RATED							
			ACTUAL	RATED	ACTUAL	RATED	ACTUAL	RATED	DUTY	MAX.	MIN.	T_s	T.C.	AMB.			
CR27	SCH25000	I_f			10	500	.05	15		100	-65	25		75	.00	.650	.750
		V_R	15000	25000													
		V_f		33													
CR28	SCH2500	I_f			10	500	.05	15		100	-65	25		75	.00	.65	.75
		V_R	15000	25000													
		V_f		33													
CR29	PS510B	I_f			4.2		.003	0.6		175	-65	25	2.0	75	.00	.007	.200
		V_R	3	225													
		V_f		.8													
CR31	PS510B	I_f			4.2	400	.003	0.6		175	-65	25	2.0	75	.00	.007	.200
		V_R	25	225													
		V_f		.8													
CR32	PS510B	I_f			4.2	400	.003	0.6		175	-65	25	2.0	75	.00	.007	.200
		V_R	25	225													
		V_f		0.8													
CR33	PS510B	I_f			4.2	400	.003	0.6		175	-65	25	2.0	75	.00	.007	.200
		V_R	25	225													
		V_f		0.8													

T_s = Temperature at which derating begins

T.C. = Derating slope

STRESS ANALYSIS SHEET

PRELIMINARY

CIRCUIT SYMBOL	PART NUMBER	PARA.	MAX. VOLTAGE (VOLTS)		MAX. CURRENT (ma)		MAX. POWER (WATTS)			TEMPERATURE IN °C					STRESS RATIO	FAILURE RATE 10^{-6}	
										RATED							
			ACTUAL	RATED	ACTUAL	RATED	ACTUAL	RATED	DUTY	MAX.	MIN.	T_s	T.C.	AMB.			HRS
CR34	P3510B	I_f			4.2	400	0.003	0.600		175	-65	25	2.0	75	0.00	.007	200
		V_R	25	225													
		V_f		.8													

T_s = Temperature at which derating begins

T.C. = Derating slope

STRESS ANALYSIS SHEET

PRELIMINARY

CIRCUIT SYMBOL	PART NUMBER	PARA.	MAX. VOLTAGE (VOLTS)		MAX. CURRENT (ma)		MAX. POWER (WATTS)			TEMPERATURE IN °C					STRESS RATIO	FAILURE RATE 10^{-6}	
										RATED							
			ACTUAL	RATED	ACTUAL	RATED	ACTUAL	RATED	DUTY	MAX.	MIN.	T_s	mw/°C T.C.	AMB.			HRS
Q1	HST5503	I_c			210	2000	0.075	4.0		200	-55	100	40	75	0.02	.140	.390
		$V_{CE(SAT)}$		.35													
		V_{CE}	12	80													
		V_{EB}		8													
Q2	2N2906A	I_c			21	600	0.010	400		200	-65	25	2.3	75	0.03	.014	.140
		$V_{CE(SAT)}$		40													
		V_{CE}	-32	-60													
		V_{EB}		5													
Q3	2N2222	I_c			2.57	500	<.001	1.8		175	-65	25	12	75	.00	.013	.100
		$V_{CE(SAT)}$		.30													
		V_{CE}	18	30													
		V_{EB}		5.0													
Q4	2N2222	I_c			0.32	500	<.001	1.8		175	-65	25	12	75	.00	.013	.100
		$V_{CE(SAT)}$		.30													
		V_{CE}	20	30													
		V_{EB}		5													

T_s = Temperature at which derating begins

T.C. = Derating slope

STRESS ANALYSIS SHEET

PRELIMINARY

CIRCUIT SYMBOL	PART NUMBER	PARA.	MAX. VOLTAGE (VOLTS)		MAX. CURRENT (ma)		MAX. POWER (WATTS)			TEMPERATURE IN °C					STRESS RATIO	H.R. FAILURE RATE 10^{-6}	MIL. FAILURE RATE 10^{-6} HRS
										RATED							
			ACTUAL	RATED	ACTUAL	RATED	ACTUAL	RATED	DUTY	MAX.	MIN.	T_s	MW/°C T.C.	AMB.			
Q5	2N2222	I_C			6.05	500	<.001	1.80		175	-65	25	12	75	0.00	.013	.100
		$V_{CE(SAT)}$		.30													
		V_{CEO}	9	0													
		V_{EB}	1.2	5													
Q6	2N2222	I_C			0.40	500	<.001	1.80		175	-65	25	12		0.00	.013	.100
		$V_{CE(SAT)}$		.30													
		V_{CEO}	9.0	30													
		V_{EB}	1.2	5													
Q7	2N2222	I_C			0.55	500	.005	1.80		175	-65	25	12	75	0.00	.013	.100
		$V_{CE(SAT)}$		.30													
		V_{CEO}	7.7	30													
		V_{EB}	.5	5													
Q8	2N2222	I_C			0.55	500	.010	1.80		175	-65	25	12	75	0.00	.013	.100
		$V_{CE(SAT)}$		.30													
		V_{CEO}	14.5	30													
		V_{EB}	.50	5													
Q9	2N2222	I_C			40	500	.012	1.8		175	-65	25	12	75	0.00	.013	.100
		$V_{CE(SAT)}$		.30													
		V_{CEO}	6	30													
		V_{EB}	1.2	5													

T_s = Temperature at which derating begins

T.C. = Derating slope

STRESS ANALYSIS SHEET

PRELIMINARY

CIRCUIT SYMBOL	PART NUMBER	PARA.	MAX. VOLTAGE (VOLTS)		MAX. CURRENT (ma)		MAX. POWER (WATTS)			TEMPERATURE IN °C					STRESS RATIO	H.R FAILURE RATE 10^{-6} HRS	MIL FAILURE RATE 10^{-6} HRS
			ACTUAL	RATED	ACTUAL	RATED	ACTUAL	RATED	DUTY	RATED MAX.	RATED MIN.	RATED T_s	RATED T.C.	AMB.			
Q10	2N2222	I_c			40	500	.012	1.80		175	-65	25	12	75	.00	.013	.100
		$V_{CE(SAT)}$		30													
		V_{CEO}	6	30													
		V_{EB}	1.2	5													
Q11	HST5503	I_c			420	2000	0.15	4.0		200	-55	100	40	75	.04	.140	~~.140~~ .440
		$V_{CE(SAT)}$		35													
		V_{CEO}	20	80													
		V_{EB}		8													
Q12	HST5503	I_c			420	200	0.15	4.0		200	-55	100	40	75	.04	.140	.440
		$V_{CE(SAT)}$		.35													
		V_{CEO}	20	80													
		V_{EB}		8													
Q13	2N4918	I_p				.012		.450		175	-55	25	4.0	25	.00	.050	.430
		V_p		25													
Q15	2N2329	I_F				160				125	-55	85°C				.050	.430
		I_H				3.0											
		V_{GF}		1.0													
		V_{BOO}		400													
		V_F		1.5													

T_s = Temperature at which derating begins

T.C. = Derating slope

STRESS ANALYSIS SHEET

PRELIMINARY

CIRCUIT SYMBOL	PART NUMBER	PARA.	MAX. VOLTAGE (VOLTS)		MAX. CURRENT (ma)		MAX. POWER (WATTS)			TEMPERATURE IN °C					STRESS RATIO	H.R. FAILURE RATE 10^{-6}	MIL HRS
										RATED							
			ACTUAL	RATED	ACTUAL	RATED	ACTUAL	RATED	DUTY	MAX.	MIN.	T_s	T.C.	AMB.			
Q14	HST5503	I_C			210	2100	0.075	4.0		200	-55	100	40	75	0.04	.140	440
		$V_{CE(SAT)}$		.35													
		V_{CEO}	12	80													
		V_{EB}		8													

T_s = Temperature at which derating begins

T.C. = Derating slope

STRESS ANALYSIS SHEET

PRELIMINARY

CIRCUIT SYMBOL	PART NUMBER	PARA.	MAX. VOLTAGE (VOLTS)		MAX. CURRENT (ma)		MAX. POWER (WATTS)			TEMPERATURE IN °C					STRESS RATIO	H.R FAILURE RATE 10^{-6}	MIL FAILURE RATE ERS
										RATED							
			ACTUAL	RATED	ACTUAL	RATED	ACTUAL	RATED	DUTY	MAX.	MIN.	T_s	T.C.	AMB.			
T1	F.S.				1										—	.020	.200
T2	F.S.				420										—	.020	.200
T3	F.S				2										—	.020	.200
L1		100mh			420										—	.020	.200
L2		500mh			10										—	.020	.200
L3		2.4mh			420										—	.020	.200
FT	SMFB-A2															.020	.200
FT	SMFB-A2															.020	.200
SR-1	F.S.															.020	.200

T_s = Temperature at which derating begins

T.C. = Derating slope

REFERENCES

II-1. U. Hochuli and P. Haldemann, "Cold cathodes for possible use in 6328Å single mode He-Ne gas lasers," Rev. Sci. Instr. 36, 1493 (1965).

III-1. E. I. Gordon and A. D. White, "Similarity laws for the effects of pressure and discharge diameter on the gain of He-Ne lasers," Appl. Phys. Letters 3, 199 (1963).

III-2. A. D. White, "Increased power output of the 6328Å gas maser," Proc. IEEE 51, 1669 (1963).

III-3. E. F. Labuda and E. I. Gordon, "Microwave determination of average electron energy and density in He-Ne discharges," J. Appl. Phys. 35, 1647 (1964).

III-4. J. Y. Wada and H. Heil, "Electron energy spectra in neon, xenon, and helium-neon laser discharges," IEEE J. Quantum Electron. QE-1, 327 (1965).

III-5. W. W. Rigrod, "Gain saturation and output power of optical masers," J. Appl. Phys. 34, 2602 (1963).

III-6. A. D. White, E. I. Gordon, and J. D. Rigden, "Output power of the 6328Å gas maser," Appl. Phys. Letters 2, 91 (1963).

III-7. P. W. Smith, "The output power of a 6328Å He-Ne gas laser," IEEE J. Quantum Electron. QE-2, 62 (1966).

III-8. P. W. Smith, "On the optimum geometry of a 6328Å laser oscillator," IEEE J. Quantum Electron. QE-2, 77 (1966).

III-9. P. W. Smith, "Linewidth and saturation parameters for the 6328 Å transition in a He-Ne laser," J. Appl. Phys. 37, 2089 (1966).

III-10. A. D. White and E. I. Gordon, "Excitation mechanisms and current dependence of population inversion in He-Ne lasers," Appl. Phys. Letters 3, 197 (1963).

III-11. J. Haisma "Construction and properties of short stable gas lasers," Phillips Research Reports Supplement No. 1, (1967).

III-12. L. Allen and D. G. C. Jones "The He-Ne laser," Advan. Phys. 14, 479 (1965).

III-13. U. Hochuli and P. Haldemann, "Cold cathodes for possible use in 6328 Å single mode He-Ne gas lasers," Rev. Sci. Instr. 36, 1493 (1965).

III-14. R. Turner, K. M. Baird, M. J. Taylor, and C. J. Van der Hoeven, "Lifetime of He-Ne lasers," Rev. Sci. Inst. 35,996 (1964).

III-15. U. Hochuli, P. Haldemann, and D. Hardwich, "Cold cathodes for He-Ne gas lasers," presented at 1967 IEEE conference on Laser Engineering and Applications, Washington, D. C., June 1967.

APPENDIX A

1.0 PURPOSE

1.1 The purpose of this document is to outline the steps and conditions to be implemented in qualifying an integrated laser and its power supply for space application.

2.0 APPLICABLE DOCUMENTS

2.1 Qualification Test Procedure

2.2 Laser Outline and Mounting Drawings

3.0 SCOPE OF TESTS

3.1 The qualification tests are designed to evaluate the laser and power supply performance in severe simulated space environments. These tests are to consist of temperature cycling, vibration, shock, acceleration, and thermal-vacuum environments. The environmental qualification tests will be performed on one unit in accordance with a documented test procedure.

3.2 At the conclusion of the environmental qualification tests, the laser will be placed on reliability life test. The reliability life tests will consist of a two month thermal vacuum test followed by a sixteen month continuous life test under normal laboratory conditions. Each laser unit will undergo functional tests at the time intervals specified in Table I.

3.3 The environmental qualification test sequence to be performed and the stress levels are specified in Table I and Section 5.0 respectively. The chosen stress levels shall provide an indication of the ruggedness of the metal-ceramic design approach. A review of Section 5.0 reveals the severity of the environmental extremes through which the laser package must successfully perform. Table II compares the laser qualification stress levels with those of other space programs.

TABLE 1

TEST SEQUENCE

ENVIRONMENTAL QUALIFICATION TESTS

		TESTING MODE
1.	Complete Functional Test	
2.	Sinusoidal Vibration	Non-Operational
3.	Complete Functional Test	
4.	Random Vibration	Non-Operational
5.	Complete Functional	
6.	Shock	Non-Operational
7.	Complete Functional	
8.	Temperature Cycling	Non-Operational
9.	Complete Functional Test	
10.	Acceleration Test	Non-Operational
11.	Complete Functional Test	

RELIABILITY LIFE TESTS

1.	Thermal-Vacuum Test (60 days)	ON-OFF Cycle
2.	Complete Functional Test	
3.	Life Test for 16 Months	Continuous-Operation
4.	Perform Daily Visual Test on Normal Days	
5.	Perform Complete Functional Test at 500 ± 50 hours intervals and record data	

TABLE II

PROGRAM NAME	SINUSOIDAL VIBRATION		RANDOM VIBRATION		SHOCK TESTS			THERMO VACUUM			ACCELERATION LEVELS	
	Freq. Hz	Peak-G Level	Freq. in cps	Peak G Level g^2/cps	Level	Time	Shape	Temperature °C Low	°C High	Vac.in Torr.	G Level	Time
APOLLO			100-480 480-570 570-630 630-670 670-2000	0.07 2.40 0.07 2.20 0.07	36g's	11 ms	-	25	100	10^{-4}	20g's	5 min.
ATS	10-25 25-250 250-400 400-2000	1.5 7.7 12.3 5.0	20-150 150-300 300-2000	0.01 3db/oct Ramp. 0.02	20g's	8 ms	1/2 sine	4	38	10^{-5}		
ITT	10-35 35-120 120-2000	.4% DA 18.0 3.5	20-150 150-300 300-2000	0.03 0.06	100g's	6 ms	1/2 sine	-24	84	10^{-5}	18g's	180 sec.
LUNAR ORBITER	5-22 22-2000	0.9 DA 12	20-2000	0.45	30g's	5.5 ms	1/2 sine	-12.3	43.2	10^{-2} 10^{-14}	14g's	5 min.
PIONEER	10-500 500-2000	5 10	20-500 500-2000	0.03 0.07	50g's	6 ms	**S.T.	-20.5	65.5	10^{-5}	50g's	3 min.
VOYAGER	5-26 26-52 52-500	± 1.3g .036DA ± 5.0g	150-300 Roll off below 150Hz Above 300 Hz	$1.0g^2$ 4db/oct 6db/oct	2" drop on fir bench 4" drop on each edge			-36	5	780 to $2.5x10^{-13}$	Thrust axis 5.6g 1.0g's normal to thrust axis	5 min.
LASER 3072H	5-30 30-2000	0.2 DA 8.6	5-30 30-700 700-900 900-2000	.02-.61 .61 18db/oct 0.18	78g's	10 ms	**S.T.	0*	50*	10^{-5}	10g's 20g's	3 min.

* Minimum and maximum temperature can be changed to the specific mission requirement, but the deviation (Δ) must not exceed 50°C to maintain specified performance.

** Sawtooth

3.4 The electrical and environmental requirements are described in Sections 4.0 and 5.0 respectively. The qualification tests shall be performed in accordance with the applicable paragraphs of a Qualification Test Procedure, and in the sequence of tests as listed in Table I whenever possible. Environmental tests may be performed in any sequence if availability of environmental test equipment is a determining factor.

4.0 ELECTRICAL REQUIREMENTS

4.1 The integrated laser and power supply shall meet the electrical requirements applicable to the 3072H Laser. The following is a tabulation of the electrical parameters for the 3072H Laser:

OPERATIONAL MODE	TELEMETRY OUTPUTS	
Input Voltage, 24 to 32 VDC	Temperature	0-5 VDC
Turn-on Time, 6 seconds	Pressure	0-5 VDC
Command-ON, 4 to 8v pulse	No. 1 Anode Voltage	0-5 VDC
Output Power, 5mw minimum, CW, TEM_{oo}	No. 2 Anode Voltage	0-5 VDC
Frequency, 6328°A	Output Power	0-5 VDC
Input Power to be Specified.	No. 1 Anode Current	0-5 VDC
Polarization, .001	No. 2 Anode Current	0-5 VDC
Beam Diameter, 2mm Maximum		
Divergence — to be Specified		
Angular Deviation — to be specified		

The complete functional test shall include a verification these specified parameters. Other tests shall be added if additional information is needed to optimize design and performance.

5.0 ENVIRONMENTAL REQUIREMENTS

5.1 The environmental tests are designed to qualify the laser for the most prevalent space environments. These environmental tests are similar to those required on other space programs. A Qualification Test Procedure shall be employed to provide orderly methods of testing the laser.

5.1.1 Vibration shall be in each of three mutually perpendicular axes as follows:

5.1.1.1 Sinusoidal Vibration

0.2" D.A. from 5-30 cps

8.6 G's peak from 30-2000 cps

Sweep the frequency range up and back once at a sweep rate of one octave per minute. Resonance frequencies shall be noted, dwell at the four main resonance peaks for two minutes.

5.1.1.2 Random Vibration

5-30 cps from 0.02 to 0.61 g^2/cps

30-700 cps -- 0.61 g^2/cps

700-900 cps -18 db/octave

900-2000 cps -- 0.18 g^2/cps

Duration - five minutes per axis.

5.1.2 Shock shall be in each of three mutually perpendicular axes.

5.1.2.1 The shock pulse shall be a terminal peak sawtooth of 78 G's ± 10% for a duration of 10^{+5}_{-0} milliseconds. The decay rate shall be not more than 10% of the total duration.

5.1.3 Temperature cycling shall be from -40°C to 74°C.

5.1.3.1 The temperature cycle shall be as follows:

25°C to -40°C remain for one hour

-40°C to 74°C remain for one hour

74°C to 25°C

Repeat the above temperature cycle three times.

5.1.4 Acceleration shall be in each of three mutually perpendicular axes for a duration of three minutes each.

5.1.4.1 Acceleration shall be 10 G's ± 10% in each axis, followed 20 G's ± 10% in each axis.

6.0 RELIABILITY LIFE TESTS

6.1 The reliability life test will consist of a two month thermal-vacuum test and a sixteen month continuous operational test. After the thermal-vacuum test, this laser will also be placed on continuous life test for sixteen months.

6.2 The thermal-vacuum tests shall be performed at a pressure of 10^{-5} torr or below. The temperature shall be raised to 50°C and then reduced to 0°C in forty-five minutes and back to 50°C in another forty-five minutes. This cycle (ninety minute cycle) shall be performed six times prior to beginning the sixty day thermal-vacuum test.

The laser will operate within specification limits given in Section 4.0. Input power, voltage, current and TM outputs will be recorded at 200 ± 20 hours intervals during this test.

Table III shows the OFF-ON cycle to be performed during sixty day thermal-vacuum test.

TABLE III

THERMAL-VACUUM CYCLE

OFF	ON	DAYS	TEMPERATURE	PRESSURE
X		5	0°C	10^{-5} torr
	X	10	0°C	10^{-5} torr
X		5	50°C	10^{-5} torr
	X	10	50°C	10^{-5} torr
X		5	0°C	10^{-5} torr
	X	10	0°C	10^{-5} torr
X		5	50°C	10^{-5} torr
	X	10	50°C	10^{-5} torr

6.3 At the completion of the sixty day thermal-vacuum test, the laser and power supply shall be placed on a sixteen months continuous life test. The laser and power supply shall be operated within the limits of the electrical requirements of this specification. The laser performance shall not decline below the following limits:

Reliability Test Hours	Output Power
0	5 mw or above
	3 mw or above
10000	2 mw or above

The laser will be operated under normal room conditions without any coolant or exterial fans. The voltages applied to the laser for cycling shall be those of the ON or OFF command signal. The input power, voltage, current, TM outputs, and other pertaining parameters will be measured at 500 ± 50 hours intervals. The other voltages will be maintained and checked periodically during the life test program.

7.0 DOCUMENTATION

7.1 Functional test data will be recorded from initial tests through life test. This data will be included as a part of the laser log book. The log book will consist of a complete history of the laser and power supply. Any variation in test will be noted in the log book.

7.2 Any failure occurring during Phase II of the program will be documented on EDD Failure Report forms. Failure reporting and analysis will be under the direction of Hughes Electron Dynamics Division Reliability Manager. This organization will assure implementation of established procedures which will require reporting through a closed-loop system with documented analysis of each part or component failure or malfunction occurrence.

7.3 Progress reports will be released periodically documenting the results achieved during the qualification and reliability test program.

APPENDIX B

I. INTRODUCTION

This plan describes a proposed reliability program to be conducted during Phase II of the Space Qualified Laser Program. The plan establishes an integrated reliability effort which is intended to conform to the program objectives.

The program described herein is designed to provide (1) effective planning and management of the reliability effort, (2) assurance through a well designed monitoring and evaluation program, and (3) definition of major reliability engineering tasks time-phased to the engineering effort.

Section II describes the Hughes Aircraft Company reliability management plan with the organization structure and program interfaces.

Section III outlines the reliability program tasks to be undertaken. Emphasis during Phase II is placed upon an analytical evaluation of the laser design reliability and lifetime characteristics. This effort is aimed at assessment of reliability status and the elimination of failure modes and mechanisms.

Section IV describes the techniques used to monitor, evaluate and report reliability status. These techniques allow implementation of timely corrective action when potential problem areas are discovered. The specific items discussed are reliability assessment; parts program; program reviews; supplier monitoring and control; test monitoring and evaluation; failure reporting; and reliability documentation.

II. RELIABILITY MANAGEMENT

The laser program management team includes personnel from functional departments who have direct line access to top division management. The development of the Space Qualified Laser is assigned to a program manager within the Hughes Electron Dynamics Division. Functional organizations provide technical, reliability and quality assurance support for the program. The organizational structure and program interfaces for this program are shown in Figure 1.

The basic reliability philosophy is to design the optimum reliability level into the laser during the developmental and design program phases. These reliability objectives are achieved through close working relationships between the design engineers and the cognizant reliability engineer.

The reliability manager shall direct the overall reliability effort in an effective manner by time-phasing his area's activities with those of the design engineers. He has direct line access to top division management. This type of organization is keyed to the National Aeronautics and Space Administration's space programs in exerting a strong reliability assurance program.

Reliability objectives will be met through continuous evaluation of the laser package fron conceptual design to a fully qualified laser unit. Reliability assessment will be performed on all major components to optimize reliability. This and other assessments are part of reliability responsibility in uncovering potential problem areas. Special emphasis is being placed on components stress levels and laser construction to localize early in the program critical areas of marginal performance and reliability. Through a close working relationship between the designers and reliability specialists, proper application of parts and materials will be ensured.

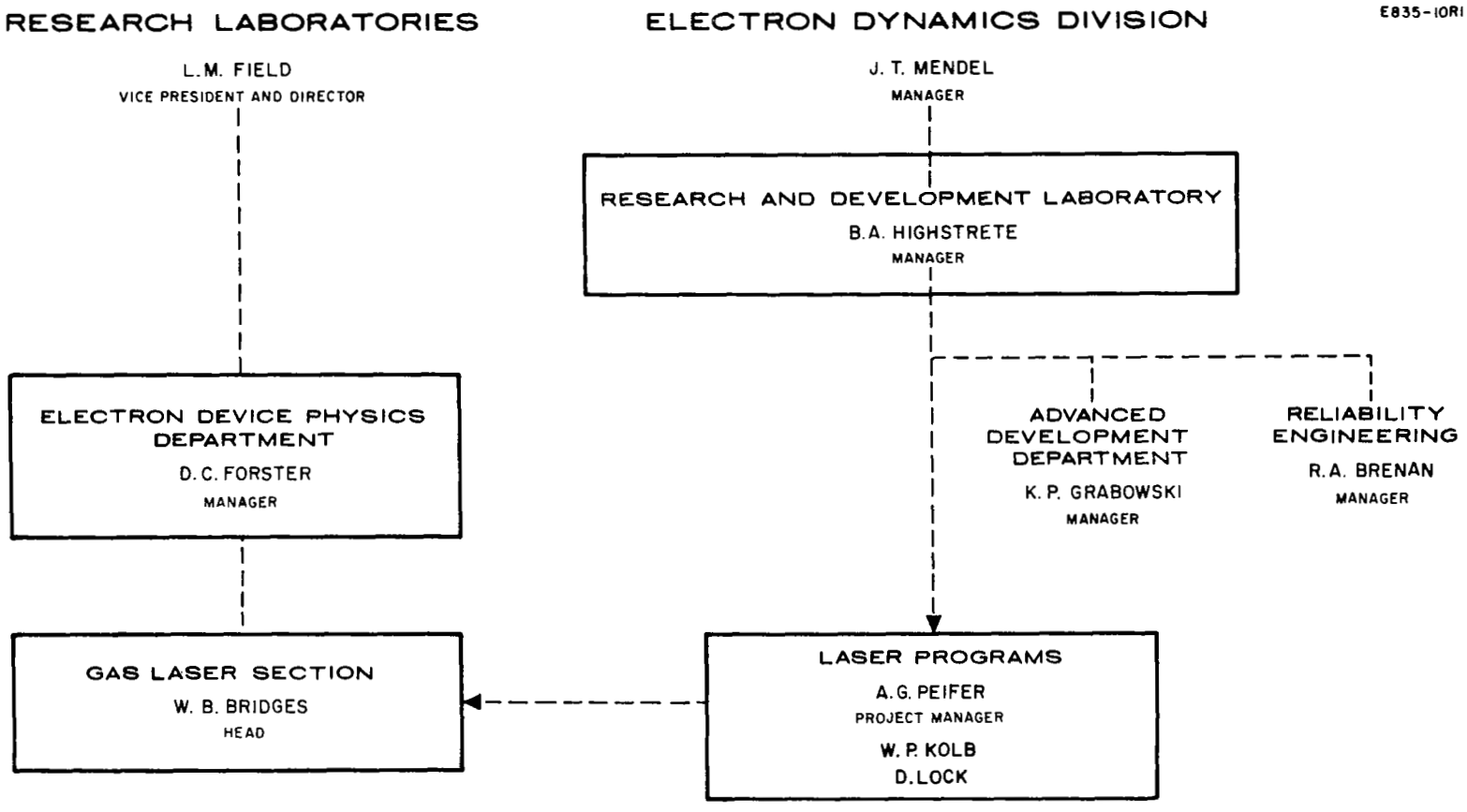

Fig. 1. Abbreviated organizational chart showing line responsibilities of personnel anticipated to be involved with this program, as well as program organization.

III. RELIABILITY PROGRAM TASKS

The following are the major reliability engineering tasks to be performed during the Phase II Space Qualified Laser Program:

1. Prepare failure modes, effects and criticality analysis based upon the evaluation of functional failure modes and mechanisms, wearout characteristics and determine their effect upon laser reliability and life.
2. Prepare reliability assessment report including a reliability prediction, and operational lifetime discussion, based upon data gathered from Phases I and II.
3. Investigate materials and processes selected for consistency with established experience.
4. Plan and monitor qualification-reliability test program.
5. Review and evaluate results obtained from qualification and reliability tests for a positive or negative effect upon reliability achievement.
6. Monitor, collect, process, analyze, and recommend corrective action on any malfunction which may occur during qualification of the integrated laser package.
7. Participate in informal HAC/ERC Program Reviews as required to support the program.

The tasks listed are integral to the program activity and constitute a basis for reliability assessment by the project engineer and reliability engineer. This effort further provides a timely means for guiding performance, reliability and environmental tradeoffs. The procedures and assessment techniques used are outlined in Section IV.

IV. RELIABILITY PROGRAM

This section further details the reliability program tasks for the Space Qualified Laser Program. The primary objective is to assess reliability status and to effect program and design improvements which will ensure attainment of the reliability and lifetime objectives.

RELIABILITY ASSESSMENT

Reliability assessment will be initiated at contract go-ahead and continue throughout the Phase II program. Scheduled milestones will occur at key points in the program. The primary reliability assessment activities include the preparation of a reliability prediction, a failure modes, effects and criticality analysis, evaluation of operational lifetime characteristics, evaluation of materials and processes, and assessment of test results. Reliability experience and achievement of similar lasers will be used whenever practical. The result of these studies will be a reliability assessment report.

Reliability assessments will be made for the laser tube, its power supplies and the integrated laser unit. During Phase I of the program, the initial reliability assessments have been based upon the conceptual design with results presented at the final Phase I Program Review.

Reliability estimates will continue through the Phase II development cycle to optimize reliability through the use of high reliability (or mil spec) parts, circuit and part derating, and to make design tradeoffs. Reliability predictions will be finalized for the qualified design configuration utilizing mean-time-between-failure histories, actual stress and duty factors and environmental stress levels.

As an important part of the early system design analysis, the project reliability engineer will develop projected analyses of the laser to determine the possible failure modes and the effects of such failures on mission success. This analysis will utilize reliability logic diagrams

to analyze the effects of various failure modes. Conceivable failures, which the designer or development engineer most familiar with the design believes could occur, will be listed on design reliability analysis forms. Accompanying the conceivable failures will be the anticipated causes, the severity and effect on performance of each type of failure, its anticipated frequency or probability or occurrence and the design and manufacturing techniques incorporated to minimize the failure occurrence probability. Such analyses will provide the means whereby an objective look may be taken at the integrated laser and its true failure possibilities and their effects evaluated. Wearout characteristics will be a natural outgrowth of this analysis.

An electrical stress analysis will determine the stress level on each electronic component in the power supply. The reliability engineer will use MIL-HDBK-217A, "Reliability Stress and Failure Rate Data for Electronic Equipment," as a guide for reliability modeling and methods for determining operating stress levels. The stress level will be used in determining the failure rate of each component. The summation of these failure rates of all components will determine the power supply reliability level. This analysis will be part of the reliability documentation package.

Reliability assessments will be revised as required by evaluation of each design change, and as data from the tests becomes available indicating a positive or negative effect upon predicted reliability.

PARTS PROGRAM

A program covering the selection, specification and application review of parts and materials will be implemented during the laser development.

Hughes places emphasis upon the procurement of parts consistent with the design requirements and to maintenance of stringent controls over all parts fabricated and procurred. In this program, maximum emphasis is placed upon approved and space qualified parts and materials with circuit and part

derating, and minimum practicable styles of generic component types. In addition, it is proposed that mil-spec electronic parts incorporated into the Phase II lasers be processed through Level II receiving-inspection (Reference Table I). Additional pre-conditioning and parameter screening methods, Level I, may be employed for space flight production units in order to achieve ultra high reliability. It may be noted that Hughes has a large number of high reliability parts specifications which are approved by NASA and other agencies for several space programs (Surveyor, ATS, Syncom, Intelsat, etc.). Parts for the laser will be selected from the Hughes list of proven space qualified parts as far as practical. This will allow substitution of high reliability screened parts for mil-spec parts in flight production hardware.

The use of non-standard parts will be discouraged; however, when a suitable part cannot be found among the Hughes preferred parts lists, a non-standard part will be selected. All data accumulated on the part will be reviewed for applicability to the design and environment prior to application approval. Space qualification data will be collected from the NASA Data Center and other satellite contractors.

Parts selection will be governed by Hughes Electron Dynamics Division Preferred Parts List which will be issued to detail for all program personnel the ground rules, as specified in the Phase II contract, for the selection of electrical and mechanical parts. This PPL will be issued by HAC/EDD Reliability Engineering at the beginning of Phase II and will be included as a requirement for all procurement documents.

Hughes Electron Dynamics Division Reliability Engineering will be directly responsible for the implementation and control of the parts program. It will maintain an up-to-date approved and qualified parts and materials list to be distributed to all design and fabrication activities. In the event that a part or material not on this list is required, a request for approval will be submitted to Hughes Reliability Engineering. Reliability Engineering will then review and approve all parts, both standard and non-standard. This

TABLE I

TESTING LEVELS FOR SPACE QUALIFIED LASER

	LEVEL I HIGH RELIABILITY	LEVEL II MIL-SPEC. PARTS
Resistors	Condition with 5 temperature cycles and 168 power burn-in. Screen on degradation criteria of ΔR.	DCR Resistance at 25°C.
Capacitors	Condition with 5 temperature cycles and high temperature bias for 168 hours. Screen on degradation criteria of ΔC, Df and ΔI_L or ΔI_R.	Measure capacitance, dissipation factor and leakage current or insulation resistance all at 25°C.
Diodes	Conditioning - Seal Test - Accelerate - High Temp Storage - High Temp Reverse Bias - 168 Hrs. Power Burn-in Screen in degradation criteria V_f and I_R and special device parameters such as T_{rr}, C_j, V_z, Z_z, etc.	Measure B_V, I_R and V_f at 25°C and perhaps high temperature I_R and special device parameter V_Z, Z_z, T_{rr}, C_g
Transistors	Conditioning - Seal Test - Acceleration - High Temp Reverse Bias for 48 hours collector base - 168 hours of power burn-in at elevated temperature. Screen on degradation criteria for I_{CBO}, I_{EBO}, H_{FE}, $V_{CE(Sat.)}$, $V_{BE(Sat.)}$ BV_{CEO}, BV_{CBO}.	Measure I_{CBO}, I_{EBO}, H_{FE}, $V_{CE(Sat.)}$, $V_{BE(sat.)}$, BV_{CEO}, BV_{CBO}, and special device parameters.

will assure maximum use of qualified parts and will allow Reliability Engineering to make recommendations for a substitute part and/or vendor of the part.

PROGRAM REVIEWS

Informal program reviews will be held periodically by the project manager to evaluate program status and resolve problem areas. Personnel from technical areas such as design, fabrication, processes, materials, reliability and quality are invited to participate. The project engineer provides an up-to-date synopsis of the performance of the laser and reviews program tasks. These reviews assure cognizance of the total program and timely achievement of the overall specification requirements.

In addition, Reliability Engineering will participate in program reviews which are held with NASA as required to resolve interface problems and provide program visibility.

SUPPLIER MONITORING AND CONTROL

To assure maximum reliability and quality of purchased parts and materials, Hughes' comprehensive program of vendor and subcontractor selection, surveillance and inspection will be implemented. As in all space programs, the quality history of every supplier is evaluated by reliability and quality representatives of the Electron Dynamics Division prior to selection.

In this program, suppliers will be required to provide Electron Dynamics Division with parts, manufacturing and process visibility to ensure maintenance or reliability and quality standards. The vendor control program will be implemented and supported by the quality assurance organization at Hughes.

TEST MONITORING AND EVALUATION

Reliability Engineering is directly responsible for the overall reliability evaluation program and for ensuring that the integrated test program adequately contributes to reliability assessment and improvement. The responsibilities designated to reliability personnel in the integrated test program encompass the following tasks:

1. Incorporation of reliability requirements into the overall test program.
2. Analysis of test results to determine capabilities of meeting reliability goals, and to identify failure modes and mechanisms.
3. Prepare Qualification-Reliability Test Program Plan.
4. Schedule and Monitor Qualification and Reliability Tests.
5. Review and follow-up of failure analyses and corrective actions for their effect on the reliability status.

The qualification-reliability test program is designed to evaluate the performance capability of the laser and is directed toward identification of problem areas which may not be revealed in the design phase or reliability evaluations. A test report will be prepared and submitted to NASA at the conclusion of the program.

FAILURE REPORTING

The effectiveness of the reliability and quality effort will be enhanced by implementation of the Hughes failure reporting system encompassing recording, collection, analysis, reporting, and corrective action with monitoring to ensure follow through.

Failure reporting will be under the direction of the Hughes Electron Dynamics Division Reliability Manager. He will assure implementation of established procedures which will require failure reporting through a closed loop system with documented analysis of each part or component failure or malfunction occurrence.

RELIABILITY DOCUMENTATION

Reliability documentation will be in accordance with the requirements of the purchase specification. Specific reliability documentation proposed includes:

1. Reliability Assessment Report
2. Qualification-Reliability Test Plan
3. Qualification-Reliability Test Report

Progress will be reported periodically as applicable to the particular program phase as part of the regular engineering progress reports.

APPENDIX C

1.0 INTRODUCTION

1.1 General

The provisions herein are the basic operating methods and disciplines used by Hughes Electron Dynamics Division (EDD) which are compatible with NPC 200-3.

2.0 BASIC REQUIREMENTS

2.1 General

Quality Assurance activities are planned and performed in conjunction with engineering, fabrication, and other functions in a manner that will assure the continuous maintenance of quality requirements throughout all phases of development and fabrication.

2.2 Change Control

2.2.1 Prints - Engineering will control the release and changes to engineering requirements in accordance with Division Operation Procedures. Print release will be through the Engineering Change Control Center and will include distribution to appropriate points available to fabrication stations, inspection stations, and the control point distribution list. Obsolete data will be destroyed at the point of change effectivity by holders of controlled prints. Quality Assurance will revise quality instructions to include the changes prior to their effectivity; and assure compliance with changes.

2.2.2 Effectivity - New part numbers will be assigned when engineering changes affect interchangeability.

Quality Assurance will assure incorporation of changes at the specific effectivity points.

3.0 DESIGN AND DEVELOPMENT

3.1 Drawing and Specification Review

3.1.1 Quality Assurance shall participate at regularly scheduled program reviews. Of primary concern will be those items which determine or control the quality of purchased or HAC/EDD produced

material such as: a) Reliability; b) Critical quality characteristics; c) Peculiar test or inspection methods: and d) Tolerances.

4.0 PROCURED MATERIAL

4.1 Procurement Documents

All purchase orders issued will be screened by the Quality Engineering section to assure compliance with specification requirements. Procurement will be from those sources on the approved supplier list.

4.2 Selection of Procurement Sources

4.2.1 General - Quality Assurance Engineering will participate during supplier survey operations. Surveys will be conducted for those suppliers that are not already approved.

4.2.2 Records - Quality Assurance will maintain records necessary for establishing and maintaining a quality history for each subcontractor and supplier in accordance with standard evaluation and rating procedure.

4.3 HAC/EDD Source Inspection

When it is not feasible to determine Quality conformance upon receipt, HAC/EDD will utilize source inspection.

4.4 Government Source Inspection

Government Source Inspection for those items specified in the contract shall be required on HAC/EDD procurement documents where the requirement is applicable.

5.0 INSPECTION AND TEST

5.1 Receiving Inspection

Receiving Inspection will have all the necessary inspection and test equipment, drawings, specifications, catalogs, processes, etc., available in order to perform its operation upon receipt of the item.

5.1.1 Characteristics inspected will be verified in accordance with applicable drawings, specifications, EDD processes, or procedures. Items not conforming are to be referred to the Materials Review Board.

5.1.2 Raw material will be chemically and physically analyzed as required.

5.1.3 Adequate methods and facilities for controlling the handling and storage of raw and fabricated material will be utilized.

5.2 Engineering drawings and specifications will be utilized as primary criteria for determining product conformance. Additional written inspection and test procedures will be provided for determining product conformance. These documents and standards shall be available to all personnel responsible for fabrication, assembly, inspection and test.

5.3 Qualification Test Procedure

A qualification test procedure will be prepared and include the following:

A. Article identification

B. Test equipment block diagrams

C. Special environmental conditions that must be maintained

D. Criteria for determining conformance or rejection

6.0 NONCONFORMING MATERIAL

6.1 Material Review

Articles and/or materials which do not conform to drawings, specifications or contractual requirements, shall be submitted to a formal Material Review Board for consideration and disposition.

6.2 Control of Nonconforming Material

Quality Assurance will provide for the segregation and identification of defective articles. Dispositions by the MRB shall be clearly documented, one copy retained on file and one shall accompany the article.

7.0 INSPECTION, MEASURING AND TEST EQUIPMENT

7.1 General

The EDD system for the calibration, maintenance, and control of inspection and test measuring equipment used to determine conformance with specifications and contract requirements meets the requirements of MIL-C-45662A.

8.0 INSPECTION STAMPS

8.1 General

The EDD quality stamp control system provides for control, issuance, traceability and usage of inspection stamps.

9.0 PRESERVATION, PACKAGING AND SHIPPING

9.1 Packaging and Shipping

9.1.1 Packaging - Packaging requirements will be defined in a manner which will assure the prevention of damage, deterioration or corrosion of the item during the packaged state. The method of packaging shall be as defined by engineering specification.

9.1.2 Shipping - Packaged articles will be identified and marked in accordance with applicable procedures and specifications. In the absence of packaging and marking requirements in the contract, packing and marking shall comply with ICC rules and regulations and shall ensure safe arrival and ready identification at destination.

10.0 SAMPLING INSPECTION

10.1 Sampling Inspection Plans

Sampling Inspection shall be in accordance with Military Sampling Plans.

11.0 QUALITY DATA AND CORRECTIVE ACTION

11.1 Quality Data

Quality data is maintained through the use of records of inspections and tests performed during the fabrication and assembly processes. The records will provide evidence that the required inspections and tests have been performed. These records will indicate part or article identification, the inspection or test involved, quantity of items conforming and nonconforming, and the nature and disposition of defects.

11.2 Corrective Action

Quality data will be continually analyzed and investigations conducted as necessary to correct discrepancies. Corrective action will be timely to prevent recurrance of the discrepancies.

12.0 AUDIT OF QUALITY PERFORMANCE

12.1 Performance of Audits

Audits of the adequacy of quality procedures, inspection, tests and process controls will be performed on a scheduled basis by an impartial team of quality supervisors and/or quality engineers.